
Kingdom of Saudi Arabia
King Abdulaziz City For Science
and Technology
General Directorate of
Research Grants Programs

AR-14-77

**FINAL REPORT**
**(Part 1- Main Report)**

# GEOTECHNICAL INVESTIGATION FOR EARTHQUAKE RESISTANT DESIGN IN THE KINGDOM - PHASE I - WESTERN COAST

**PROJECT TEAM**

**Dr. Mohammad Al-Haddad** (P.I.)
**Dr. Talal O. Al-Refeai** (Co-I)
**Dr. Abdullah M. Al-Amri** (Co-I)

**KING SAUD UNIVERSITY**
**RIYADH**

**2001 G**

gdrgp@kacst.edu.sa ص.ب ٦٠٨٦ -الرياض ١١٤٤٢-هاتف ٤٨٨٣٥٥٥-٤٨٨٣٤٤٤-فاكس ٤٨١٣٨٧٨ ب.ا
P.O.Box 6086-Riyadh 11442-Tel.4883555-4883444-Fax 4813878 E-mail: gdrgp@kacst.edu.sa

# GEOTECHNICAL INVESTIGATION FOR EARTHQUAKE RESISTANT DESIGN IN THE KINGDOM - PHASE I - WESTERN COAST

**PROJECT TEAM**

# ACKNOWLEDGEMENT

Funding for this research project was provided by King Abdulaziz City for Science and Technology (KACST) under grant No. AR-14-17. The investigators express their gratitude to King Saud University for its cooperation during this research and allowing unlimited use of computer facilities of the Civil Engineering Department. Also gratitude is due to the Ministry of Interior and Ministry of Municipalities and Rural Affairs for their cooperation and help during the field trips made in the project period. Thanks are also due to the Deputy Ministry for Mineral Resources, Jeddah, Ministry of Petroleum and Mineral Resources and the Saudi Arabian Mission of the U.S. Geological Survey for allowing referencing to their geological and geotectonic maps.

# TABLE OF CONTENTS

# LIST OF TABLES

# LIST OF FIGURES

# LIST OF FIGURES

# الملخص


يحتوي هذا التقرير النهائي للمشروع البحثي أت-١٤-٧٧ والمكون من جزئين (الرئيس والملاحق) على إنجازات المشروع خلال مراحله المختلفة وآلتي سبق نشر بعضها في التقارير الدورية الستة السابقة.

تهـــدف الدراســـة اساساً إلى إجراء التمنطق الزلزالي الدقيق لمواقع محددة في مدن مختارة على إمتداد الساحل الغربي للمملكة العربية السعودية. وهي : حقل ، ينبع ، جدة ، جيزان و الوجه.

ويمكن تلخيص مراحل الدارسة على النحو التالي :-

أ- تجميع المعلومات الجيوتقنية لإختبارات التربة في كل من : جده ، ينبع و جيزان.

ب- حفـــر خمـــس ثقوب إختبارية إشتملت على إختبارات الإختراق القياسي **SPT** في كل من مدينتي حقل و الوجه.

ت- قياســـات الجـــس الكهربائي العمودي **VES** بواقع خمس إختبارات في كل مدينة لتحديد مستوى سطح الماء وعمق صخور القاعدة.

ث- عمل مقاطع سرع موجات القص **SWV** بواقع ٨ – ١٤ موقع في كل مدينة.

الجـــزء التحليـــلي من هذه الدراسة تضمّن تحليل المعلومات الزلزالية والجيوتقنية والجيوفيزيائية لتطوير المعـــاملات الزلزالـــية الدقيقة لكل موقع. إشتملت هذه المعاملات على إجراء مقاطع للتربة في كل موقع مع ما يقابلها من المعاملات الزلزالية المرتبطة بالتمنطق الزلزالي لكل موقع وقدرة تميع التربة.

عموماً يمكن وصف المقاطع السائدة للتربة لمناطق الدراسة على النحو التالي : معظم المواقع المختبرة في كـــل من حقل و الوجه وكل المواقع المختبرة في كل من ينبع و جده تصنف على أنها تمثل مقاطع تربة صـــلبة إلى صـــخريه هشه ذات تصنيف زلزالي من نوع **SC**. ولقد إقترحت على ضوء ذلك المعاملات الزلزالية المرتبطة بالتمنطق الزلزالي لكل مدينة .

جمـــيع المواقـــع المختبرة في مصاطب الصبخة في جيزان. وموقع واحد فقط في كل من مدينتي حقل و الوجـــه لها قابلية التميع. وبالتالي فإن المعاملات الزلزالية لهذه المواقع إعتمدت على التصنيف الزلزالي للتربة من نـــوع **SE** خلافـــاً لمـــا تم تصـــنيفه بأنه من نوع **SD** إستناداً على نتائج إختبارات سُرع موجات القص **SWV**. و هـــذه المعاملات يوصي بها عند تصميم المباني القياسية (العادية). أما المباني التي لها تصنيف خاص أو رئيسي في نظام البناء فإنها تتطلب تقويم جيوتقني محدد للموقع للتأكد من صنف التربة **SF**.

يمكـــن إعتبار ما توصلت إليه هذه الدراسة على أنه مرحلة أولية لعمل خرائط التمنطق الزلزالي الدقيق لـــلمدن الـــتي تم دراستها. و يعتبر الخبراء في كثير من الدول أن خرائط التمنطق الزلزالي الدقيق المعتمده على ظروف تربه الموقع عنصر أساس في التخطيط العمراني وبرامج تقليل الخطر الزلزالي ، ومن أهم ما توصلت إليه الدراســـة توفيرها لمعلومات عن الخصائص الزلزالية للمواقع التي تم دراستها بناءاً على التصنيف الحديث المتبع حالياً.

# ABSTRACT

This Final Report (Part 1-main Report and Part 2- Appendices) of the research project AR-14-77 culminates the study reported earlier in six progress reports. The study was mainly aimed at site-specific seismic zonation of selected cities located on the western coast of the Kingdom of Saudi Arabia (KSA). These cities are Haql, Yanbu, Jeddah, Jizan, and Al-Wajh. The investigations made for the study included: a) Collection of geotechnical data of soil tests in the cities of Yanbu, Jeddah, and Jizan, b) Drilling of 5 boreholes for soil investigations and standard penetration tests in each city of Haql and AlWajh, c) Vertical Electrical Sounding (VES) measurements at 5 sites in each city to define the groundwater and bedrock depths, and d) Shear wave velocity (SWV) profiling at 8-14 sites in each city.

The analytical part of the study involved systematic incorporation of earthquakes, geotechnical and geophysical data into development of the seismic site-specific parameters. These included, definition of the site-soil profiles and the corresponding seismic coefficients which are related with the seismic zone of the respective city and liquefaction potential. The prevalent soil profiles of the cities studied can be described as follows:

Majority of the tested sites in both Haql and Al-Wajh, and all tested sites in both Yanbu, and Jeddah, were classified as very dense soils and soft rock profiles with seismic site-soil category SC. The seismic coefficients which are associated with the seismic zone of the respective city were suggested accordingly. All sites tested in Sabkha terrains in Jizan, as well as one location each in Haql and AlWajh were found to be susceptible to liquefaction. Therefore, seismic coefficients recommended for these sites were based on site-soil category SE rather than soil category SD as determined solely based on SWV results. These coefficients were recommended for standard buildings. However, the buildings which are classified as special or essential in the seismic design code, require geotechnical site-specific evaluation, to check for softer soil category (SF).

The main outcome of this study is the consistence of the results with the current trend of definition of soil-site categories for seismic design. It is believed that the outcome of this study can be considered as an initial step toward the seismic microzonation of the cities studied. Experts in many countries consider the seismic microzonation mapping based on site-specific soil conditions as the most essential element for their urban land use management plans and seismic risk reduction programs.

# CHAPTER 1

# INTRODUCTION AND PREVIEW

This Introductory Chapter highlights the significance of the project, objectives, and the major elements of the methodology of the study.

Building design codes have long recognized the effects of Site-Soil conditions on design ground motion. Experience and knowledge gained over the past 20 years indicate that there were significant deficiencies and limitations in the old site categories and coefficients such as those of the 1994 Uniform Building Code (UBC 94)[1] and 1991 provisions of NEHRP (2). In the recent versions of these codes, soil site provisions have been subjected to significant evolution, not only on the definition of the site class but also on its associated coefficient. But such recent provisions are based on difficult and costly field geotechnical and geophysical measurements of soil site characteristics. Furthermore, such measurements need to be conducted by experienced and well-equipped staff. This requirement of experienced staff along with the high cost of mobilization of equipment make determination of soil profile class of individual sites very difficult or even prohibitive in some cases. The site-specific seismic zonation (microzonation) has therefore been recognized as the most appropriate and economical solution for site categorization. Experts in many countries consider the seismic microzonatin as the most essential element for their urban land use management plans and seismic risk reduction programs.

The idea of this study is to initiate and explore the concept of the seismic microzonation of selected cities in the Kingdom of Saudi Arabia (KSA). Efforts of the study involved systematic geotechnical and geophysical field tests. The results were generally formulated to be consistent with the current trend of definition of Soil- Site categories. An equally important outcome of the study is the gained experience and mobilization of advanced equipment. This is considered an essential step for further studies in this area, that are needed for updating the seismic design criteria proposed for KSA and furnishing the essential data for evaluation of the seismic performance of existing buildings.

## 1.1 OBJECTIVE AND SCOPE

The scope of the study was limited to five cities on the western coast of the Kingdom. These cities are Haql, Yanbu, Jeddah, Jizan, and Al-Wajh. In each city, the following objectives were accomplished.

a) Characterizing soil profiles and assessment of the dynamic soil properties, that includes a vast site characterization database of shear wave velocity (SWV) profiles to depth reaching 50 m.

b) Evaluation of the potential of amplification of the seismic response of the ground and the associated soil site coefficients. Site coefficients will be defined in terms of the mean shear wave velocity in the upper 30 m of the soil profile according to the recent trend of provisions on effect of local site conditions on ground motions.

c) Evaluation of the liquefaction potential.

## 1.2 SITE SELECTION FOR FIELD WORK

Although sites were selected with a principal objective of covering different soil types in each city, accessibility of the field equipment, and availability of open and level surface influenced the final selection of the sites. Locations and geographical co-ordinates of the selected sites in the cities of the study are tabulated and located on maps of the cities in Appendix A.

## 1.3 METHODOLOGY

### 1.3.1 Executive work

The major tasks executed to achieve the objectives of this project were comprehensive literature reviews on state-of-the art-methods to measure shear wave velocity and methods for evaluation of the liquefaction potential, analyzing the collected geotechnical data and conducting field tests.

### 1.3.2 Field tests

a) **Soil investigation:** The field explorations were assigned to a local geotechnical firm. The. scope of the fieldwork was outlined in detail by the research team. The contract provisions include:

1) Standard Penetration Test (SPT) in accordance with ASTM D-1586 [3] at 1.5 m intervals or at every change of stratum.
2) Collection of disturbed soil samples by means of split barrel sampling procedure.
3) Laboratory tests to evaluate the basic physical properties of the various materials that underlie each site.

All data obtained from the fieldwork is presented on the drilling logs in Appendix B. Sieve analysis was conducted to determine the grain-size characteristics of selected soil samples. Gradation curves and classification are presented also in Appendix B.

b) **Vertical Electrical Sounding Investigation**: Vertical electrical sounding (VES) work was carried out to evaluate the depth to bedrock and indicate the water level. An Schlumberger sounding technique was utilized with a half current electrode separation extended up to 400 m. This means that the investigation maximum depth was about 60 m. The field data was interpreted by using the Schlumberger automatic interpretation program. The methodology and results are presented in Chapter 3 of this report.

c) **Shear wave velocity**: The Controlled Source Spectral Analysis of surface waves (CXW) explained in detail in appendix D is employed in the project for measurements of (SWV). The (CXW) has been recognized as a relatively non-invasive and cost-effective approach to obtain SWV data [4]. The CXW technique measures the dispersion of Rayleigh waves produced by means of a controlled vibrator, using accelerometers and a digital data processing unit. The electromagnetic, 700 kg source is made to vibrate with a periodic random signal produced by the signal analyzer and amplified by a 20 Amp power amplifier. The signal has a flat spectrum over the frequency range considered. The system produces Rayleigh waves in the range of 3 to 100 Hz with a wavelength of up to 59 m. During the test the velocity of the components of the wave is obtained by measuring the phase of the cross power spectrum between two receivers located at given distances from the source. The velocity is obtained from the phase lag and the distance between receivers. The typical spacing used is 1, 2, 5, 10 and 15 m, and frequencies are between 3 and 100 Hz. From the test data and further analysis it is possible to determine the SWV profile of a site typically to a depth of 30 m. Field measurement are presented in Appendix F.

# CHAPTER 2

# LITERATURE REVIEW

## 2.1 CURRENT TREND OF SITE-SOIL PROVISIONS IN THE DESIGN CODE

It has long been recognized that the effects of site-soil conditions on design ground motion should be considered in earthquake resistant design of building. Building design codes generally take into account the effect of local site conditions on the design ground motion by introduction of a "site coefficient". This to modify basic design response acceleration parameters determined for firm rock sites to appropriate values for other site conditions. In most international and old editions of US codes a single site coefficient is assigned for each site class. In ATC-3-06 [5] the site coefficient (S) associated with the three site classes of S1, S2 and S3 were respectively 1.0, 1.2, and 1.5. In NEHRP [2], UBC [6], and UBC [1], and based on experience gained form 1985 Mexico City Earthquake, a fourth site class, "S4" was added with a site coefficient of 2.0. In the recent versions of these codes, soil site provisions have been subjected to significant evolution, not only on site class definition but also on the associated coefficients. Experience and knowledge gained from 1985 Mexico City and 1998 Loma Prieta earthquakes was the major factor promoting the need for improvement in codifying site effects.

Strong motion data from 1989 Loma-Prieta earthquake and extensive geotechnical investigations have yielded new definitions for site classes and the accompanying empirical amplification factors (Boore and Joyner [7]; Borcherdt [8]). In their regression analysis for the prediction of site-specific response spectra Boore et al. [9] have classified the sites into four groups on the basis of average shear wave velocity, Vs (m/s), in the top 30m. Site class A has Vs>750 m/s, B between 360-750 m/s, C between 180-360 m/s and D less than 180 m/s. Similar site classes have also been proposed by Borcherdt [8]. The amplification potentials of these site classes are low to very low (A); low to intermediate (B); intermediate to high (C); and high to very high (D). Such shear-wave velocity based site classification is the current methodology in recent earthquake resistant design codes..

Boore et al. [9] have used the site categorization A, B and C, delineated on the basis of average shear wave velocity ranges, to model the site variations in their regression analysis to estimate the Pseudo Spectral Velocity (PSV) from the western North American strong-motion data. This regression analysis can be used for the mapping of the spectral amplitudes at specific frequencies. Borcherdt [8] has described the amplification capability of the four site categories and obtained the associated Average Horizontal Spectral Amplification (AHSA) factors from Loma Prieta earthquake strong-motion data. The AHSA represents the average spectral ratio between the horizontal ground motion at a site with respect to a nearby rock site, and in general, can be expressed as the ratio of the average shear wave velocity of a reference site (Vo) to that of the given site (Vs) raised to some power: AHSA =3D (Vo/Vs)^M. The ASHA increases with decreasing average shear wave velocity, and especially at sites with soft soils, this increase is less for short period motion than other period ranges.

## 2.2 DEFINITION OF SOIL-SITE CATEGORIES

Rinne [10] presented a state of knowledge paper on the site coefficients for building codes in United States of America (USA). The paper outlines deficiencies and limitations of the old site categories and coefficients of the Uniform Building Code (UBC 94)[1]. Experience and knowledge gained over the past 20 years indicate the following:

- The old site categories are not well defined,
- Old site coefficients do not apply to short period amplification,
- Categories do not correspond to logical breaks in site coefficients revealed by recent research,
- Old site coefficients do not account for the non-linearity of site response with varying input motion,
- Definitions of site categories leave considerable room for interpretation that in many cases places a site in an inappropriate category.

The paper also outlines the evolution of development of new site coefficients from data and research through a workshop sponsored by the following scientific agencies (in USA).

1. NCEER, National Center for Earthquake Engineering Research.
2. SEAOC, Structural Engineers Association of California.
3. BSSC, Building Seismic Safety Council.

The NCEER/SEACO/BSSC Workshop integrated the research efforts into the proposed new code provisions and was thus a landmark meeting in the development of new site coefficients. The workshop was held in November 1992 at the University of Southern California in Los Angeles, with a wide representation of over 65 geoscientists, geotechnical engineers, and structural engineers. R.D. Borcherdt, R. Dory, and R.B. Seed presented draft proposals for new site coefficients at the workshop. The resulting coefficients were found to be similar in each proposal. These proposals were merged at the workshop into a consensus proposal for the 1994 update of the NEHRP 1991 provisions [1]. Site categories were generally defined in terms of the mean shear wave velocity, $\overline{V}_S$, in the upper 100-ft of the soil profile based on the empirical relationship by Borcherdt's [9]. $\overline{V}_S$ is considered as the main definition of the site categories and shall be used if it is available. The new site categories have been incorporated in NEHRP provisions since 1994 [11] with more detailed geotechnical definitions. In recognition of the fact that in some cases $V_S$ is not available, alternative definition in term of standard penetration resistant (N) and undrained shear strength ($S_u$) are included. The new site categories of NEHRP provisions are adopted in UBC97 [13] as shown in Table 2.1. They are also adopted in the final draft of the International Building Code 2000 (IBC 2000) [13] as shown in Table 2.1.

**Table 2.1 NEHRP Soil Profile Type Classifications**

| Site Class | Soil Profile Name | AVERAGE SOIL PROPERTIES IN TOP 30 m. | | |
|---|---|---|---|---|
| | | Soil Shear Wave Velocity, $\overline{V}_S$ (m/s) | SPT, $\overline{N}$ | Unconfined Soil Shear Strength, $S_u$ (kPa) |
| A | Hard Rock | > 1,500 | not applicable | not applicable |
| B | Rock | 760 to 1,500 | not applicable | not applicable |
| C | Very Dense Soil and Soft Rock | 360 to 760 | > 50 | > 100 |
| D | Stiff Soil | 180 to 360 | 15 to 50 | 50 to 100 |
| E | Soft Soil | < 180 | < 15 | < 50 |
| F | 1-Liquefiable soils, quick and highly sensitive clays, collapsible weakly cemented soils<br>2-Layers of peats and/or highly organic clays with thickness (H) of more than 3 m.<br>3-Very high plasticity clays (PI > 75) with H > (8 m)<br>4-Very thick, soft/medium stiff clays with H > (36 m) | | | |

Table 2.1 indicates that $S_F$ soil profile requires site-specific evaluations. The criteria prescribed for the required evaluation are as follows:

- Soils vulnerable to potential failure or collapse under seismic loading such as liquefiable soils, quick and highly sensitive clays, and collapsible weakly cemented soil.

- Peats and /or highly organic clays of thickness H >3 m.

- Very high plasticity clays (H >8m, with PI >75).

- Very thick soft/medium stiff clays (H> 36 m)

The following steps are prescribed in NEHRP provisions for classifying a site:

**Step 1:** Check for the four categories, mentioned above, of site class $S_F$ requiring site-specific evaluation. If the site corresponds to any of these categories, classify the site as Site Class $S_F$ and conduct a site-specific evaluation.

**Step 2:** Check for Site Class $S_E$, see table 2.1.

**Step 3:** Categorize the site using one of the definitions prescribed in Table 2.1.

The rock site classes $S_A$ and $S_B$ are not allowed if there are more than 3m of soil between the footing and the rock surface. Also, such categories shall be supported by shear wave velocity measurements ($V_S$). However, shear wave velocity may be estimated for site class $S_B$ for competent rock with moderate fracturing and weathering. For softer and more highly fractured weathered rock, $V_S$ shall be measured on site otherwise; the site shall be classified as class $S_C$.

Definitions of site classification parameters ($\overline{V}_S$, N, and $S_u$) are prescribed in both UBC-97 [12] and NEHRP provisions. These definitions apply to the upper 30m of the site profile. If the site profile contains distinctly different soil layers, the site shall be subdivided into those layers. Each distinct layer shall be designated by a number that range from 1 to n, where there are a total of n distinct layers in the upper 30 m profile of the site. The site parameters then are computed as the average of the inverse of the layered values of the respective parameter as explained later in Chapter 6.

It is obvious that determination of site categorizing parameters, especially $\overline{V}_S$, require difficult and costly field geotechnical and geophysical measurements. Furthermore, such measurements need to be conducted by well-experienced and equipped staff. This requirement of experienced staff along with the high cost of mobilization of equipment make determination of soil profile class of individual sites very difficult or even prohibitive in some cases. Therefore, the site-specific seismic zonation (microzonation) has been recognized as the most appropriate and economical solution of site categorizing. Most countries are considering the seismic microzonatin as the most essential element for their urban land use management plans and seismic risk reduction programs. This is what made the idea of this study, which aims at seismic microzonation of most seismically active region in the Kingdom, to come up.

## 2.3 MODIFICATION OF PEAK GROUND ACCELERATION (PGA)

A large number of empirical attenuation relationship investigations have studied the dependence of peak ground motion parameters on site conditions. Boore et al. [9] have estimated the PGA from the western North American strong-motion data on the basis of the site classes A, B and C, with all other parameters being the same. The ratio of the PGA on Class B sites to that on Class A is given by the factor 1.45. A factor of 1.79 is applicable for the ratio of the PGA on Class C sites to that on Class A. Campbell and Bozorognia [14] have used an extensive set of worldwide accelerograms to develop a PGA attenuation relationship. Results indicate that PGA on rock is higher than those on alluvium at short distances while the reverse is true at longer distances. PGA on soft rock is systematically higher than that on hard rock at all distances.

The response spectra starts at the PGA and sharply raises up to a maximum value that is then maintained constant until a given period and then declines usually as a function of the inverse of the period. Depending on the soil type the maximum value of the response is higher for stiffer soils than for softer soils for low periods. However, the extent of this maximum value is related to the fundamental period of vibration of the soil deposit which is higher for softer and deeper soils. The effect of the local conditions on the response spectra makes it different for different types of structures depending on its fundamental modes of vibration. This is the main reason of the selective damage observed on similarly constituted structures during earthquakes.

## 2.4 SHEAR WAVE VELOCITY (SWV) MEASUREMENTS

Several seismic methods have been developed for in-situ SWV evaluation. These methods are based on the propagation of elastic waves generated at one point (source) and monitored at other locations (receivers). Rodriguez-Ordonez [4] provided an excellent overview of available geophysical methods for SWV profiling including advantages and disadvantages of each method. These methods can be classified into two major groups: drilling based group (intrusive methods), surface techniques based (non-invasive methods). Intrusive methods such as down-hole and cross-hole SWV measurements, have several advantages. For instance, they allow one to determine SWV directly with higher precision and at the same time permit one to obtain geologic logs (texture, hardness, fracture spacing, age, density) of formations. They also allow one to measure standard penetration resistance. However, because of the requirement of drilled holes, these methods are much more costly (at least by a factor of 5) compared to any surface measurement technique. These costs make direct SWV methods (such as down-hole and cross-hole) prohibitive in seismic microzonation studies that cover large areas and many different sites especially for depths larger than 30 m.

Non-invasive techniques have long been recognized as a cost-effective approach to obtain SWV data essential for seismic response analysis including site amplification and liquefaction. The controlled-source measurement of surface wave dispersion (CXW) [4], as explained in detail in Appendix (D), is a non-invasive method that is being used for site characterization in the USA and Japan. In March 1997, the Japan Ministry of Construction (JMOC) certified the CXW method as a standard test in Japan (JMOC 1997), similar to an ASTM designation in the USA.

The propagation velocity of surface waves (Vs) depends on the structure of the soil. If the properties of the soil profile are constant with depth, surface waves of different wavelengths (or frequencies) travel at the same velocity. However, if soil properties vary, surface waves of different wavelengths travel at different phase velocities. This variation of the phase velocity (Vf) with wavelength is referred-to as dispersion. The process of obtaining **Vs** structure from measured **Vf** data is referred to as the Vf-Vs method. The Vf-Vs principle is used in several different methods such as the spectral analysis of surface waves (SASW), the controlled source measurements of surface waves dispersion (CXW), and other techniques based on the use of background vibrations or earthquake data to define the surface wave dispersion.

The objective of the Vf-Vs method is to obtain a SWV profile for a site by using the measured dispersion curve. This is an inverse problem in which the properties of the system are computed from the response to an excitation of stress waves. The main tool available for the solution of this inverse problem is the forward modeling of elastic wave propagation. Using these models, the dispersion curves can be computed for known soil profile. Nonlinear optimization formulations are used with the forward modeling to compute a soil profile with a dispersion curve that is compatible with the measured one.

Inversion procedures for Vf-Vs methods available to date have serious limitations. They require extensive computations, results are not unique, and there are no appropriate means to evaluate the resolution and accuracy of the results. These procedures also require highly specialized and experienced analysts. These drawbacks have limited the general use of Vf-Vs methods. The CXW approach alleviates these limitations and extends the application areas of these methods.

The CXW method may be regarded as a combination of the steady-state Raleigh waves and the spectral-analysis of surface waves, offering the advantages of most methods described in the literature.

In the CXW method, a powerful electromagnetic exciter (the controlled-source) generates operator-selected, repeated surface vibrations that are recorded by two vertically oriented receivers placed at some known distance near the controlled source. Various modes of repeated source excitation might be used for accurate data averaging. The control unit of the system is used both as signal generator and as advanced signal analyzer.

In this project, the CXW system and interpretation method will be used to obtain dense grids (of about 500-x 500 m) of SWV profiles to depth reaching 30 m in the study area. The SWV and site characterization data will be used for earthquake response analysis, seismic microzonation and other related applications.

## 2.5 RELEVANT PREVIOUS LOCAL STUDIES

Two independent teams were sent for reconnaissance reporting on the Nov 1995 Gulf of Agaba earthquake ($M_b$ = 5.9). One team was assigned by KACST [15], and Ministry of Petroleum and Mineral Resources assigned the other [16]. The estimations of Modified Mercalli Intensity (MMI) distribution of the earthquake of the two reports are

consistent. In the area of this study (City of Haqel and Ad-Durrah costom) the prevalent MMI is estimated to be VII. Complete collapse of three reinforced concrete-framed sheds in Ad-Durrah-customhouse, about 87 km from the epicenter, would qualify for a site-specific MMI of IX. This case was not considered in assessment of the intensity because it was considered an isolated case of collapse that attributed to construction and soil problems. The foundation soil is lose fill near a cliff. Great amplification of ground motion due to the site soil and topography conditions is expected. Actually, the preliminary data obtained from the Jordanian strong motion network indicates that the level of the horizontal components of the PGA of the main shock on rock and lose soil in city of Al-Aqaba which is located only 17 km from the site, were about .067g and 0.156 respectively. In this study, the site-specific response of this area will be studied in detail.

KACST have funded several national research projects in the area of seismology and earthquake engineering. A major study has been funded in the area of earthquake engineering. The study is entitled, "Study Leading to Preliminary Seismic Design Criteria in the Kingdom of Saudi Arabia" [17]. The study represents regional consistent and systematic collection and critical treatment of the limited historical and instrumental data on earthquakes and seismotectonics of the region, and development of seismic design criteria. The results of the probabilistic seismic hazard assessment indicate that the highest relative predicted ground-motion occurs near the northwestern border neighboring the Gulf of Aqaba and also near the southwestern border, neighboring Yemen. Based on iso-acceleration map for 10% probability of being exceeded in 50 years, for the seismic design purposes the Kingdom are delineated into four seismic zones. Following the 1991 Uniform Building Code UBC) [6] format, the seismic zones are assigned numbers 0, 1, 2A and 2B. Such parameters defining seismic hazard are estimated from the activity of seismogenic sources and the attenuation of the ground acceleration with distance at a given probability of exceedence. The effect of local soil conditions is not included in this estimate.

# CHAPTER 3

# GEOLOGIC SETTING & ELECTRICAL SOUNDING MEASUREMENTS

## 3.1 GEOLOGIC SETTING OF THE SELECTED SITES

### 3.1.1 INTRODUCTION

The Tertiary deposits of the Red Sea coast of Saudi Arabia crop out along narrow coastal plain whose average width is 5-10 km. The total thickness of sediments ranges between 2000 and 5000 m and the deposits show considerable facies variations. The major subsidence and sedimentation took place between the end of the Oligocene and the end of the lower Miocene. It was followed by some tectonic readjustment as well as salt diapirism during the Upper Pliocene and Pleistocene.

The coastal plain of the Red Sea is bounded to the east by the Arabian Shield escarpment and to the west by the sharp break-in slope marking the edge of the Red Sea trough.

The coastal plain in the Gulf of Aqabah area range in width from 35 to 45 km and becomes very narrow north of Al-Wajh. It consists of irregular fault controlled strip occupied by Miocene sediments and Quaternary alluvium and gravel.

Between Al-Wajh and Jeddah, both the shelf and coastal plain widen significantly across the two embayments of Al-Wajh- Umm Lajj and Yanbu-Jeddah. The coastal plain has an average width of 15 km along this part of the coast.

From Umm Lajj north to the Gulf of Aqabah, raised surfaces have been measured lying 6m , 10m , 20m and 30m above sea level. These surfaces are formed mainly of coralline rocks and have been caused by vertical movements of fault blocks. The maximum

uplift of the Pleistocene terraces occurs on Tiran island, at the mouth of the Gulf of Aqabah, where the reef stands 520 m above sea level.

South of Jeddah, the shelf expands gradually until off the coast at Jizan, where it includes Farasan islands, it reaches a maximum width of over 100 km. The coastal plain also widens south from Jeddah, being 40 km at Jizan.

In the south, there is no relief to the flat coastal plain other than Jizan salt dome, which rises 50 m above sea level. North of Jeddah , low hills of Tertiary strata crops out on the coastal plain.

### 3.1.2 HAQL SITE

Haql city is located at the extreme NW of Saudi Arabia along the Gulf of Aqabah. and bounded by lat. 29 and 30 N and long. 34.5 and 36 E.

Precambrian rocks in Haql consist of the Hinshan formation, which represents the oldest rock unit , composed of low-grade metavolcanic and metasedimentary rocks and a variety of granitic rocks. The lower Paleozoic Quweira, Ram and Umm Sahm sandstones unconformably overlies the Precambrian rocks in the central part of the area and are overlain in the eastern part by the Ordovician to Devonian Tabuk formation, which consists of sandstone and shale (Fig. 3.1).

The Quaternary coastal zone at Haql is 6 to 10 km wide, apart from some Precambrian in liers adjacent to the coast south of the town. Most of the zone consists of a broad outwash fan which dips at several degrees towards the coast as the result of uplift associated with the Dead sea transform. The fan is well exposed in Wadi Umm Jufayn to the SE of Haql. where an older sequence of silt and sand with some conglomerate beds is overlain by coarser sequence of conglomerate and sand forming the present surface.

Terrace deposits form one of the most significant features along the coast and constitute much of the landscape west of the Precambrian hills. The thickness of the terrace deposits is as much as 150 m. It consists of a succession of pebble to boulder gravels and medium to coarse sand. The sand is poorly to well bedded.

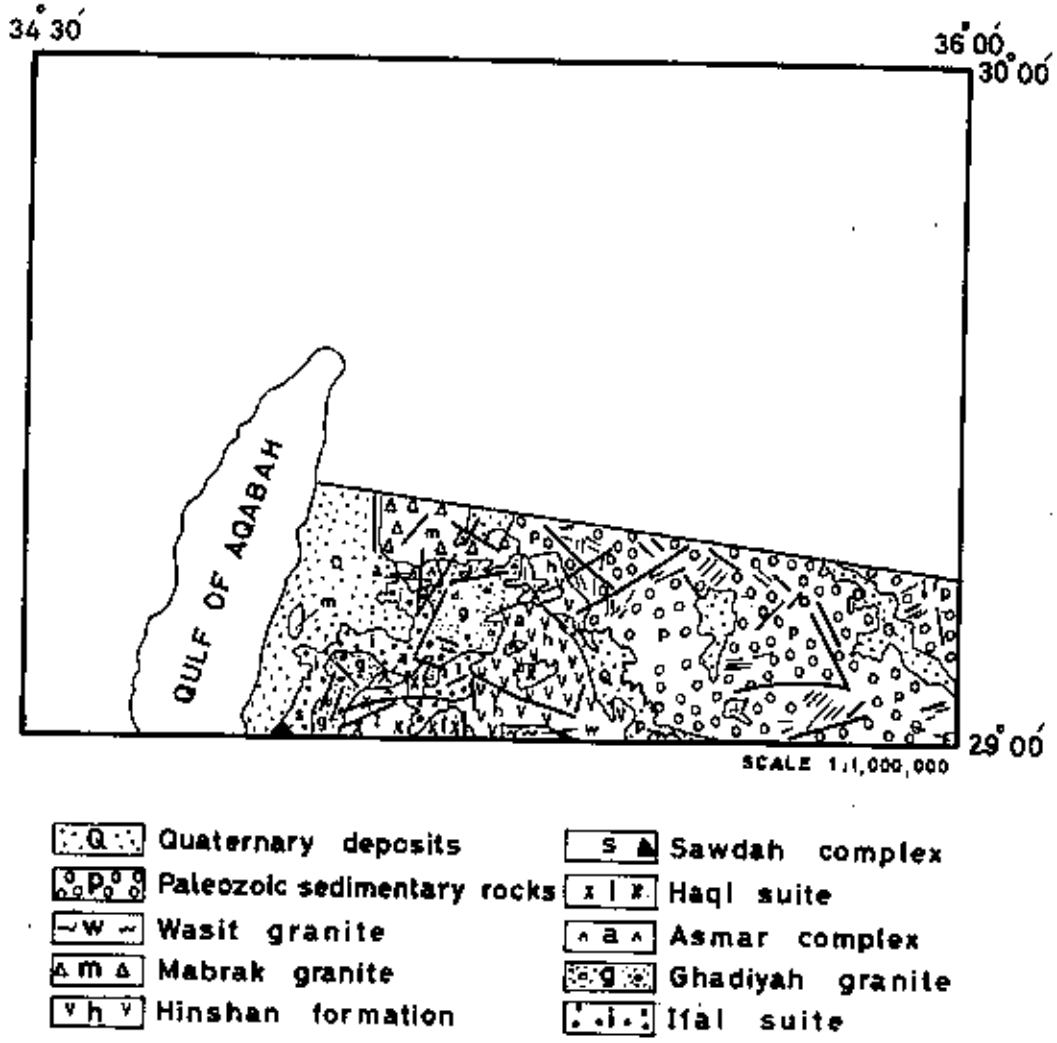


Fig. 3.1: Geologic map of Haql area showing major structural features [18].

Reef limestone forms small, isolated headlands on the coast of the Gulf of Aqabah. It overlies the terrace deposits. The yellow limestone composed of corals and fossils which interbedded with sandy beds and reaches as much as 15 m thick [18].

Three principal Wadis are present : Wadi Mabrak in the NW, Wadi ad Dabr in the SW drain westward and the third is Wadi Umm Jurfayn drains in the northwestward to the Gulf of Aqabah. These wadis are as much as 500 m wide and are bounded by vertical faces as much as 25 m high. Wadi alluvium consists of sand, silt and gravel and fills the bottoms of channels and Wadis.

### 3.1.3 AL-WAJH SITE

Al-Wajh site is located on the northern Red Sea coast between lat. 26-27 N. and long. 36-37 E. In Al-Wajh , the Tihamah is between one and two kilometers wide and is underlain by Tertiary and Quaternary reef limestone and clastic sedimentary rocks. Raised beaches with maximum elevations of about 10 m are common. Westerly draining Wadis have incised V-shaped valleys through the uplifted beach deposits.

Tectonically, the Arabian Shield consists of folded and metamorphosed plutonic and stratiform rocks. The oldest exposed rocks in Al-Wajh are represented by Usaylah suite which is composed of highly deformed and metamorphosed volcanic, plutonic and migmatitic rocks [19]. The Zaam group is the oldest unit of stratiform rock which consists of argillites, siltstone, shale, limestone and volcanic rocks. The Bayda group lies unconformably upon the Zaam group as autochthonous unit in the west and as thick para-autochthonous and allochthonous thrust sheets in the eastern and northern parts. Deposition of Thalbah group in the late Precambrian (clastic rocks, predominantly conglomerates) was followed by a tectonic phase characterized by regional folds and thrusts associated with a major crustal thickening tectonic regime and finally by formation of ductile shear belts of the Najd wrenchfault system (Fig. 3.2).

Arkosic sandstone of Cambrian crops out in the NIE. Cretaceous , Tertiary, and Quaternary marine and continental sediments were deposited in a major graben which is believed to be related to the opening of the Red Sea. Outliers of Tertiary basalt in the extreme NE are part of the Harrat al Uwayrid.

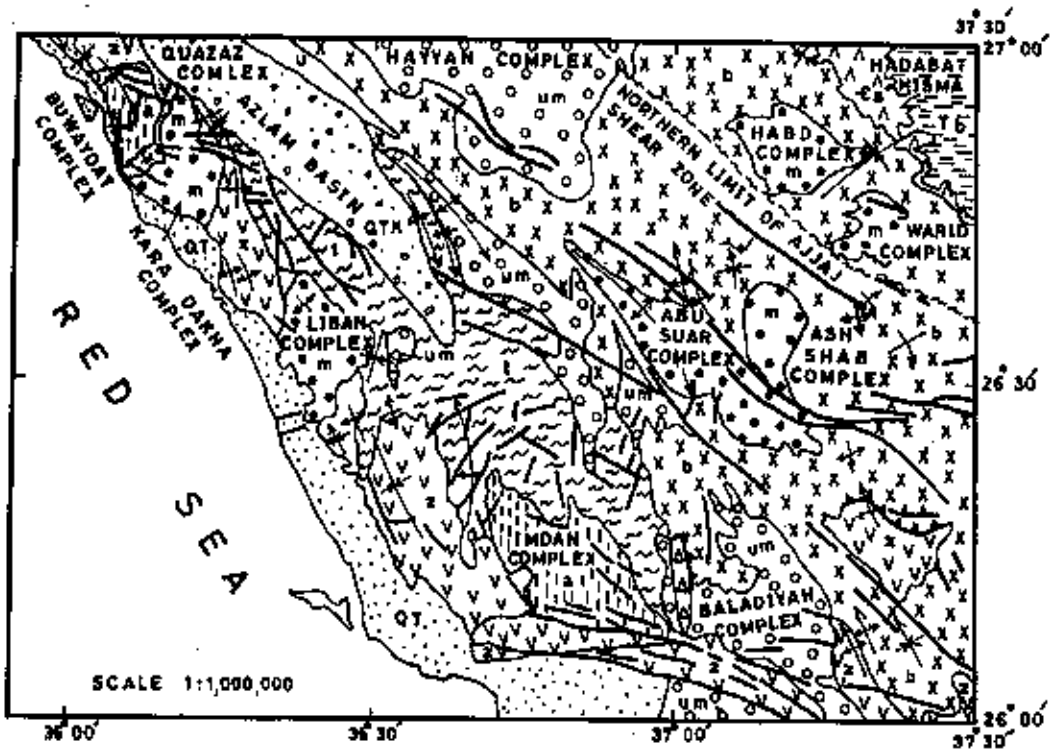


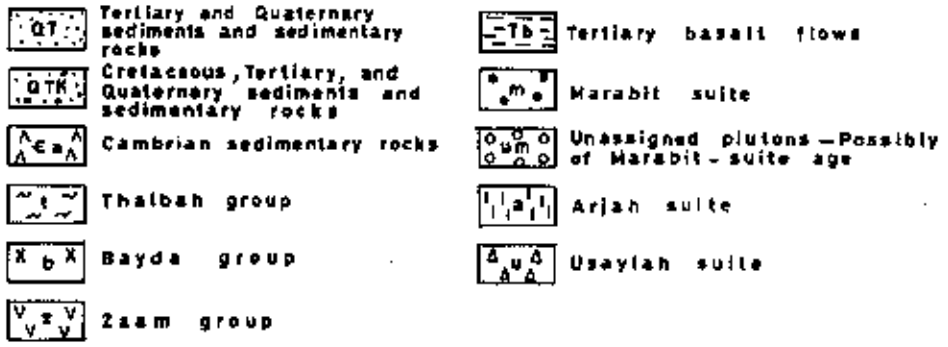


Fig. 3.2: Geologic map of Al-Wajh area showing structural features [19].

***Raghama Formation***

This formation crops out along the Red Sea coast and consists of three members: The sandstone member , the basal unit of the Raghama formation is composed of sandstone, siltstone and conglomerates. The predominant rock is fine-grained sandstone with a clay matrix intercalated with beds of polymictic conglomerate.

The conglomerate member lies unconformably on Precambrian rocks. It has no obvious stratification and is composed of subrounded, poorly sorted clasts.

The limestone member, overlies the conglomerate member and is widely distributed throughout the Tertiary deposits. South of Al-Wajh, several inlier of Precambrian rock show through the Tertiary deposits, revealing proximity of basement rocks. North of Al-Wajh, the limestone member, which overlies the Precambrian basement and infills the paleorelief, comprises a sequence of beds that dip uniformly westward.

***Quaternaiy Deposits***

Marine and continental deposits of Quaternary age crop out on the coastal plain, and surficial deposits are widespread in Wadis and coastal areas.

Near Al-Wajh, raised reef limestone crops out along the coast and rises inland to a height of 50 m above sea level. The flat-lying raised reef is a complex of coralline limestone, massive reef limestone, and back-reef deposits of calcareous mudstone.

North of Wadi Marwah in the northern coastal area the raised reef limestone is underlain in some places by a thin, unsorted polymictic conglomerate. Near Wadi Antar, dipping reef limestone wedges out southerly and is separated from a flat-lying raised reef by gravel deposits.

In the Hawd az Zalm, the Cretaceous- Tertiary Azlam formation is overlain by gravel sheet, which wadis have eroded into terraces. The gravel were probably deposited in shallow intermontaine lakes drained by Wadi Thalibah. Unconsolidated wadi sediments and wind-blown sand occur in the Hawd az Zalm and on the coastal plain.

### 3.1.4 YANBU SITE

Yanbu site incorporates the Red Sea coast and the west of the Arabian Shield between lat. 24 and 25 N. and long. 37.5 and 39 E. Most of the area is occupied by outcrops of Upper Proterozoic rock, locally covered by Cenozoic basalt flows and eolian sand deposits; the narrow coastal strip contains Tertiary-Quaternary marine and continental coastal plain sediments [20].

The oldest Proterozoic rocks are represented by two units: 1) the Al Hinu formation composed of granitized gneiss, amphibolite and leptite: 2) the volcanic and sedimentary Farri group with serpentinized ultramafic rock. This group is unconformably overlaid by Al Ays group of clastic sediments and mafic rocks. An orogeny followed deposition of Al Ays with emplacement of Jabal Salajah granitic batholith and the Wadi Kamal gabbroic and anorthositic complex (Fig. 3.3).

Extensive deformation folded the Precambrian rocks and imparted an intense schistosity. Faulting attributed to the Najd system is the last Precambrian tectonic movement. During the Miocene, olivine basalt flows making up plateaux and marine sediments of the Raghama formation which underlie the coastal plain are event related to the opening of the Red Sea trench.

The distribution of the Tertiary sediments (Raghama formation) was controlled by syndepositional faulting and graben formation related to the development of the Red Sea. A generalized section across the coastal plain from the Precambrian basement in the east to the coast in the west would be:

1. Beds of shale and conglomerate sandstone alternating with siltstone.
2. Thin Tertiary reefoid limestone with the Miocene coral , rising above the coastal plain and alternating with sandstones and silts.
3. Shale covered by sand and gravel.
4. Raised reef limestone terraces of Quaternary age.

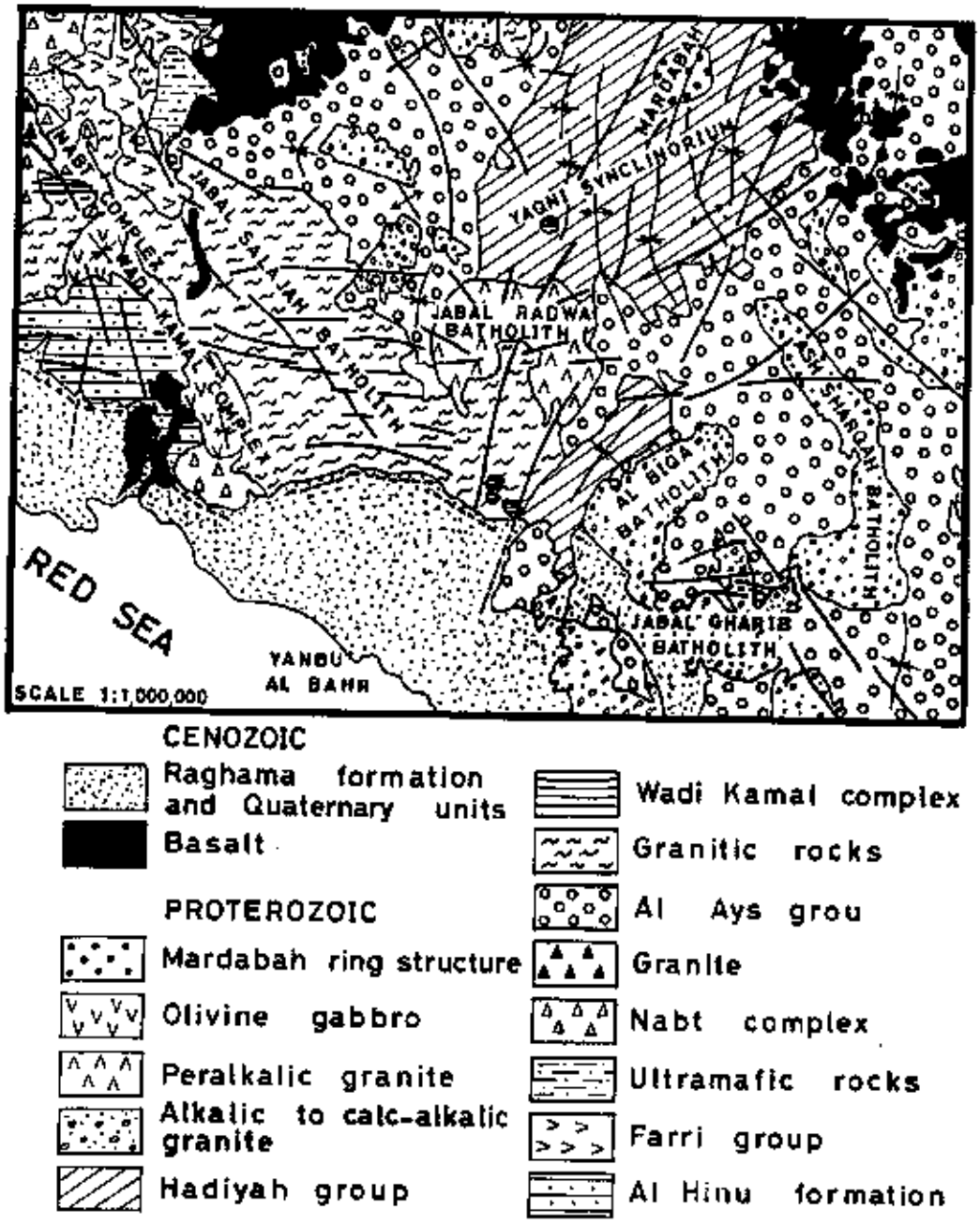


Fig. 3.3: Geologic map of Yanbu Al-Bahr showing major structural features [20].

The marine Quaternary deposits are represented mainly by reef terraces which lies several meters above sea level. Sand and mud in the lower zones of the Sharms intermixed with contemporaneous alluvial material.

Continental Quaternary deposits are represented by:

1. a sandy mantle covering a wide area which has a composite origin incorporating fluviate and eolian transport.

2. gravely or sandy spreads dissected by very close drainage.

3. gravel spreads related to the degradation of the older terraces.

### 3.1.5 JEDDAH SITE

Jeddah site is located in the west-central part of the Arabian Shield bordering the Red Sea. It is underlain by Precambrian layered rocks (10%) and plutonic rocks (90%), by Tertiary sedimentary rocks in the west, and by Miocene to Pliocene lavas in the north [21].

The Tertiary deposits and Precambrian rocks are capped by flat-lying Tertiary basalts of Harrat Rahat. Coral reefs fringe the coast. A Quaternary raised reef forms a coastal terrace in Jeddah area. Alluvial fans are conspicuous features at the mouths of Wadis along the coastal plain north of Jeddah. Eolian sand covers the alluvial fans on the coastal plain south of Jeddah.

Generally, the Quaternary deposits have been divided into seven units, The oldest is raised reef limestone that crops out along the coast, north of Jeddah the outcrop is 5-10 km wide but south of Jeddah is less than 1 km wide. Inland, the reef limestone is covered by terraced gravels, alluvial fan deposits and in the south by wind-blown sand.

Talus deposits have accumulated at the foot of steep mountain slopes. The most recent deposits are alluvial sands and gravels of Wadis, and Sabkhah gypsiferous sands, silts and clays that overlies the reef limestone.

The thickness of the alluvial cover varies widely. Over large areas of the coastal plain it is from a few centimeters to several meters thick. A drill hole in south Jeddah

intersected about 85 m of alluvial deposits [22] suggesting that there is, in places, substantial thickening of the alluvial cover inland.

### 3.1.6 JIZAN SITE

Jizan site is located in the southern Arabian Shield between lat. 17 and 17.5 N and long. 42.5 and 43.25 E. The geology of the area is the product of three major periods. These periods encompass late Proterozoic rocks of the Arabian Shield, remnants of sedimentary rocks deposited on the Shield between the Cambrian and early Tertiary times, and igneous and sedimentary rocks deposited in the Red Sea basin between the middle Tertiary and the present [23].

The Arabian Shield rocks consist of late Proterozoic quartz-rich schists that were intruded by strongly foliated to gneissic granite. Deposition of the Cambrian to lower Tertiary rocks was controlled by fluctuations in the positions of the shorelines of the surrounding marine basins. These tectonically quiescent conditions terminated with the onset of volcanism.

In a traverse from west to east, the following units are encountered : the Sabkhah unit (200-300 m), abroad zone of Quaternary alluvial deposits (30-35 km). Quaternary basalts, then a narrow zone of Tertiary igneous rocks with Ordovician sandstones which are exposed by faulting. To the farther east, The Precambrian basement complex forms the elevated mountains (Fig. 3.4).

Rock salt and associated cap rocks consist mostly of gypsum which have diapirically moved through the overlying country rocks of the Baid formation. These cap rocks are extremely faulted and disturbed , but the succession at the salt dome is as follows:

1. Massive halite with thin anhydrite reach about 1500 m thick.

2. 50 m of fine silty sandstone and shale rich in organic matter.

The bottom of the salt dome is estimated to reach about 5000 m below sea level. When a salt dome surfaces, most of the overlying country rock and cap rock are subsequently removed by erosional processes.

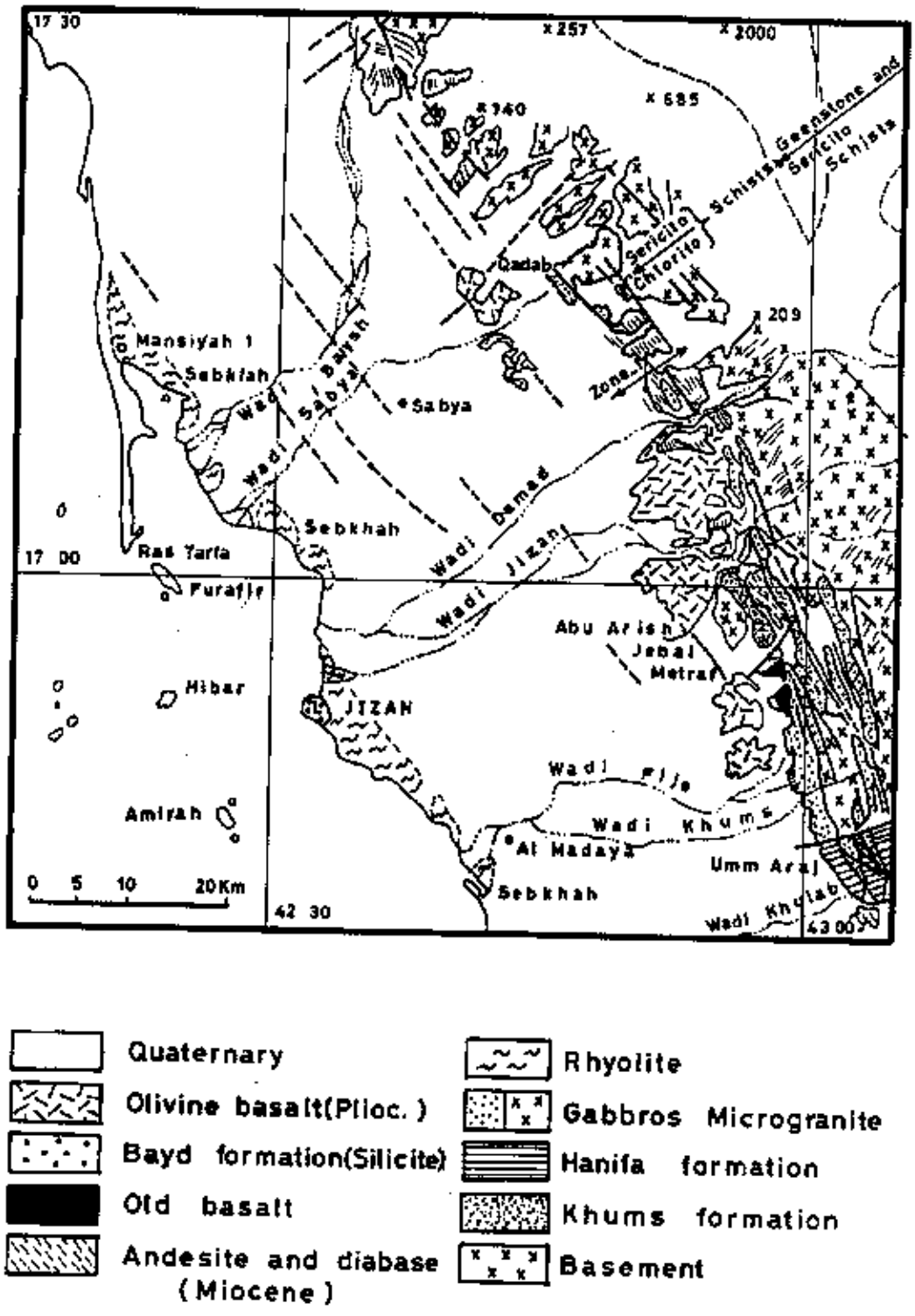


Fig. 3.4: Geologic map of the Jizan coastal plain [22].

***Quaternary Sediments***

Alluvial terrace deposits constitute about 40 % of the Quaternary deposits. They are composed primarily of sands and gravels, with lesser amounts of cobbles and finer silts.

Along the Red Sea coast large elongated bodies of Sabkhah deposits occur dissected by alluvium or eolian sands. These are believed to result from tidal flats where layers of saline mud were interlard with saline sands. The thickness is estimated to be a few meters 5-6.

Alluvial deposits occupy all the major streams. They range in thickness from a few meters in the upstream to more than 100 m near the sea. It consists of flood plain and terrace deposits. These deposits consist of gravels, sands, silts and clay deposits. Silts and associated fine sediments which locally are gypsiferous.

## 3.2 ELECTRICAL SOUNDING MEASUREMENTS

### 3.2.1 INTRODUCTION

The primary objectives of this study are to obtain details about the location, depth and resistivity of subsurface layers and to define the groundwater and depth to the bed rock.

In this study, Schlumberger Vertical Electrical Sounding (VES) measurements were conducted by using a portable ABEM SAS-306C instrument with booster transmitter capable of producing a maximum of 500 Volt D.C. voltage. During the field measurements the maximum half current electrode spacing AB/2 extended up to 400 m from the center. These measurements (resistance) are converted to apparent resistivity values by scaling them by a geometrical factor that depends on the spacing between the electrodes.

At larger AB/2 values, some sounding curves indicated noise interferences. This could be due to the low power of the resistivity instrument, which can not provide sufficient signal strength to exceed the required signal to noise ratio. The field data were re-examined as individual soundings and unacceptable errors in the apparent resistivity curves have been removed during processing.

The results were then plotted on a bi-logarithmic paper, and appropriate methods of interpretation were then used to compute the resistivities and thickness of layers.

A total of 28 soundings were made: 8 soundings at 4 sites in Haql City, 5 soundings at Wajh City, 5 soundings at Yanbu City , 6 soundings in Jeddah City and 4 soundings in Gizan City. Table 3.1 shows some geophysical parameters in study cities.

Interpretations were initially made by using Zohdy's automatic interpretation computer program (ATO). The final interpretations was made by using RESIX-PLUS program by INTERPEX Ltd. The results have been used for the interpretation of the geoelectrical cross-section for each area.

### 3.2.2 TEST RESULTS

#### 3.2.2.1 Haql City

In Haql City 8 Schlumberger Vertical electrical soundings (VES) were measured, two soundings at Site No. l. (HIA and AlB) near to the Al-Dahara Dam (Fig. 3.5). At site No. 2. Al-Sahban District two soundings H2A and H2B were measured at the shore of Aqabah Gulf Coast. At site No. 3 Al-Humida District two soundings H3A and H3B were measured (Fig. 3.6). At site No.4 near to the Prison, far away from the coast two soundings H4A and H4B were conducted.

The field Sounding curves within Haql city were three Layers type resulted from three geoelectric layers. At site No. 1 (Fig. 3.5) the geoelectric section showed a top soil composed of silty sandy calcareous gravels having resistivity ranging between 300 to 800 ohm.m and depth about 3 m. This layer is underlain by a dry layer of coralline limestone with a resistivity between 1000 to 2000 ohm.m and depth about 30 m and this layer represents the unsaturated aquifer. The third layer is the saturated aquifer consists of wet coralline limestone with resistivity less than 100 ohm.m; depending on the quality of the contained water. This layer is very thick, more than 60 m, and for this reason the bedrock depth is greater than 60m.

At site No. 2. the geoelectric section consisting of top soil composed of calcareous sand having resistivity between 20 to 75 ohm.m and depth about 2 m - This layer is underlain by saturated layer of coralline limestone with a resistivity less than 10 ohm.m and depth more than 60 m. The coralline limestone layer represents the saturated aquifer and the

Table (3.1): Summary of some geophysical parameters.

| City | Site No. | Depth to Water-table | Depth to the Bed Rock |
|---|---|---|---|
| Haql | H1A | 10 m | > 60 m |
| | H1B | 10 m | > 60 m |
| | H2A | 5 m | > 60 m |
| | H2B | 3 m | > 60 m |
| | H3A | 6 m | > 60 m |
| | H3B | 8 m | > 60 m |
| | H4A, H4B | > 60 m | > 60 m |
| Wajh | W1 | 40 m | > 60 m |
| | W 2-5 | 2 – 4 m | > 60 m |
| Yanbu | Y1 | 4 m | > 60 m |
| | Y 2-5 | 2 m | > 60 m |
| Jeddah | J 1,3 | 2 – 4 m | > 60 m |
| | J 2,5 | 3 m | > 60 m |
| Jizan | G 1,5 | 0.5 m | > 60 m |

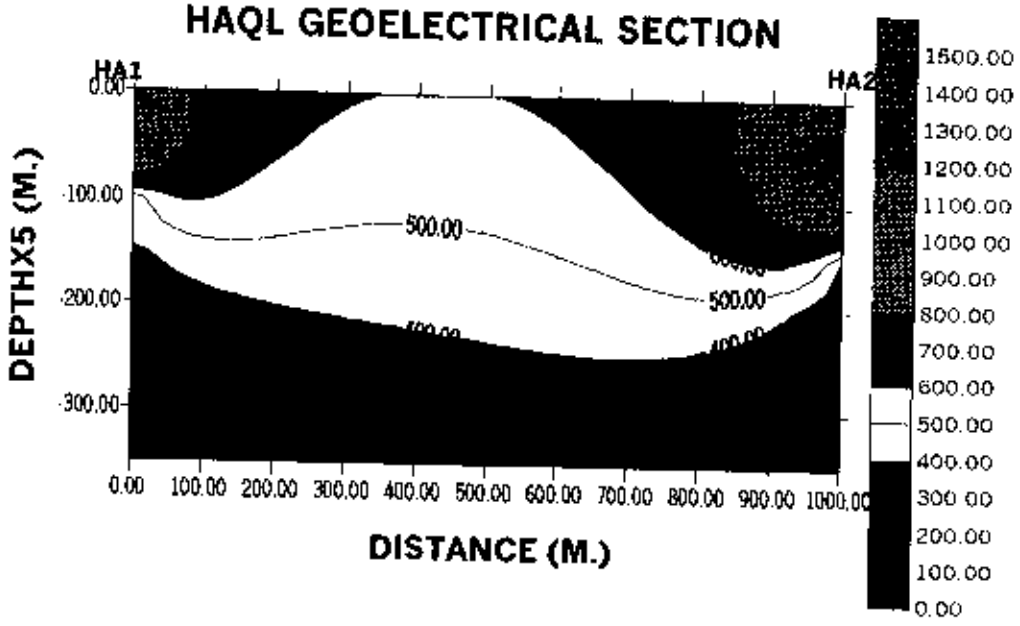


Fig. 3.5: Interpreted resistivity contour section connecting soundings H1A and H1B in Haql city.

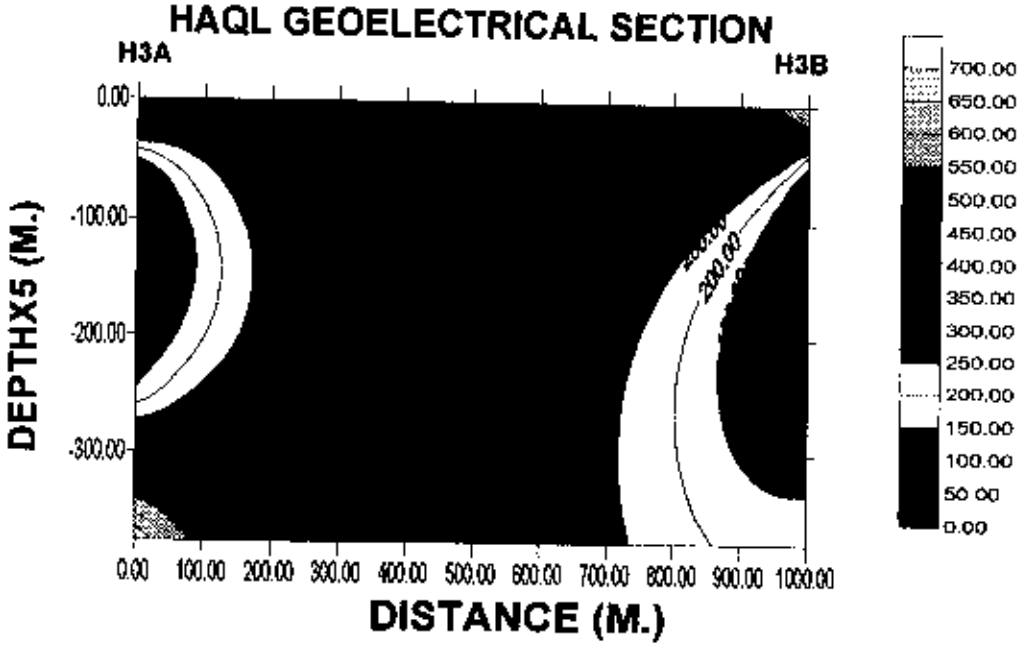


Fig. 3.6: Interpreted resistivity contour section connecting soundings H3A and H3B in Haql city.

contained water quality at this site (No. 2) is relatively highly saline. The depth to the bedrock is greater than 60m.

At site No. 3, as shown in Fig. (3.6), the geoelectric section consists of top soil composed of gravelly sand with a resistivity between 200 to 700 ohm.m and depth about 10m . This layer is underlain by a saturated weathered layer having resistivity less than 50 ohm.m and depth about 50 m. The third layer is unsaturated layer composed of limestone and the depth is more than 60m.

At site No. 4 near to the Prison the field curves of the two soundings H4 and H5 show one layer very thick. The geolectrical section consists of a very thick layer composed of gravelly silty sand having resistivity ranging between 100 and 1000 ohm.m and depth greater than 60 m. At 10 m depth there is a saturated layer of small thickness and containing water quality relatively less saline. The basement bed rock depth more is than 60m.

### 3.2.2.2 Al-Wajh City

In Al-Wajh City 5 vertical electrical soundings were carried out at 5 sites. The field sounding curves within Al-Wajh were of two types resulted from two geoelectrical layers. At site No. 1, away from the Red Sea coast, the geoelectrical section consists of top soil composed of silty sand having a resistivity ranging between 100 to 500 ohm.m and depth about 20 m. This layer is underlain by a saturated aquifer consisting of a wet layer having resistivity less than 10 ohm.m. The water level ranges between 40 - 50 m below surface and water quality is highly saline. The bed rock depth is grater than 60 m. The other four sites are located along the Red Sea Coast and the geoelectrical sections at these sites (VES 2, VES 3 and VES4 in Fig. 3.7): consists of a soil layer composed of silty sand having resistivity about 10 ohm.m and depth ranging between 2 to 4m. This layer is underlain by a saturated aquifer layer consisting of wet sands with resistivity 1 ohm.m at depth 2 m and the contained water quality relatively highly saline. The depth to the bed rock is more than 60m (Fig. 3.7).

### 3.2.2.3 Yanbu City

In Yanbu City 5 vertical electrical soundings were measured at 5 sites. The field sounding profiles within Yanbu were of two types and resulted from two geoelectrical

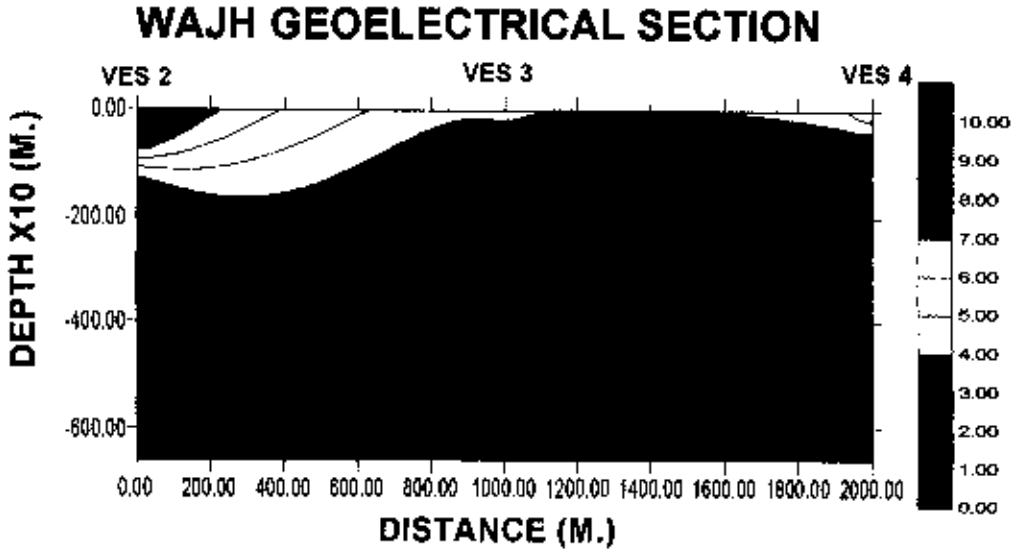


Fig. 3.7: Interpreted resistivity contour section connecting soundings VES2, VES3, and VES4 in the coastal area of Al-Wajh city.

sections. At site No. 1 the geoelectrical section consists of a top soil composed of dry gravelly sand having resistivity ranging from 10 to 50 ohm.m and depth 3.5 m. This layer is underlain by a saturated aquifer with contained water quality highly saline. The water level was 4m. The bed rock depth greater than 60 m. The rest of the soundings (VES2, 3 and 4) presents two layers, the top soil layer is silty sand very thin about 2 m thick and having resistivity about 4 ohm.m (Fig. 3.8). This layer is underlain by a saturated aquifer with resistivity 1 ohm.m. The water level is 2m and water quality is very saline. The bed rock depth is deep (Fig. 3.8).

### 3.2.2.4 Jeddah City

In Jeddah City 5 vertical electrical soundings were measured at 5 sites. The field sounding profiles within Jeddah were of two types. At site No. 1, at the Airport, and site No. 3, at the Sea port, the geoelectrical section showed top soil composed of silty sand having resistivity ranging between 5 to 10 ohm.m and depth ranging between 2-5 m. This layer is underlain by a saturated aquifer layer having resistivity 1 ohm.m; the contained water quality is very saline. The bed rock at these sites is very deep, more than 60 m. At site No. 2 near to Meridian Hotel and site No. 5 the geoelectrical profile (Fig. 3.9) shows dry top soil composed of sandy clay having resistivity ranging between 20 to 100 ohm.m with depth about 3 m. This layer is underlain by a saturated aquifer layer having resistivity 1 ohm.m and the water level is at 3 m. The saturated layer at Jeddah city is very thick and the water quality is relatively very saline. Similar to all locations the bed rock at Jeddah City is deeper than 60 m (Fig. 3.9).

### 3.2.2.5 Gizan City

In Gizan City 5 sites were investigated by Schlumberger vertical electrical sounding. All the investigated sites are located near the coast and so the field sounding profiles within Gizan were of one type. The geoelectrical section in Fig. (3.10) show a saturated aquifer, composed of salty silty clay. The water level is about 0.5 m and the water quality is very saline. The saturated saline layer is very thick having resistivity less than 1 ohm.m. The bed rock is also deeper than 60 m (Fig. 3.10).

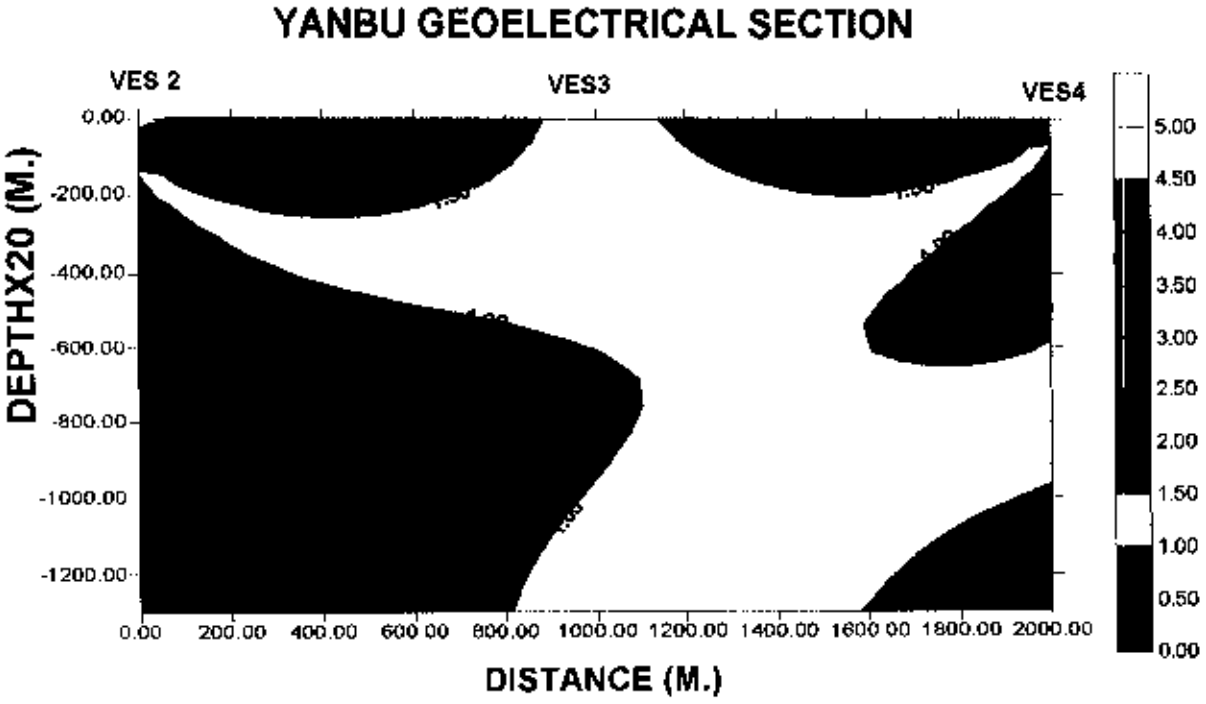


Fig. 3.8: Interpreted resistivity contour section connecting soundings VES2, VES3, and VES4 in the coastal area of Yanbu city.

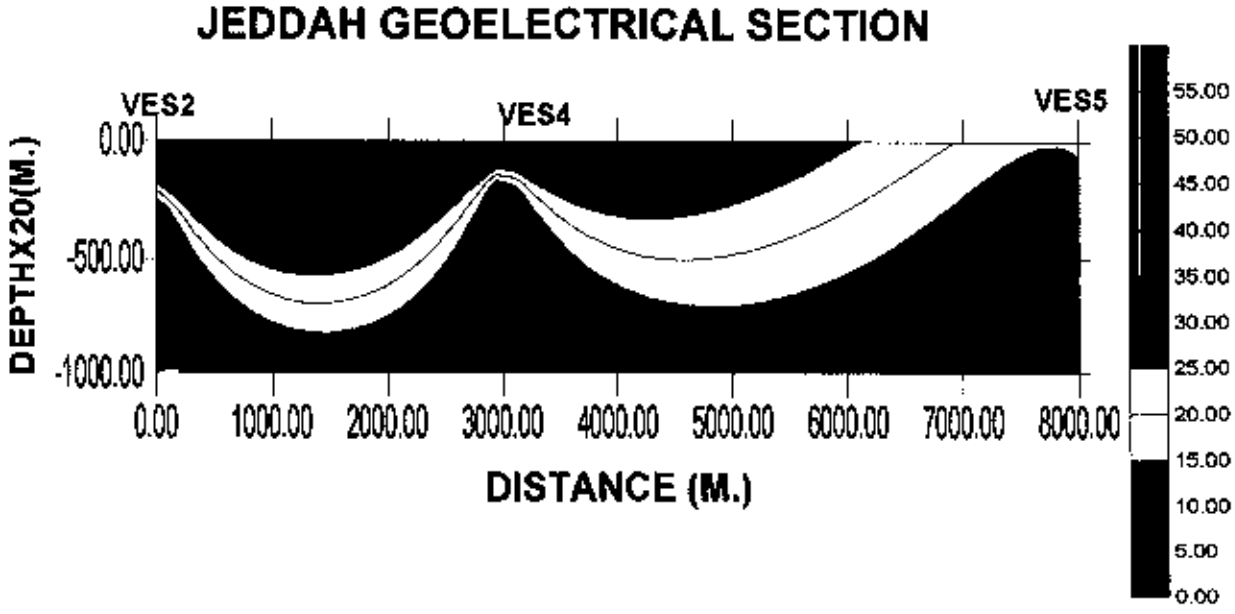


Fig. 3.9: Interpreted resistivity contour section connecting soundings VES2, VES4, and VES5 in Jeddah city.

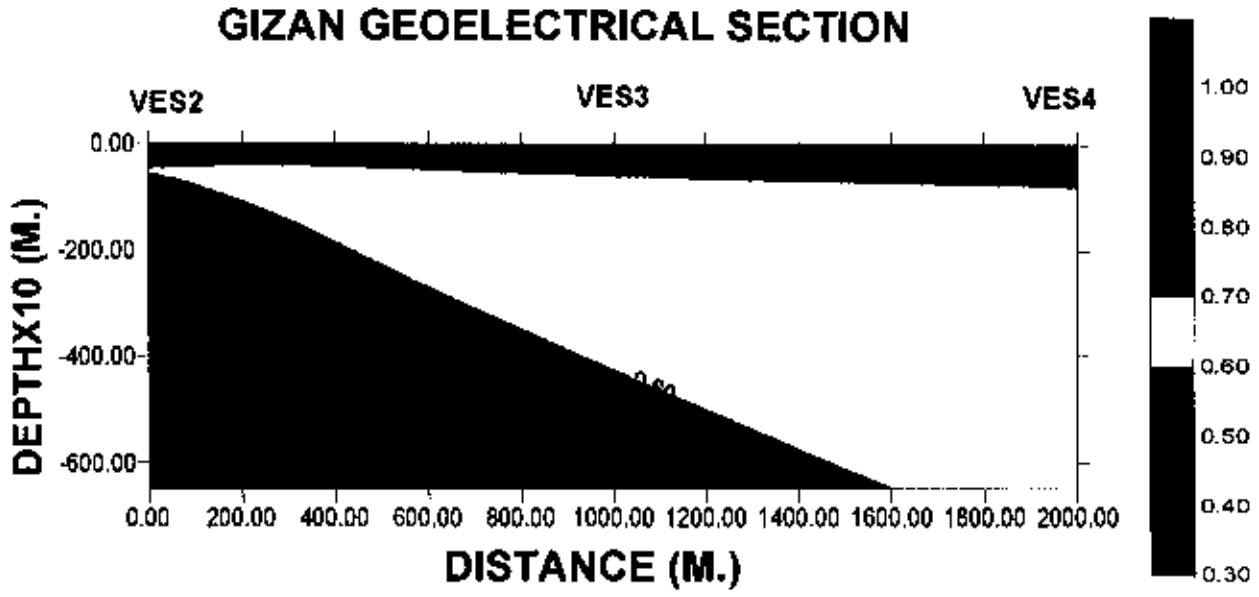


Fig. 3.10: Interpreted resistivity contour section connecting soundings VES2, VES3, and VES4 along the coastal area of Gizan city.

# CHAPTER 4

# GEOTECHNICAL CHARACTERIZATION OF SITES

## 4.1 INTRODUCTION

Local soil conditions can have enormous effects on ground surface motions and the behavior of supported structures. The strong ground shaking and collapse of a large number of buildings in Mexico City in 1985 were related directly to the dynamic characteristics of the soft clay in Mexico City [24, 25]. During the Armenia Earthquake of 1988 the large horizontal amplifications and increased damages in Leninakan, as compared with the damages in relatively close Kirovakan, have been correlated with the characteristics of local geologic deposits [26]. Recent studies show that such effects of local soil conditions mainly depend on the geotechnical properties of the soils involved, i.e, on the types of the soils [24, 27] and their depth. Based on study of liquefaction occurrences during past earthquakes and the sedimentary units affected, Youd and Perkins [28] have developed the criteria listed in Table 4.1. These qualitative relations form the basis for most of the geologic criteria used for the mapping of the liquefaction susceptibility.

The strategy of these investigators to evaluate the liquefaction potential at the selected sites was initially focused on collection of information from borings carried out in these areas in order to characterize the engineering properties of the various geologic units. The soil logs of each city were obtained from several soil testing companies, engineering firms and government agencies. SPT-N values, grain size data and soil classification data have been the primary information compiled. Boring logs in Haql and Al-Wajh were not of adequate scale to be able to define subsurface conditions in these two cities. Therefore a field investigation program was conducted in those two cities. The program consisted of drilling and sampling of 5 boreholes to a depth of 20 m in each city. For this purpose a truck mounted rotary type drilling rig CME-model 55 was used. Drilling was performed using auger tools.

To supplement our collected data, 8 to 14 carefully selected sites were tested in each city, using the CXW (controlled measurements of surface wave dispersion) technique for

**Table 4.1 Susceptibility of Sedimentary Deposits to Liquefaction During Strong Shaking** [28].

| Types of Deposit | General Distribution of Cohesionless Sediments in Deposits | Likelihood that Cohesionless Sediments, When Saturated, Would be Susceptible to Liquefy (by Age of Deposit) | | | |
|---|---|---|---|---|---|
| | | < 500 yrs | Holocene | Pleistocene | Pre-Pleistocene |
| **Continental Deposits** | | | | | |
| River Channel | locally variable | very high | high | low | very low |
| Flood plain | locally variable | high | moderate | low | very low |
| Alluvial fan and plain | widespread | moderate | low | low | very low |
| Marine terraces and plains | widespread | — | low | very low | very low |
| Delta and fan-delta | widespread | high | moderate | low | very |
| Lacustrine and playa | variable | high | moderate | low | very low |
| Colluvium | variable | high | moderate | low | very low |
| Talus | widespread | low | low | very low | very low |
| Dunes | widespread | high | moderate | low | very low |
| Loess | variable | high | high | high | very low |
| Glacial till | variable | low | low | very low | very low |
| Tuff | rare | low | low | very low | very low |
| Tephra | widespread | high | high | ? | ? |
| Residual soils | rare | low | low | very low | very low |
| Sebka | locally variable | high | moderate | low | very low |
| **Coastal Zone** | | | | | |
| Delta | widespread | very high | high | low | very low |
| Estuarine | locally variable | high | moderate | low | very low |
| Beach: High wave energy | widespread | moderate | low | very low | very low |
| Beach: Low wave energy | widespread | high | moderate | low | very low |
| Lagoonal | locally variable | high | moderate | low | very low |
| Fore shore | locally variable | high | moderate | low | very low |
| **Artificial** | | | | | |
| Uncompacted fill | variable | very high | — | — | — |
| Compacted fill | variable | low | — | — | — |

characterization of these sites in terms of mean shear wave velocity, $V_s$, in the upper 30 m. Sites selected for field work pertaining to Haql, Al-Wajh, Yanbu, Jeddah and Jizan, respectively are shown in Figures 4.1 to 4.5. Description of each site is summarized in Tables 1 to 5 in Appendix A. The coordinates of each site are shown in Tables 6 to 10 in Appendix A.

Soil conditions based on collected data and data obtained from field work in each city are presented in the following parts sections.

## 4.2 SOIL CONDITIONS IN CITY OF HAQL

The analysis of the field exploration results – records of borehole in the city of Haql are shown in Figures 1 to 5 in Appendix B. These constitute of the following main characteristics:

1. The old city of Haql lies within a narrow coastal zone, 5 to 10 meters above the sea level. This area is underlain by dense to very dense sand and gravel deposits. These deposits are in average 2 to 7 m thick and are underlain by a coral formation. Water level in this area is 2 to 11 m below ground surface.

2. The growing urban and commercial areas to the east and west of the old city of Haql are underlain by the elevated terrain (known locally as Al-Dhahra) 30 meters above sea level. Surface data suggest that soil deposits in this area are 20 m or more in thickness. The deposits typically are dry dense to extremely dense gravelly sand or sandy gravel.

3. Construction is prohibited on the massive thick dune sand areas north of Haql along the shoreline toward Al-Dorah city.

## 4.3 SOIL CONDITIONS IN CITY OF AL-WAJH

Soil data from five boreholes, Figures 6 to 10 in Appendix B (refer to Figure 4.2 for locations), show that subsurface sediments at Al-Wajh, generally consist of coralline silty, gravelly sand in dense to very dense conditions. At Wadi Zaem (north of Al-Wajh toward Duba), the subsurface soil consists of gravelly sand in loose to medium dense conditions to a depth of 20 m.

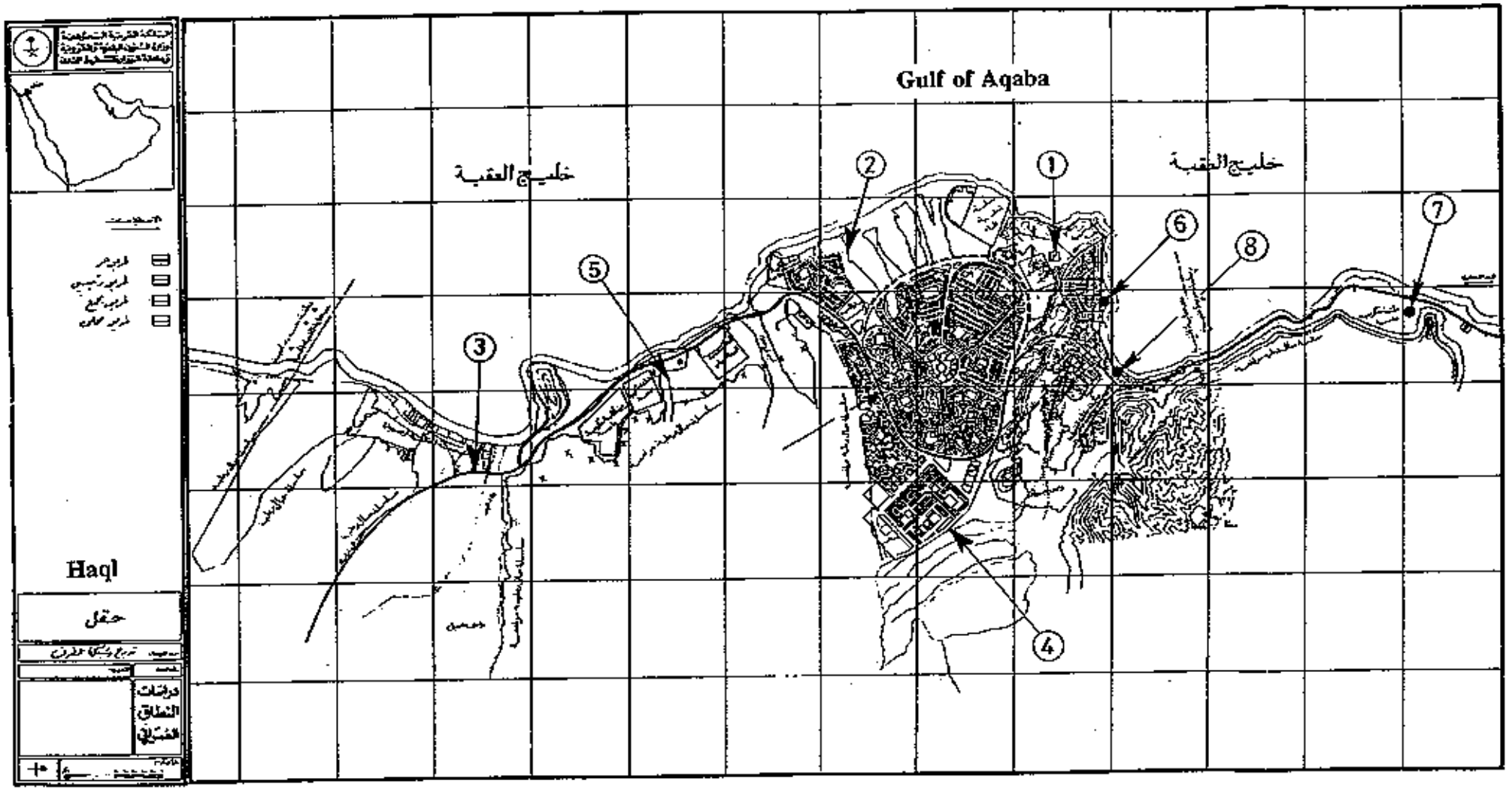


Figure 4.1 Location of Study Sites in Haql

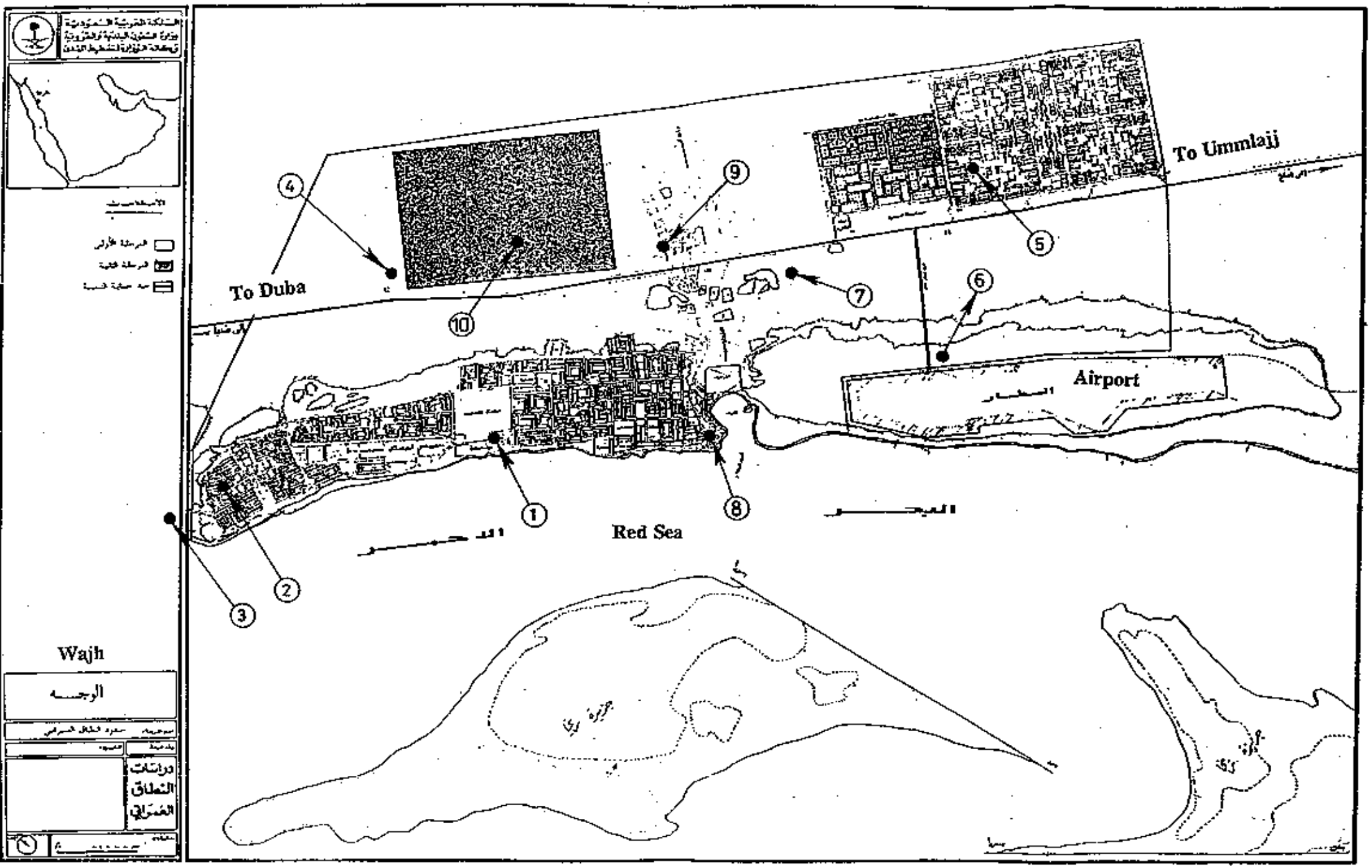


Figure 4.2 · Location of Study Sites in Wajh

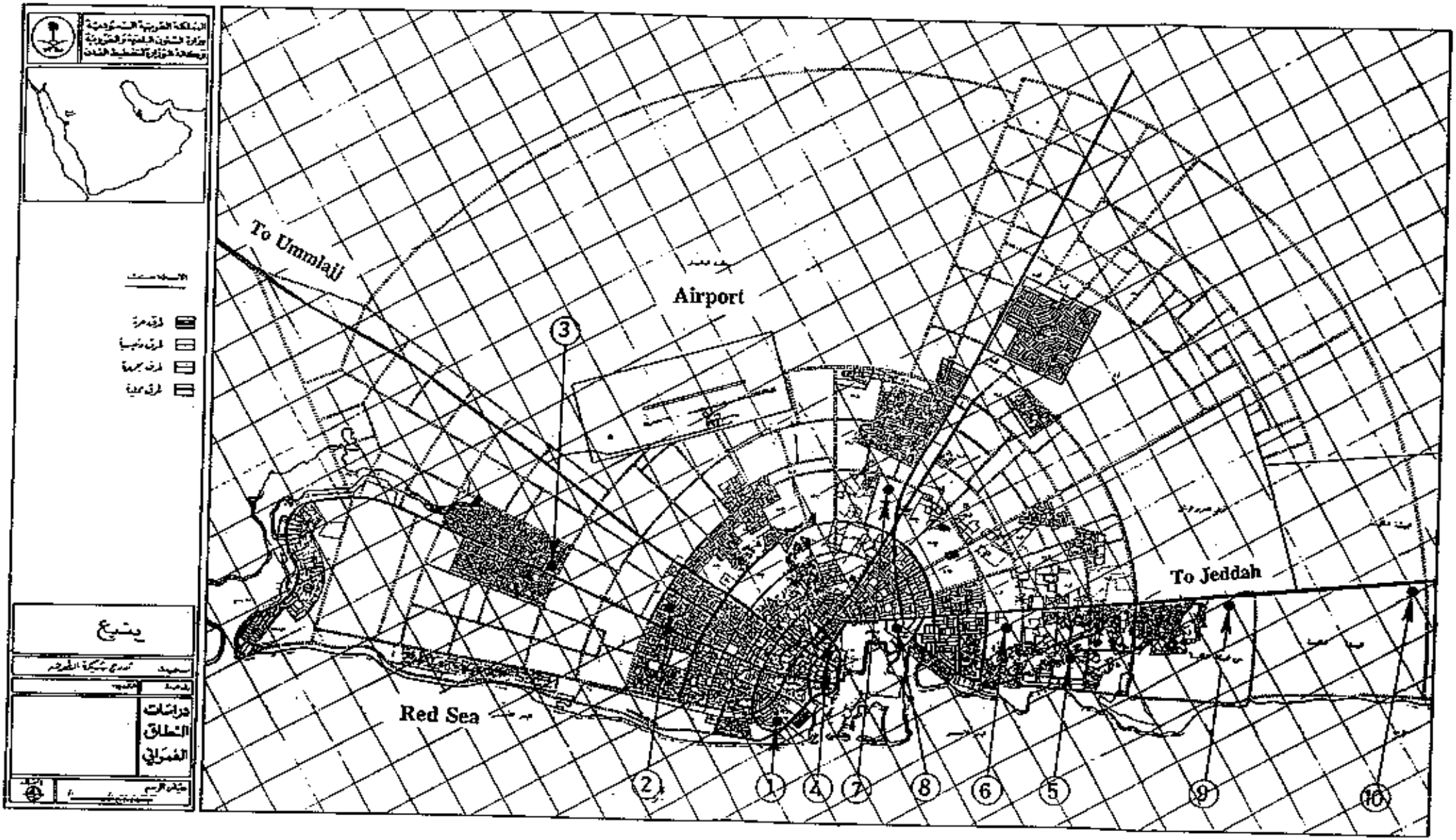


**Figure 4.3** Location of Study Sites in Yanbu

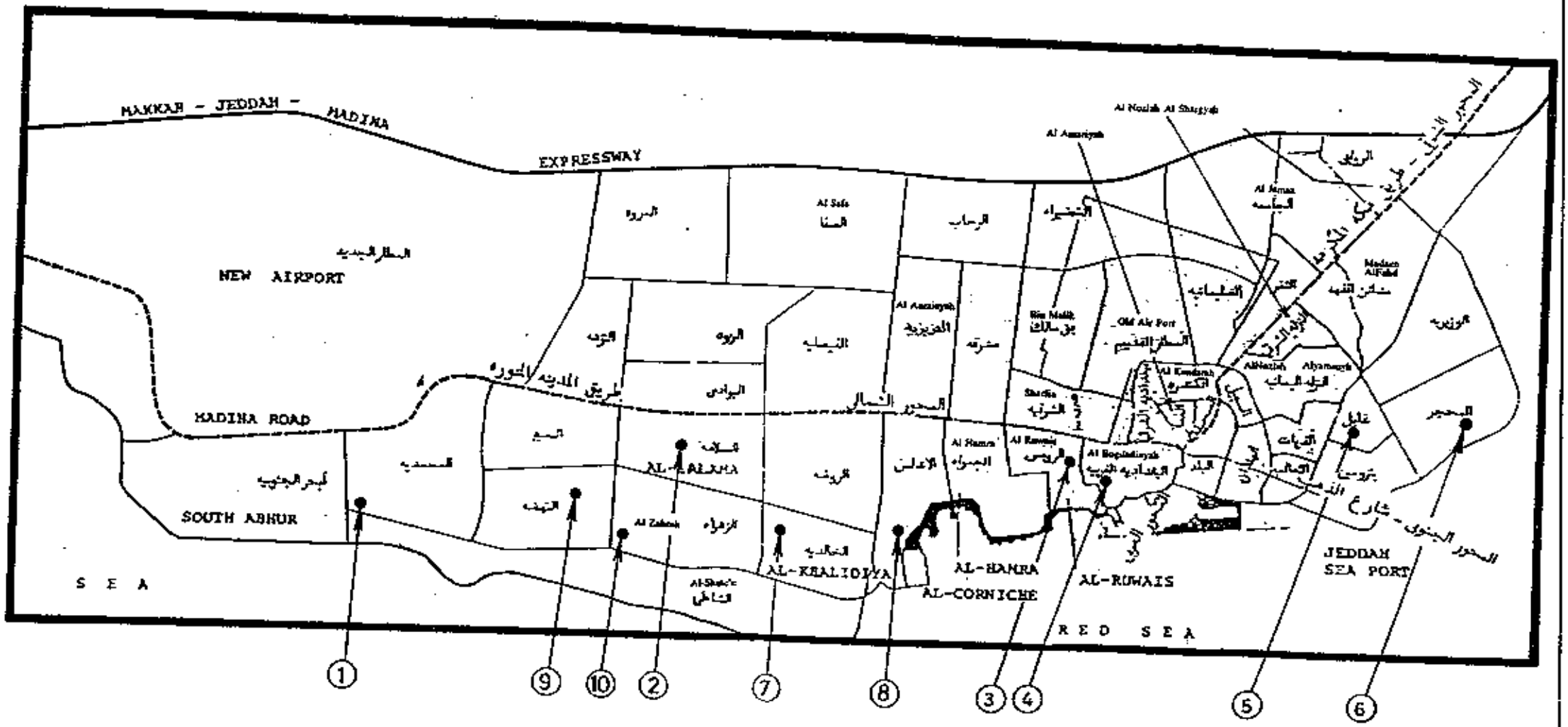


Figure 1.5 Location of Study Sites in Jeddah

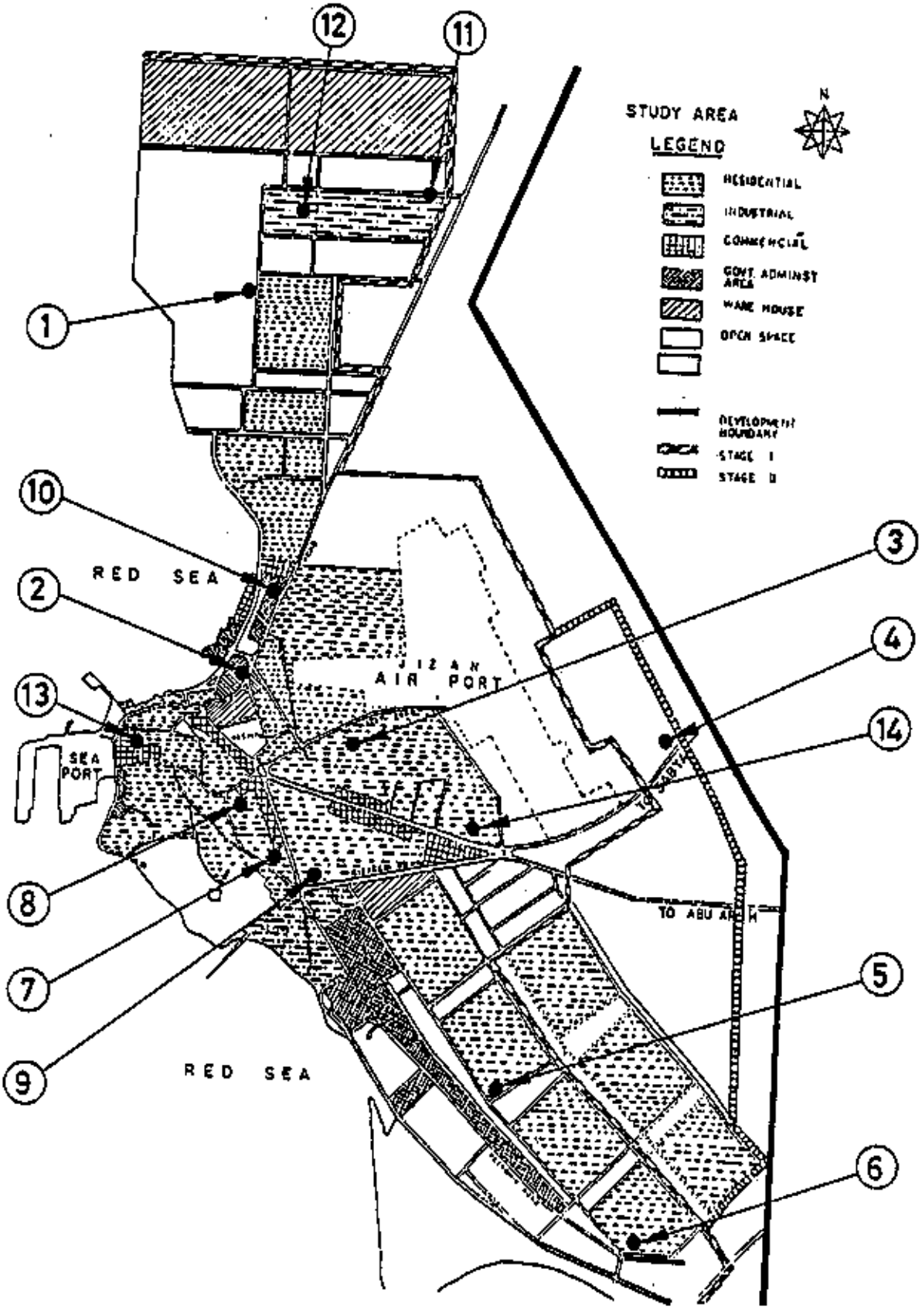


**Figure 1.6** Location of Study Sites in Jizan

## 4.4 SOIL CONDITIONS IN CITY OF YANBU

Although the ground conditions in Yanbu are significantly different within the sites, the investsigators were able to collect around 106 boring logs in the city of Yanbu (two of them to a depth of 15 m, while the rest 10 m deep), and 167 boring logs in the industrial area, 35 kms south of Yanbu (in this case most of them 20 m deep). Based on the analysis of the collected data (See Table 11 in Appendix B), the subsurface conditions can be designated as extremely variable, complex and composed of the following profiles:

**Profile 1.** There are extremely loose to loose fine to medium sand deposits from the surface to 15 m below the surface with a very shallow groundwater table (less than 1 m).

**Profile 2.** A thin top layer of compact shattered coral (2 - 5 meters with SPT-N values 20 to 50) underlain by thick layer of very loose to loose fine sand with some gravel and/or silt (6 - 8 meters with SPT-N values between 5 to 25) below ground level.

**Profile 3.** Dense to very dense layer of silty sand with gravel and cobbles.

**Profile 4.** Coral limestone interbedded with coralline sand and fines. It is medium dense to very dense specially at deeper depths (35 km south of Yanbu).

## 4.5. SOIL CONDITIONS IN CITY OF JEDDAH

Jeddah lies on a narrow coastal plain, varying in width from 2 to 40 km from south to north, which runs parallel to the Red Sea. The coastal deposits in Jeddah area can be divided into two parts. The first deposits are chiefly depositional coralline while the others are mainly sands and silts originated from variable rocks. Clays are occasionally encountered, but less prevalent. However, coral reefs are abundant, both on and offshore, and vary in thickness from centimeters to tens of meters. These coral deposits are sometimes completely weathered. More

than 440 boreholes (see Table 12 in Appendix B) have been drilled in different districts, to study subsurface conditions in Jeddah. The subsurface conditions are variable, distinct variations exist among different areas. Selected soil profiles encountered in these areas are given below:

**Profile 1. Wadi Ghalil Profile**

Wadi Ghalil channel is running across the southern part of Jeddah. Soil types encountered in this wadi are as follows:

i) Silty gravelly sand in the upper 3 to 9 meters. The soil is dry and medium to very dense.

ii) A stratum of gravelly sand to sand and gravel with rock boulders with a maximum thickness of 8 meters. This material is saturated and dense to very dense.

iii) The third layer consists of very dense silty to clayey sand with rock boulders with a maximum thickness of about 15 m.

iv) At a depth of about 26 m to 40 m from the ground a layer of highly to moderately weathered meta-andesite is encountered.

Groundwater level in this wadi is at a depth of about 8 meters.

**Profile 2. Wadi Fatimah Profile**

Wadi Fatimah slopes gently towards the sea, to the west, by about 0.4%. These wadi deposits (alluvial deposits) that originated from weathering of igneous and metamorphic rocks consist of gravelly sand to sandy gravel and/or sand and gravel. The subsoil strata in this area are as follows:

i) The upper 1-2 meters is a silty gravelly sand. It is saturated and very dense.

ii) The second layer consists of silty fine to coarse sand, saturated and very loose to loose (SPT-N=5 to 15). The average thickness of this layer is 6 meters.

iii) The third layer consists of saturated and very dense sand to sandy gravel with various amounts of silt and clay and extend to a depth of 40 meters below the ground.

The ground water level is at a depth of 1 meter.

**Profile 3. Southern Coastal Plain**

The subsoil strata in the coastal plain which is bounded by Wadi Fatimah on the east and the Red Sea (Naval Base) on the west, are as follows:

i) The first layer consists of clayey silty sand, saturated and very loose to loose. The thickness of this layer is about 2 meters.

ii) A layer of clayey to silty carbonate sand and gravel (mainly derived from disintegration and decomposition of coral formation) is encountered below the first layer. The thickness of this layer is about 8 meters. The soil is saturated and of medium to very dense state (SPT-N = 20 - 50).

iii) A layer of silty gravelly, sandy gravel and/or silty sand and gravel is underlying the second layer to a depth of 40 meters below the ground. It is saturated and in very dense state.

**Profile 4. Northern Coastal Plain**

The coastal deposits in Al-Shatee district consist of the following layers.

i) 0-3 m a layer of loose silty sand with coral fragments (SPT-N value = 6) or a layer of silty sand with gravel in medium dense to very dense state (SPT-N values between 15 to 100).

ii) (a) 3 - 10 m a layer of clayey sand with gravel medium dense to very dense.

(b) 3 - 5 m a layer of coralline sand with boulders and coral fragments, very dense.

iii) 5 - 30 m coralline sand with coral fragments, medium dense to very dense.

The groundwater level is at 2 m below the ground surface.

**Profile 5. Sabkha Profile**

Sabkha soils are present in Abhur, Al-Khalidiya, Al-Salama, Al-Hamra, Al-Ruwais, Al-Corniche and in Jeddah Sea Port districts (see Figure 8 in 2nd Progress Report). Following is a typical soil profile in Al-Hamra district:

(i) 0-3 m a layer of silty sand with gravel (SP) and coral fragments, saturated loose to medium dense (SPT-N between 10 and 17).

(ii) 3-20 m a layer of coralline sand (SP, SP-SM, SM) with coral fragments, saturated, loose to medium dense (SPT-values between 8 to 25).

The ground water level is at 1 meter below the ground surface.

## 4.6 SOIL CONDITIONS IN CITY OF JIZAN

The city of Jizan is situated on an elevated terrain underlain by a salt dome measuring 4 sq. kms in area and reaching 50 m above the see level (Figure 4.6). Two categories of geologic units are recognized in and around the city of Jizan, namely sand dunes and sabkha. Subsurface conditions in these two zones were studied based on data from more than 320 borings (see Table 13 in Appendix B).

**Sand Dune Deposits:** These aeolian sand deposits varies in thickness from 0 m to as deep as 20 meters, underlain by salt rock. The sand has a uniform grain size distribution as shown in Figure 13 in Appendix B. It is primarily composed of fine quartz grains and volcanic rock fragments with fines contents from 7% to 30% with an average of 19.8%. Natural water content for the sand ranges from 4% to 20% with an average of 12.7%. The relative density of the sand highly varies from loose at shallow depth (0-2 m), loose to medium at intermediate depth (2-10 m) and dense to very dense below that. Standard penetration resistances vary from location to location as shown in Figure 14 in Appendix B and appear to range from 4 and 18 for the upper 5 to 10 meters.

**Sabkha Deposits:** The flat coastal plain surrounding the elevated terrain in the north and south is covered by thick sediments of recent age consisting of soft/loose organic saline soils known locally as sabkha. The deepest boring within the sabkha was 25 m which did not reach the underlying bedrock. Soil profile in the sabkha areas consists of three units, depth to the groundwater table is at 1 m or less. The thickness of the top layer ranges from 1 to 2 m and consisting of fine grained sediments (silty sand and/or fine sand with silt and gravel), with SPT-N values = 4 - 30. The second layer with a thickness of 8 m to 12 m is of soft and/or loose deposits that is composed of soils varying from nonplastic fine sands to silt and clay with a very

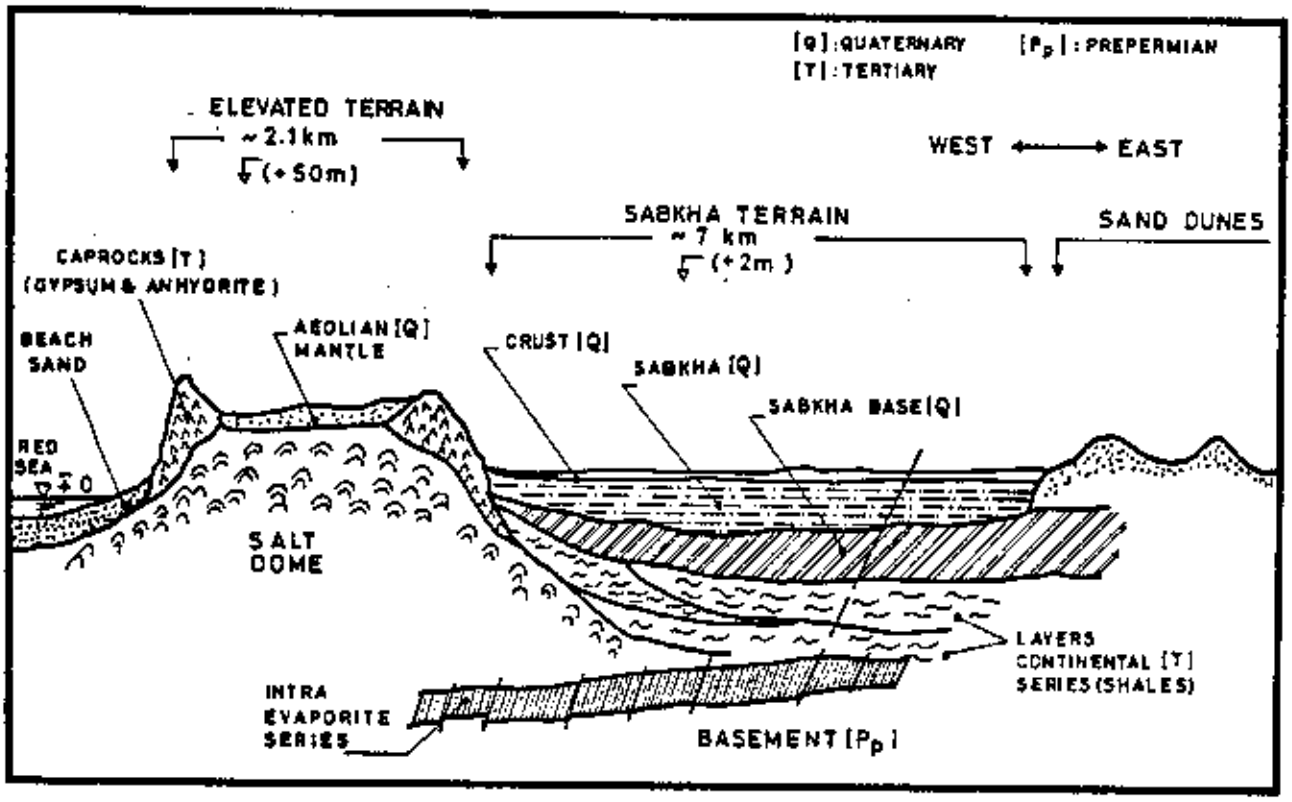


Figure 4.6 **Representative East-West Cross-Section of Jizan Region** [29].

low SPT-N values (1 to 4). The base layer consists of fine to coarse dense to very dense sand. Figure 4.7 is from an aerial photograph showing the Quarternary geology around the city of Jizan.

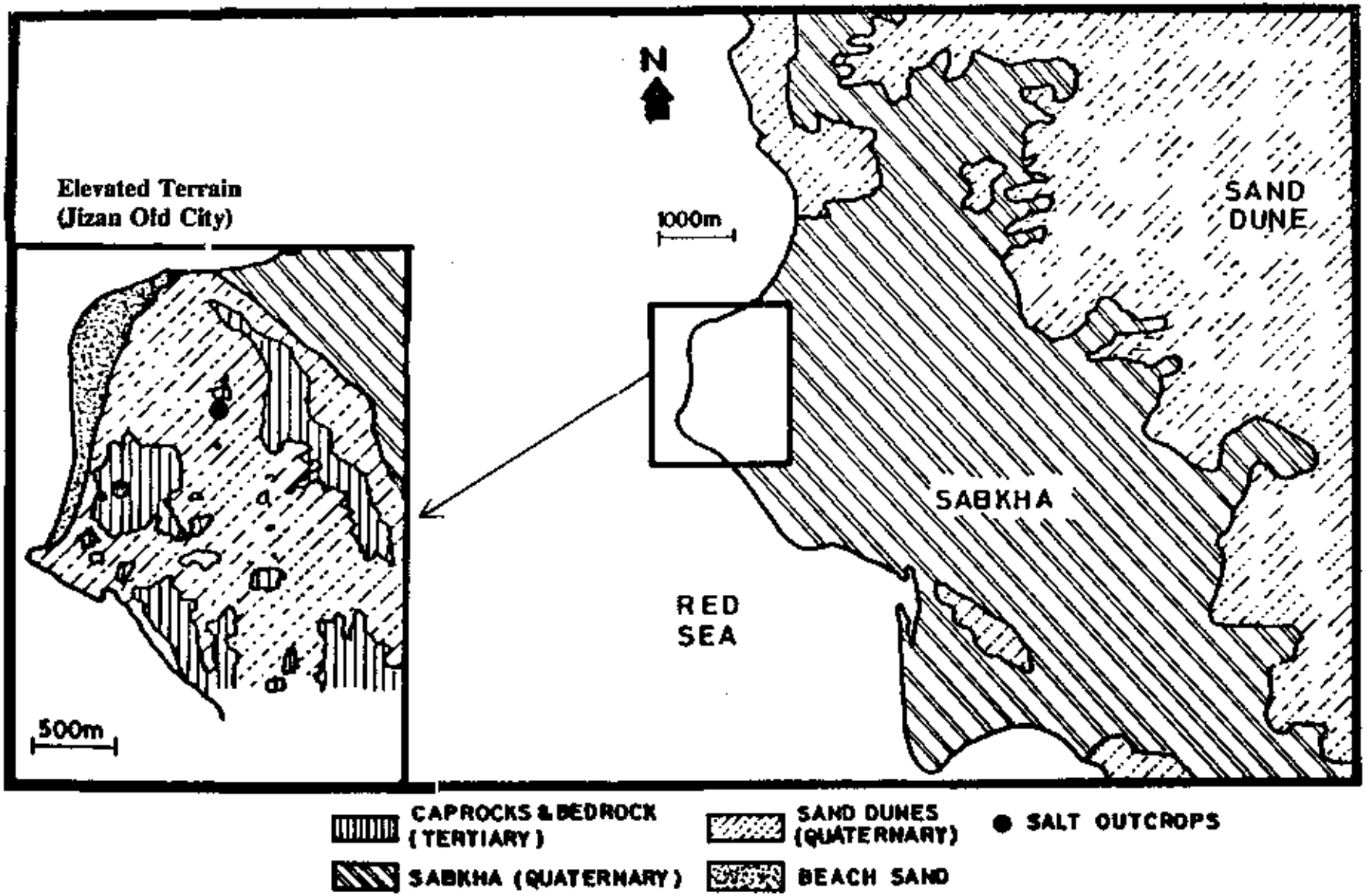


Figure 4.7: **Recent Sediments In Jizan Region** [30].

# CHAPTER 5

# EVALUATION OF LIQUEFACTION RESISTANCE

## 5.1 INTRODUCTION

In this research, we will use the simplified procedure to identify layers susceptible to liquefaction. The following briefly outlines the simplified procedure as adopted by the NCEER Workshop in 1996.

Over the past twenty-five years, a procedure, termed the "simplified procedure", has evolved for evaluating liquefaction resistance of soils. This procedure has become the standard of practice in North America and throughout much of the world. Following disastrous earthquakes in Alaska and in Niigata, Japan in 1964, Professors H.B. Seed and I.M. Idriss developed and published the basic "simplified procedure". The procedure, which is largely empirical, evolved over the decades primarily through summary papers by H.B. Seed and his colleagues. In 1985, Professor Robert V. Whitman convened a workshop on behalf of the National Research Council (NRC) in which thirty-six experts reviewed the state-of-knowledge and the state-of-the-art for assessing liquefaction hazard. No general review or update of the simplified procedures has occurred since that time.

In 1996, Professors Leslie Youd and Izzat Idriss convened a workshop sponsored by the National Center for Earthquake Engineering Research (NCEER) in which twenty-one experts reviewed developments and gained consensus for future augmentations to the procedure. The scope of the workshop was limited to procedures for evaluating liquefaction resistance of soils on level to gently sloping ground.

The participants developed consensus recommendations on the following topics: (1) use of the standard and cone penetration tests for evaluation of liquefaction resistance,

(2) use of shear wave velocity measurements for evaluation of liquefaction resistance, (3) use of the Becker penetration test for gravely soils, (4) magnitude scaling factors, (5) correction factors $K_\alpha$ and $K_\sigma$, and (6) evaluation of seismic factors required for the evaluation procedure.

The recommendations of the workshop regarding standard penetration tests and shear wave velocity method will be presented as follows:

## 5.2 CYCLIC STRESS RATIO (CSR) AND CYCLIC RESISTANCE RATIO (CRR)

Calculation or estimation of two variables is required for evaluation of liquefaction resistance of soils. These variables are the seismic demand placed on a soil layer, expressed in terms of cyclic stress ratio (CSR), and the capacity of the soil to resist liquefaction, expressed in terms of cyclic resistance ratio (CRR), hereafter referred to as liquefaction resistance or liquefaction resistance ratio. CRR is a symbol proposed by Robertson and Wride that was endorsed by the workshop. Previously, this factor had been called the cyclic stress ratio required to generate liquefaction, or the cyclic strength ratio, and had been given different symbols by different writers (CSRL, CSR, etc.).

Seed And Idriss [31] formulated the following equation for calculation of CSR:

$$CSR = \tau_{av} / \sigma'_{vo} = 0.65(a_{max} / g)(\sigma_{vo} / \sigma'_{vo}) r_d \qquad (5.1)$$

where $a_{max}$ is the peak horizontal acceleration at ground surface generated by the earthquake, g is the acceleration of gravity, $\sigma_{vo}$ and $\sigma_{vo}'$ are total and effective vertical overburden stresses, respectively, and $r_d$ is a stress reduction coefficient. The latter coefficient provides an approximated correction for flexibility of the soil profile. The workshop participants recommend the following minor modification to the procedure for calculation of CSR. For noncritical projects, the following equations may be used to estimate average values of $r_d$.

$$r_d = 1.0 - 0.00765\, z \quad \text{for } z \le 9.15 \text{ m} \qquad (5.2a)$$

$$r_d = 1.174 - 0.0267\, z \quad \text{for } 9.15 \text{ m} < z \le 23 \text{ m} \qquad (5.2b)$$

$$r_d = 0.744 - 0.008\, z \quad \text{for } 23 < z \le 30 \text{ m} \qquad (5.2c)$$

$$r_d = 0.50 \qquad \text{For } z > 30 \text{ m} \qquad (5.2d)$$

where z is depth below ground surface in meters. Mean values of $r_d$ calculated from Equation 5.1 are plotted on Figure 5.1 along with the mean and range of values proposed by Seed and Idriss [31]. The workshop participants agreed that for convenience in programming spreadsheets and other electronic aids, and to be consistent with past practice, $r_d$ values determined from Equation 2 are suitable for use in routine engineering practice.

As an alternative to Equation 5.2, Thomas F. Blake (Summary report, [32]) approximated the mean curve plotted on Figure 5.1 by the following equation:

$$r_d = \frac{(1.000 - 0.4113z^{0.5} + 0.04052z + 0.001753z^{1.5})}{(1.000 + 0.4177z^{0.5} + 0.05729z - 0.006205z^{1.5} + 0.001210z^2)} \qquad (5.3)$$

Equation 5.3 yields essentially the same values for $r_d$ as Equations 2a-d, but is easier to program for many applications and may be used in routine engineering practice.

## 5.3 STANDARD PENETRATION TEST (SPT)

Criteria for evaluation of liquefaction resistance based on standard penetration test (SPT) blow counts have been rather robust over the years. Those criteria are largely embodied in the CSR versus $(N_1)_{60}$ plot reproduced in Figure 5.2. That plot shows calculated CSR and $(N_1)_{60}$ data from sites where liquefaction effects were or were not observed following past earthquakes along with CRR curves separating data indicative of liquefaction from data indicative of nonliquefaction for various fines contents. The CRR curve for a fines content less than five percent is the basic penetration criterion for the simplified procedure and is referred to hereafter as the "simplified base curve." The CRR curves in Figure 5.2 are valid only for magnitude 7.5 earthquakes.

### 5.3.1 CLEAN SAND BASE CURVE

Several changes to the SPT criteria were endorsed by workshop participants. The first change is to curve the trajectory of the simplified base curve at low $(N_1)_{60}$ to a projected CRR intercept of about 0.05 (Figure 5.2). This adjustment reshapes the base curve to achieve consistency with CRR curves developed from CPT data and probabilistic

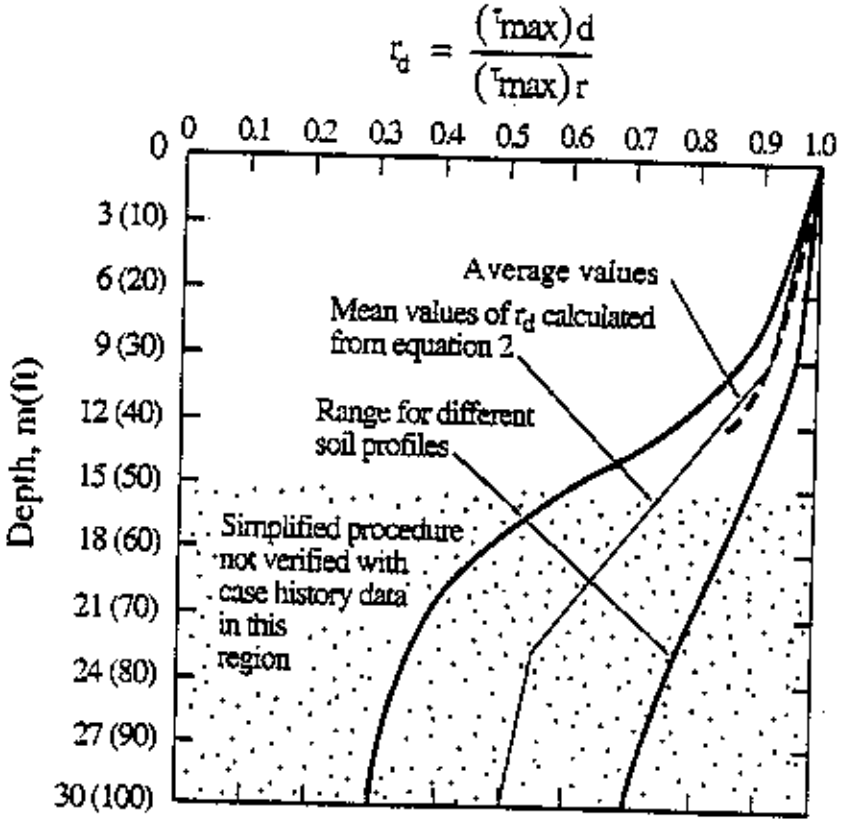


**Figure 5.1: $r_d$ Versus Depth Curves Developed by Seed and Idriss (1971) with Added Mean Value Lines from Equation 2**

(Summary report, [32])

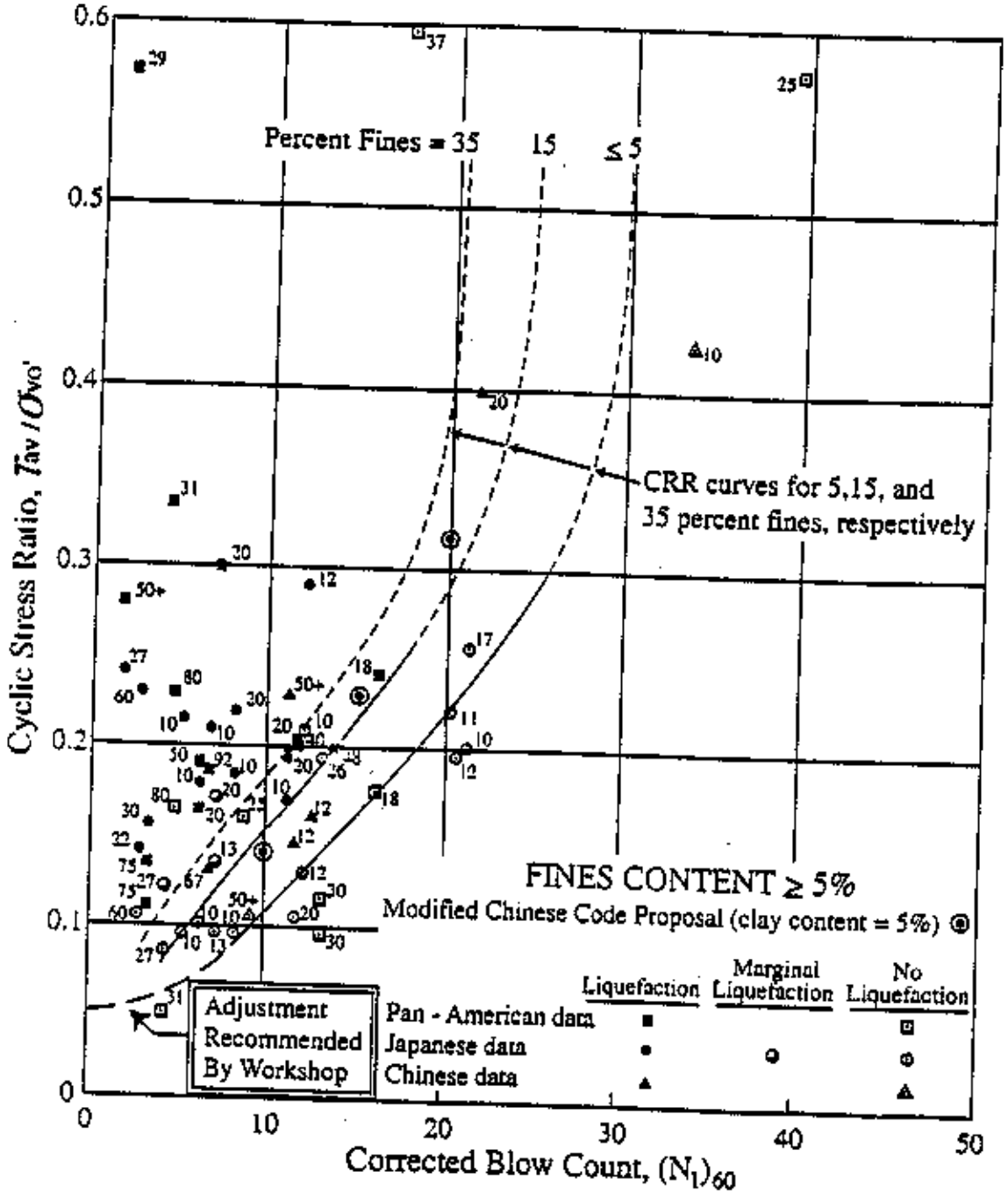


**Figure 5.2: Simplified Base Curve Recommended for Calculation of CRR from SPT Data along with Empirical Liquefaction Data (modified From Seed et al., 1985)**

(Summary report, [32] )

analyses by Liao et al. [33] and Youd and Noble [34]. Seed and Idriss [35] originally projected that curve through the origin, but there were few data to constrain the curve in the lower part of the plot. A better fit to the present empirical data is to bow the lower end of the base curve as indicated in Figure 5.2.

Thomas F. Blake (Summary report, [32]) approximated the simplified base curve plotted on Figure 5.2 by the following equation:

$$CRR_{7.5} = \frac{a + cx + ex^2 + gx^3}{1 + bx + dx^2 + fx^3 + hx^4} \qquad (5.4)$$

Where $CRR_{7.5}$ is the cyclic resistance ratio for magnitude 7.5 earthquakes; $x = (N_1)_{60}$; a = 0.048; b = 0.1248; c = 0.004721; d = 0.009578; e = 0.0006136; f = 0.0003285; g = -1.673E-05; and h = 3.714E-06. This equation is valid for $(N_1)_{60}$ less than 30 and may be used in spreadsheets and other analytical techniques to approximate the simplified base curve for engineering calculations.

### 5.3.2 CORRELATIONS FOR FINES CONTENTS

Another change was the quantification of the fines content correction to better fit the empirical data and to support computations with spreadsheets and other electronic computational aids. In the original development, Seed et al. [36] found that for a given $(N_1)_{60}$, CRR increases with increased fines content. It is not clear, however, whether the CRR increase is because of greater liquefaction resistance or smaller penetration resistance as a consequence of the general increase of compressibility and decrease of permeability with increased fines content. Based on the empirical data available, Seed et al. Developed CRR curves for various fines contents as shown on Figure 5.2.

After a lengthy review by the workshop participants, consensus was gained that the correction for fines content should be a function of penetration resistance as well as fines content. The participants also agreed that other grain characteristics, such as soil plasticity may affect liquefaction resistance; hence any correlation based solely on penetration resistance and fines content should be used with engineering judgment and caution. The following equations, developed by I.M. Idriss with assistance from R.B. Seed are

recommended for correcting standard penetration resistance determined for silty sands to an equivalent clean and penetration resistance:

$$(N_1)_{60cs} = \alpha + \beta(N_1)_{60} \tag{5.5}$$

where $\alpha$ and $\beta$ are coefficients determined from the following equations:

$$\alpha = 0 \quad \text{for FC} \leq 5\% \tag{5.6a}$$

$$\alpha = \exp[1.76-(190/FC^2)] \quad \text{for } 5\% < \text{FC} < 35\% \tag{5.6b}$$

$$\alpha = 5.0 \quad \text{for FC} \geq 35\% \tag{5.6c}$$

$$\beta = 1.0 \quad \text{for FC} \leq 5\% \tag{5.7a}$$

$$\beta = [0.99+(FC^{1.5}/1000)] \quad \text{for } 5\% < \text{FC} < 35\% \tag{5.7b}$$

$$\beta = 1.2 \quad \text{for FC} \geq 35\% \tag{5.7c}$$

where FC is the fines content measured from laboratory gradation tests on retrieved soil samples.

These equations may be used for routine liquefaction resistance calculations. Back calculation of CRR curves as a function of fines content and $N_1(60)_{60}$ for magnitude 7.5 earthquakes using Equations 5.5-5.7 yield curves that are essentially identical to the curves plotted on Figure 5.2.

### 5.3.3 OTHER CORRECTIONS

In addition to grain characteristics, several other factors affect SPT results. One of the more important of these factors is the energy delivered to the SPT sampler. An energy ratio, ER, of 60% has generally been accepted as the reference value. The ER delivered by a particular SPT setup depends primarily on the type of hammer and anvil in the drilling system and on the method of hammer release. Approximate correction factors ($C_E$ = ER/60%) to modify the SPT results to a 60% energy ratio for various types of hammers and anvils are listed in Table 5.1. Because of variations in drilling and testing equipment and differences in procedures used, a rather wide range in the energy correction factor, $C_E$, has been observed as noted in the table. Even when procedures are carefully monitored to conform to established standards, such as ASTM D-1686, considerable variation in $C_E$ may

**Table (5.1): Corrections to SPT Modified from Skempton, [32]**

| Factor | Equipment Variable | Term | Correction |
|---|---|---|---|
| Overburden Pressure | | $C_N$ | $(Pa/\sigma'_{vo})^{0.5}$ CN ≤ 2 |
| Energy ratio | Donut Hammer<br>Safety Hammer<br>Automatic-Trip Donut-Type Hammer | $C_E$ | 0.5 to 1.0<br>0.7 to 1.2<br>0.8 to 1.3 |
| Borehole diameter | 65 mm to 115 mm<br>150 mm<br>200 mm | $C_B$ | 1.0<br>1.05<br>1.15 |
| Rod length | 3 m to 4 m<br>4 m to 6 m<br>6 m to 10 m<br>10 to 30 m<br>> 30 m | $C_R$ | 0.75<br>0.85<br>0.95<br>1.0<br>< 1.0 |
| Sampling method | Standard sampler<br>Sampler without liners | $C_S$ | 1.0<br>1.1 to 1.3 |

occur because of minor variations in equipment and procedures. Even within a given borehole variations in energy ratio between hammer blows or between tests typically may vary by as much as ten percent. Thus, the recommended practice is to measure the energy ratio frequently at each site where the SPT is used. Where measurements can not be made, careful observation and notation of the equipment and procedures is required to estimate a $C_E$ value for use in liquefaction resistance calculations. Use of good-quality testing equipment and carefully controlled testing procedures conforming to ASTM D-1686 will generally yield more consistent energy ratios and $C_E$ values from the upper parts of the ranges listed in Table 5.1.

Additional correction factors are required for rod lengths less than 10 m and greater than 30 m, borehole diameters outside the recommended interval (65 mm to 125 mm), and sampling tubes without liners. Ranges of correction values for each of these variables are listed in Table 5.1. Careful documentation of drilling equipment and procedures, including measurement of ER, is required to select the most appropriate values for these correction factors. Even so, some uncertainty remains in the actual factors that should apply for any field operation.

Based the SPT N-value also varies with effective overburden stress, an overburden stress correction factor is also applied. This factor has commonly been calculated from the following equation [37]:

$$C_N = (P_a / \sigma'_{vo})^{0.5} \tag{5.8}$$

where $C_N$ is a factor to correct measured penetration resistance for overburden pressure and $P_a$ equals 100 kPa or approximately one atmosphere of pressure in the same units used for $\sigma'_{vo}$, applied in this equation should be the overburden pressure that was effective at the time the SPT test was conducted. Even though the ground water level may have changed and a different water table level applied in the calculation of CSR (Equation 5.1), the correction of blow count requires use of the effective pressures that were effective at the time of drilling and testing.

The SPT N-value corrected for each of the above variables is given by the following equation:

$$(N_1)_{60} = N_m C_N C_E C_B C_R C_S \tag{5.9}$$

where Nm is the measured standard penetration resistance, Ce is the correction for hammer energy ratio (ER), CB is a correction factor for borehole diameter, CR is the correction factor for rod length, and CS is the correction for samplers with or without liners. Suggested ranges of values for each of these correction factors are listed in Table 5.1. Selection of appropriate factors from within these ranges requires specific information on equipment and drilling procedures and engineering judgment.

A final change recommended by workshop participants is the use of revised magnitude scaling factors rather than the original [35] factors to adjust $CRR_{7.5}$ to CRR for other earthquake magnitudes. Magnitude scaling factors are addressed later in this part of the report.

## 5.4 SHEAR WAVE VELOCITY

During the past decade, several simplified procedures have been proposed for the use of field measurements of small-strain shear wave velocity, $V_S$, to assess liquefaction resistance of granular soils [38 through 43]. The use of $V_S$ and CRR are similarly influenced by void ratio, effective confining stresses, stress history, and geologic age.

### 5.4.1 CRITERIA FOR EVALUATING LIQUEFACTION RESISTANCE

Robertson et al. [40] proposed a stress-based liquefaction assessment procedure using field performance data from sites in the Imperial Valley, California. These investigators normalized $V_S$ by:

$$V_{S1} = V_S (P_a / \sigma'_{vo})^{0.25} \tag{5.10}$$

where Pa is a reference stress of 100 kPa, approximately atmospheric pressure, and $\sigma'_{vo}$ is effective overburden pressure in kPa. Robertson et al. Chose to modify $V_S$ in terms of $\sigma'_{vo}$ to follow the traditional procedures for modifying standard and cone penetration test resistances. The liquefaction resistance bound (CRR curve) determined by these investigators for magnitude 7.5 earthquakes is plotted on Figure 5.3a along with data calculated from several field sites where liquefaction did or did not occur. The cyclic stress

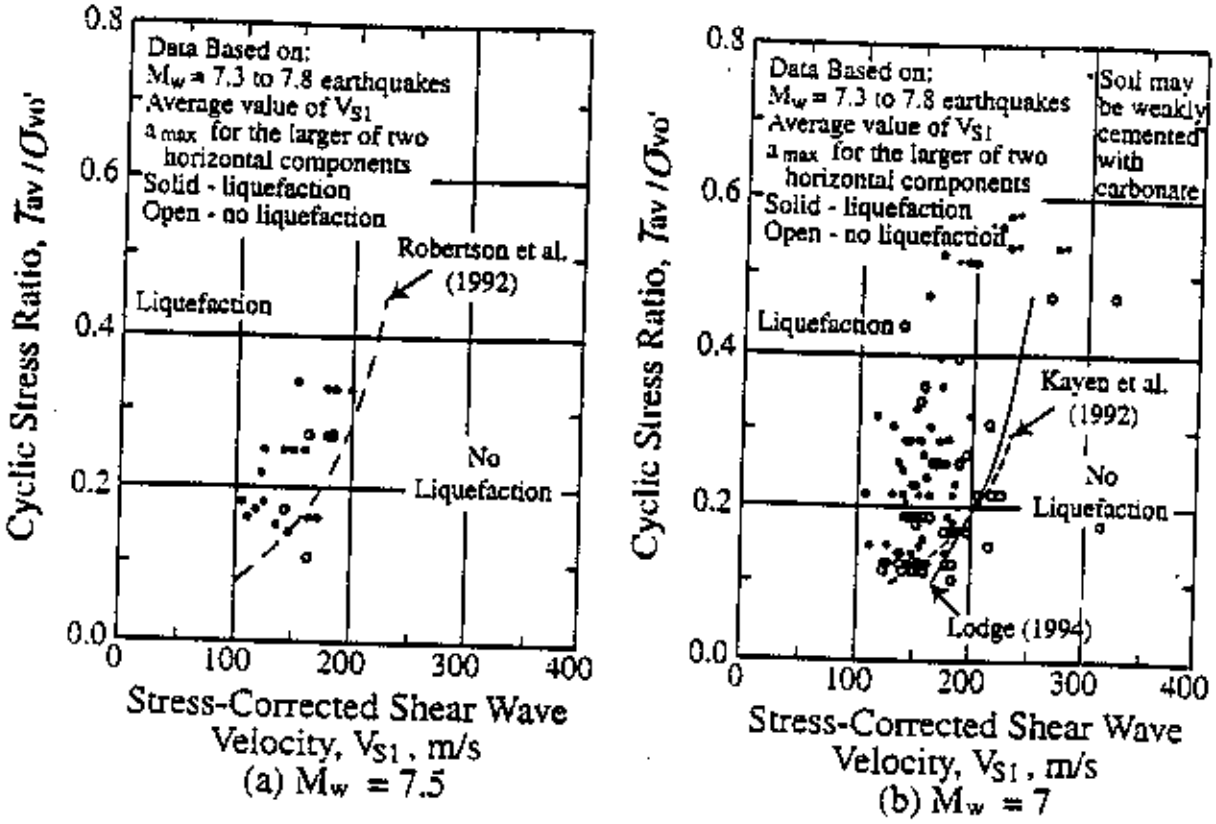


**Figure 5.3:** CSR Charts Based on Corrected Shear-Wave Velocities Suggested by (a) Robertson et al. [40], and (b) Kayen et al. [41] and Lodge [43] (Summary report, [42])

ratios were calculated using estimates of $a_{max}$ for the larger of two horizontal components of ground acceleration that would have occurred at the site in the absence of liquefaction.

Subsequent liquefaction resistance boundaries proposed by Kayen et al. [41] and Lodge [43] for magnitude 7 earthquakes are shown on Figure 5.3b. These curves are based on field performance data from the 1989 Loma Prieta earthquake. With few exceptions, the liquefaction case histories are bounded by the relationships proposed by these suggested bounds. The relationship proposed by Lodge [43] provides a conservative lower boundary for liquefaction case histories with $V_{S1}$ less than about 200 m/s. The relationship by Robertson et al. [40] is the least conservative of the three. Professor Ricardo Dobry suggested a relationship between cyclic resistance ratio and $V_{S1}$ for constant average cyclic shear strain, $\gamma_{av}$, of the form:

$$CRR = \tau_{av} / \sigma'_{vo} = f(\gamma_{av}) V_{S1}^2 \qquad (5.11)$$

where $\gamma_{av}$ is constant average shear strain. This formula supports a CRR bound passing through the origin and provides a rational approach for extrapolating beyond the limits of the available field performance data, at least for lower values of $V_{S1}$ ($V_{S1} \leq 125$ m/s).

For higher values of $V_{S1}$, Andrus and Stokoe [44] reason that the CRR bound should become asymptotic to some limiting $V_{S1}$ value. This limit is caused by the tendency of dense granular soils to exhibit dilative behavior at large strains. Thus Equation 11 is modified to:

$$\tau_{av} / \sigma'_{vo} = CRR = a(V_{S1} / 100)^2 + b / (V_{S1}) - b / V_{S1c} \qquad (5.12)$$

where $V_{S1c}$ is the critical value of $V_{S1}$, which separates contractive and dilative behavior, and a and b are curve fitting parameters.

Using the relationship between $V_{S1}$ and CRR expressed by Equation 5.12, Andrus and Stokoe drew curves to separate data from sites where liquefaction effects were and were not observed. Best fit values for the constants a and b were 0.03 and 0.9, respectively, for magnitude 7.5 earthquakes. Andrus and Stokoe also determined the following best-fit values for $V_{S1c}$.

$V_{S1c}$ = 220 m/s for sands and gravels with fines contents less than 5%

$V_{S1c}$ = 210 m/s for sands and gravels with fines contents of about 20%

$V_{S1c}$ = 200 m/s for sands and gravels with fines contents greater than 35%

Figure 5.4 presents CRR boundaries recommended by Andrus and Stokoe for magnitude 7.5 earthquakes and uncemented Holocene-age soils with various fines contents. Although these boundaries pass through the origin, natural alluvial sandy soils with shallow water tables rarely have corrected shear wave velocities less than 100 m/s, even near ground surface. For a $V_{S1}$ of 100 m/s and a magnitude 7.5 earthquake, the calculated CRR is 0.03. This minimal CRR value is generally consistent with intercept CRR values for the CPT and SPT procedures.

Equation 5.12 can be scaled to other magnitude values through use of magnitude scaling factors. These factors are discussed in a later section.

## 5.5 MAGNITUDE SCALING FACTORS

In developing the simplified procedure, Seed and Idriss [35] compiled a sizable data base from sites where liquefaction did or did not occur during earthquakes with magnitudes near 7.5. Analyses were made of these data to calculate cyclic stress ratios (CSR) and $(N_1)_{60}$ values for various sites where surface effects of liquefaction were or were not observed. Results from clean sand sites (fines content $\leq$ 5 percent) were plotted on a CSR versus $(N_1)_{60}$ plot. An updated version of that plot (Seed et al. [36]) is reproduced in Figure 5.2. A deterministic curve was drawn through the plot to separate regions with data indicative of liquefaction (solid symbols) from regions with data indicative of nonliquefaction (open symbols). Where there was a mixture of data, the curve was conservatively placed to ensure that data indicative of liquefaction plot above or to the left of the bounding curve. This curve, termed the simplified base curve or $CRR_{7.5}$ curve, is relatively well constrained by empirical data between CSR of 0.08 and 0.35 and is logically extrapolated to higher and lower values beyond that range. As shown in Figure 5.2, the workshop participants recommend bowing the lower part of the simplified base curve to intersect the ordinate of the plot at a CRR of about 0.05.

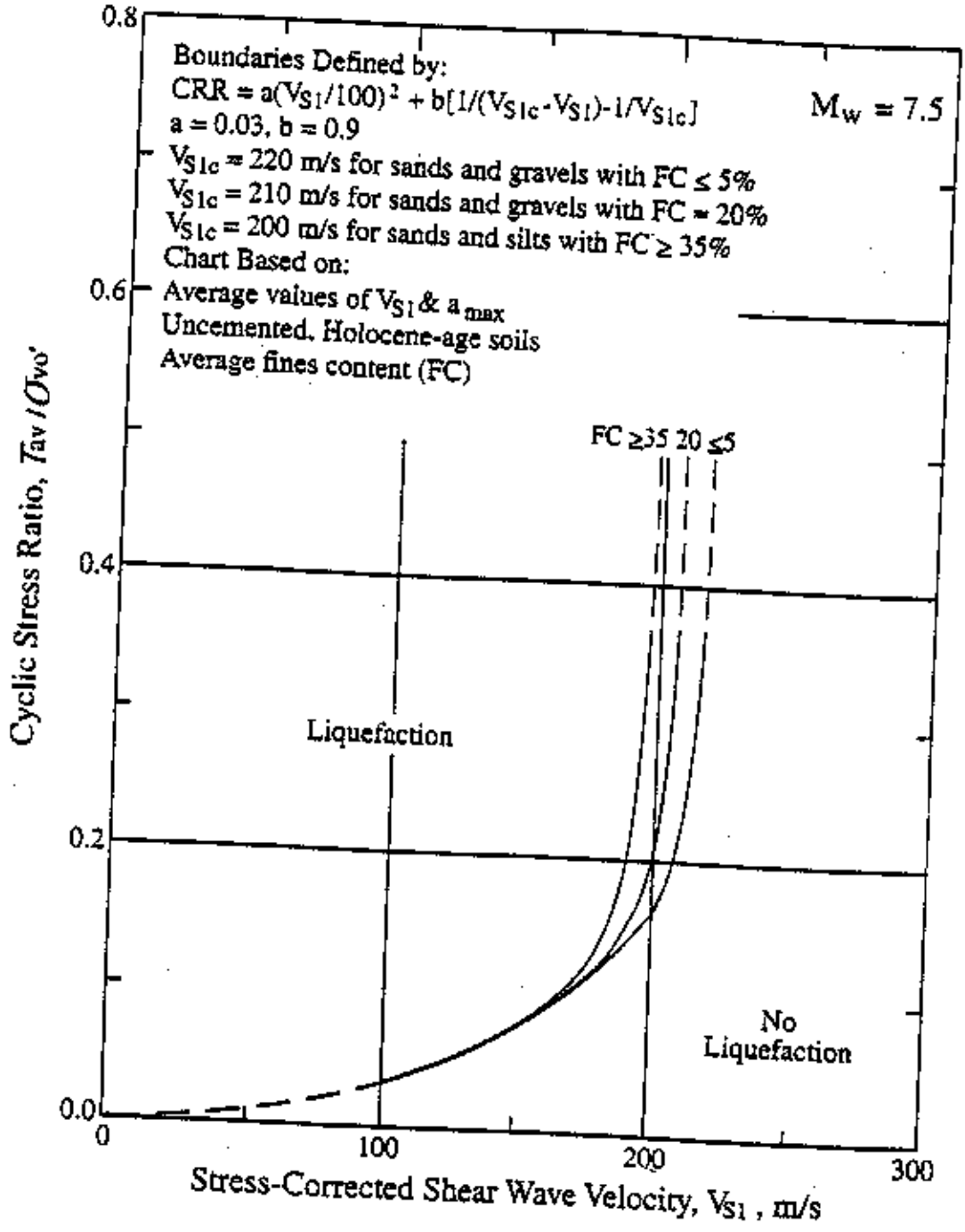


**Figure 5.4: Curves Recommended by Workshop for Calculation of CRR from Corrected Shear Wave Velocity (Summary report, [32] )**

To adjust the simplified base curve to magnitudes smaller or larger than 7.5, Seed and Idriss [35] introduced correction factors called "magnitude scaling factors." These factors are used to scale the simplified base curve upward or downward on the CSR versus $(N_1)_{60}$ plot. Conversely, magnitude weighting factors, which are the inverse of magnitude scaling factors, may be applied to correct CSR for magnitude. Either correcting CRR via magnitude scaling factors, or correcting CSR via magnitude weighting factors, leads to the same final result. Because the original papers by Seed and Idriss were written in terms of magnitude scaling factors, the use of magnitude scaling factors is continued in this report.

To illustrate the influence of magnitude scaling factors on calculated hazard, the equation for factor of safety (FS) against liquefaction can be written in terms of CRR, CSR, and MSF as follows:

$$FS = (CRR_{7.5} / CSR)MSF \tag{5.13}$$

where $CRR_{7.5}$ is the cyclic resistance ratio determined for magnitude 7.5 earthquakes using Figure 5.2 or Equation 5.4 for SPT data or Figure 5.4 or Equation 5.12 for $V_{S1}$ data. Equation 5.13 demonstrates that the factor of safety against development of liquefaction at a site is directly proportional to the magnitude scaling factor selected.

**Seed and Idriss [35] Scaling Factors**

Because of the limited empirical data available in the 1970s, Seed and Idriss [35] were unable to narrowly constrain bounds between liquefaction and nonliquefaction regions on CRR plots for magnitudes other than 7.5. Consequently, they based their scaling factors on representative loading cycles and laboratory test results. From a study of strong-motion accelerograms, the number of representative loading cycles generated by an earthquake was correlated with earthquake magnitude. For example, magnitude 7.5 earthquakes were characterized by 15 loading cycles, whereas, magnitude 8.5 earthquakes were characterized by 26 loading cycles, and magnitude 6.5 earthquakes by 10 loading cycles. Second, laboratory tests were conducted to measure the number of loading cycles required to generate liquefaction and five percent cyclic strain. Laboratory tests were conducted using a variety of clean sands, void ratios, and ambient stress conditions. From these tests, a single representative curve was developed that relates cyclic stress ratio to the number of loading cycles required to generate liquefaction (Figure 5.5). By dividing CSR values from

this curve for various numbers of cycles, representative of various earthquake magnitudes, by the CSR for 15 cycles (magnitude 7.5), the initial set of magnitude scaling factors was derived. These scaling factors are listed in Column 2 of Table 5.2 and are plotted on Figure 5.6. These magnitudes scaling factors have been routinely applied in engineering practice since their introduction in 1982.

**Idriss Scaling Factors**

In preparing his H.B. Seed memorial lecture, I.M. Idriss reevaluated the data that he and the late Professor Seed had used to calculate the original 1982 magnitude scaling factors. In so doing, Idriss re-plotted the data on a log-log plot and found that the data plotted as a straight line. He further noted that one outliner point had strongly influenced the original analysis, causing the original plot to be nonlinear and characterized by unduly low values for magnitudes less than 7.5. Based on this reevaluation, Idriss defined a new set of magnitude scaling factors. These factors are listed in Column 3 of Table 5.2, plotted on Figure 5.6 and are defined by the following equation:

$$MSF = 10^{2.24} / M^{2.56} \qquad (5.14)$$

Idriss recommends these revised scaling factors for use in engineering practice in place of the original factors.

The revised scaling factors are significantly larger than the original scaling factors for magnitudes less than 7.5 and somewhat smaller than the original factors for magnitudes greater than 7.5. Relative to the original scaling factors, the revised factors lead to a reduced calculated liquefaction hazard for magnitudes less than 7.5 and increased calculated hazard for magnitudes greater than 7.5.

**Andrus and Stokoe Scaling Factors**

From their studies of liquefaction resistance as a function of shear wave velocity, $V_s$, Andrus and Stokoe (Summary report [32]) developed Equation 12 for calculating CRR from $V_s$ for magnitude 7.5 earthquakes. Using this equation, Andrus and Stokoe drew curves on graphs with plotted values of CSR as a function of $V_{S1}$ from sites where surface effects of liquefaction were or were not observed. Graphs were plotted for sites shaken by magnitude 6, 6.5, 7, and 7.5 earthquakes. The positions of the CRR curves were visually

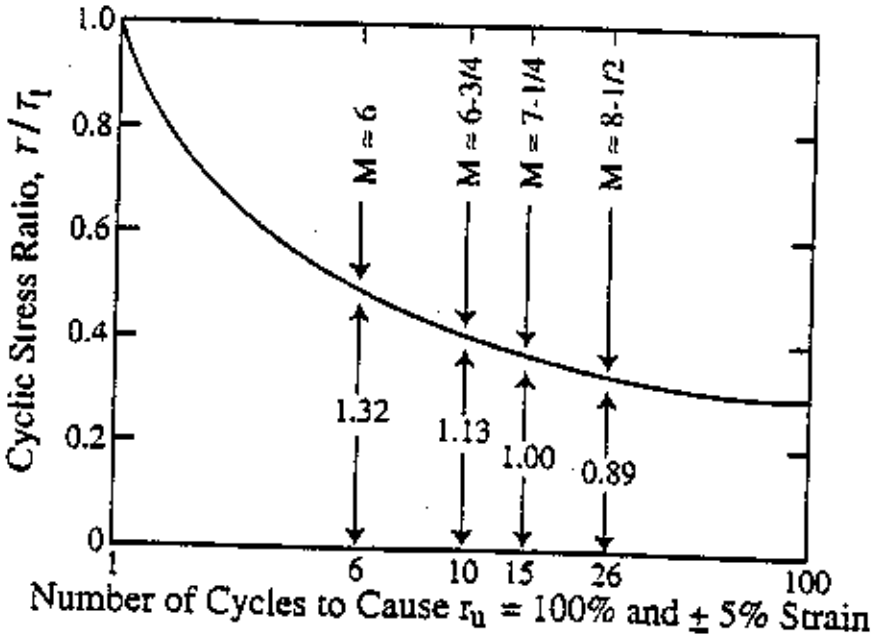


**Figure 5.5: Representative Relationship Between CSR and Number of Cycles To Cause Liquefaction and (After Seed and Idriss, [35])**

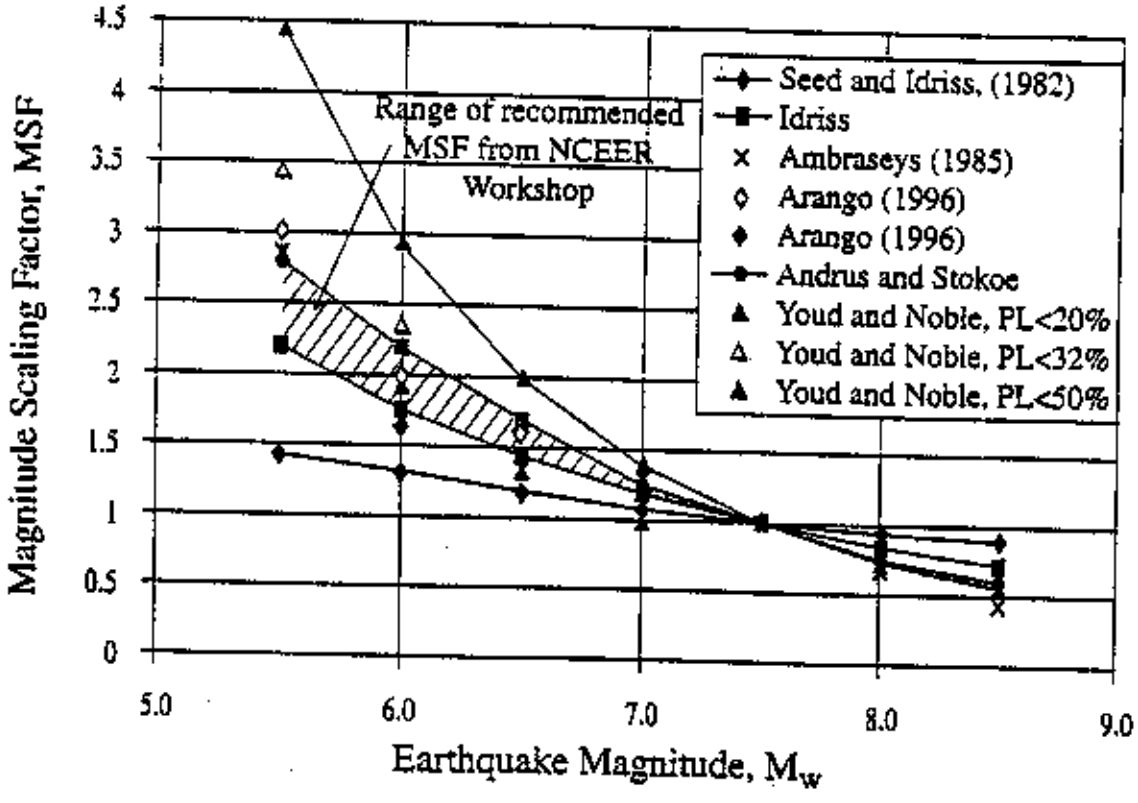


**Figure 5.6: Magnitude Scaling Factors Derived by Various Investigators (Summary report, [32])**

adjusted on each graph until a best fit bound was obtained. Magnitude scaling factors were then estimated by taking the ratio of CRR for a given magnitude to the CRR for magnitude 7.5 earthquakes. These MSF were then fitted to the following exponential function.

$$MSF = (M_w / 7.5)^{-3.3} \tag{5.15}$$

Values for magnitude less than 6 and greater than 7.5 were extrapolated from this equation. MSF values from this analysis are listed in Column 7, Table 5.2, and plotted on Figure 5.6. For magnitudes less than 7.5, the MSF proposed by Andrus and Stokoe are rather close in value (within about 5 percent) to the MSF proposed by Ambraseys. For magnitudes greater than 7.5, the Andrus and Stokoe MSF are slightly smaller than the revised MSF proposed by Idriss.

**Youd and Noble Scaling Factors**

Youd and Noble [34] used a logistic analysis to analyze case history data from sites where effects of liquefaction were or were not reported following past earthquakes. This analysis yielded the following probabilistic equation:

$$Logit(P_L) = In(P_L) = -7.633 + 2.256M_w - 0.258(N_1)_{60cs} + 3.095InCRR \tag{5.16}$$

where $P_L$ is the probability that liquefaction occurred, $1-P_L$ is the probability that liquefaction did not occur, and $(N_1)_{60cs}$ is the corrected blow count, including the correction for fines content. Youd and Noble recommend direct application of this equation to calculate the CRR for a given probability of liquefaction occurrence. In lieu of direct application, Youd and Noble define MSF for use with the simplified procedure. These MSF were developed by rotating the simplified base curve to near tangency with the probabilistic curves for PL of 50%, 32%, and 20% and various earthquake magnitudes. These MSF are defined as the ratio of the ordinate of the rotated base curve at the point of near tangency to the ordinate of the unrotated simplified base curve at the same $(N_1)_{60cs}$. Because the rotated simplified base curves lie entirely below the given probability curve, CRR calculated with these MSF are characterized by smaller probability of liquefaction occurrence than the associated probabilistic curves. Thus the MSF listed in Columns 8, 9, and 10 (Table 5.2), are denoted by $P_L<50\%$, $P_L<32\%$, and $P_L<20\%$, respectively. Because the derived MSF are less than 1.0, Youd and Noble do not recommend use of MSF for $P_L<32\%$ and $P_L<20\%$ for

**Table (5.2):** Magnitude Scaling Factor Values Defined by Various Investigators (Summary report, **[32]** )

| Mag-nitude, M | Seed and Idriss (1982) | Idriss | Ambra-seys (1988) | Arango (1996) | | Andrus and Stokoe (in press) | Youd and Noble (this report) | | |
|---|---|---|---|---|---|---|---|---|---|
| (1) | (2) | (3) | (4) | (5) | (6) | (7) | $P_L<$ 20% (8) | $P_L<$ 32% (9) | $P_L<$ 50% (10) |
| 5.5 | 1.43 | 2.20 | 2.86 | 3.00 | 2.20 | 2.8 | 2.86 | 3.42 | 4.44 |
| 6.0 | 1.32 | 1.76 | 2.20 | 2.00 | 1.65 | 2.1 | 1.94 | 2.35 | 2.92 |
| 6.5 | 1.19 | 1.44 | 1.69 | 1.60 | 1.40 | 1.6 | 1.34 | 1.66 | 1.99 |
| 7.0 | 1.08 | 1.19 | 1.30 | 1.25 | 1.10 | 1.25 | 1.00 | 1.20 | 1.39 |
| 7.5 | 1.00 | 1.00 | 1.00 | 1.00 | 1.00 | 1.00 | | | 1.00 |
| 8.0 | 0.94 | 0.84 | 0.67 | 0.75 | 0.85 | 0.8? | | | 0.73? |
| 8.5 | 0.89 | 0.72 | 0.44 | | | 0.65? | | | 0.56? |

earthquakes with magnitudes greater than 7.0. Equations for defining the Youd and Noble MSF are listed below.

$$\text{Probability, } P_L < 20\% \text{ MSF} = 10^{3.81}/M^{4.53} \quad \text{For } M < 7 \tag{5.17}$$

$$\text{Probability, } P_L < 32\% \text{ MSF} = 10^{3.74}/M^{4.33} \quad \text{For } M < 7 \tag{5.18}$$

$$\text{Probability, } P_L < 50\% \text{MSF} = 10^{4.21}/M^{4.81} \quad \text{For } M < 7.75 \tag{5.19}$$

**Ambraseys Scaling Factors**

Field performance data collected since the 1970s for magnitudes less than 7.5 indicate that the original Seed and Idriss [35] scaling factors may be overly conservative. For example, Ambraseys [45] analyzed liquefaction data compiled through the mid-1980s and plotted calculated cyclic stress ratios for sites that did or did not liquefy on CSR versus $(N_1)_{60}$ plots. From these plots, Ambraseys developed empirical exponential equations that define CRR as a function of $(N_1)_{60}$ and moment magnitude, Mw. By holding the value of $(N_1)_{60}$ constant in the equations and taking the ratio of CRR determined for various magnitudes of earthquakes to the CRR for a magnitude 7.5 earthquakes. Ambraseys derived the magnitude scaling factors listed in Column 4 of Table 5.2. These factors are also plotted on Figure 5.6. For magnitudes less than 7.5, the MSF suggested by Ambraseys are significantly greater than both the original factors developed by Seed and Idriss (Column 2, Table 5.2) and the revised factors by Idriss (Column 3). Because they are based on observational data, these factors have validity for estimating liquefaction hazard; however, they have not been widely used in engineering practice. Conversely, for magnitudes greater than 7.5 , Ambraseys factors are significantly lower than the original (Seed and Idriss, [35]) and Idriss's revised scaling factors. Because there are little data to constrain Ambraseys' scaling factors for magnitudes greater than 7.5, these factors are uncertain, are likely overly conservative, and are not recommended for engineering practice.

**Arango Scaling Factors**

Arango [46] developed two sets of magnitude scaling factors. The first set (Column 5, Table 5.2) is based on farthest observed liquefaction effects from the seismic energy source, the estimated average peak accelerations at those distant sites, and the absorbed seismic energy required to cause liquefaction. The second set (Column 6, Table 5.2) was

developed from energy concepts and the relationship derived by Seed and Idriss [35] between numbers of significant stress cycles and earthquake magnitude. The MSF listed in Column 5 are similar in value (within about 10%) to the MSF of Ambraseys (Column 4), and the MSF listed in Column 6 are similar in value (within 6%) to the revised MSF proposed by Idriss (Column 3).

## 5.6 RECOMMENDATIONS FOR ENGINEERING PRACTICE

The workshop participants reviewed the MSF listed in Table 5.2 and all but one (S.S.C. Liao) agree that the original factors were too conservative and that an increase is warranted for engineering practice for magnitudes less than 7.5. Rather than recommending a single set of factors, the workshop participants suggest a range of MSF with the engineer allowed to choose factors from within that range requisite with the conservatism required for the given application. For magnitudes less than 7.5, the lower bound for the recommended range is the revised set of magnitude scaling factors proposed by Idriss (Column 3, Table 5.2, or Equation 5.12). The upper bound for the suggested range is the MSF proposed by Andrus and Stokoe (Column 7, Table 5.2, or Equation 5.15). The upper bound values are consistent with MSF suggested by Ambraseys, Arango, and Youd and Noble for $P_L$<20% (generally within about 10 percent).

For magnitudes greater than 7.5, the factors recommended by Idriss (Column 3, Table 5.2; Equation 5.14 should be used for engineering practice. Above magnitude 7.5, these factors are smaller than the original Seed and Idriss [35] factors, and hence application of the new factors leads to increased calculated liquefaction hazard compared to the original factors. The reasoning for this recommendation is that the original factors by Seed and Idriss [35] may not have been sufficiently conservative for magnitudes greater than 7.5. There are insufficient case history data for earthquakes with magnitudes greater than 8 to support use of the lower MSF values listed in Table 5.2. These lower values were generally extrapolated from smaller magnitude earthquakes. Thus, these more conservative MSF are not recommended for engineering practice.

## 5.7 CORRECTIONS FOR HIGH OVERBURDEN PRESSURES, STATIC SHEAR STRESSES, AND AGE OF DEPOSIT

The correction factors $K_\sigma$ and $K_\alpha$ were developed by Seed [47] to adjust cyclic resistance ratios (CRR) to static overburden and shear stresses larger than those embodied in the development of the simplified procedure. As noted, the simplified procedure is only valid for level to gently sloping sites (low static shear stress) and depths less than about 15 m (low overburden pressures). The $K_\sigma$ correction factor extends cyclic ratios to high overburden pressures, while the $K_\alpha$ correction factor allows extension of the simplified procedure to more steeply sloping ground conditions. Because there are virtually no case histories available to help define these correction factors, the results from laboratory test programs have been used to develop corrections for engineering practice.

### $K_\sigma$ Correction Factor

Cyclically loaded, isotropically consolidated triaxial compression tests show that while liquefaction resistance of a soil increases with increasing confining pressure, the resistance, as measured by the cyclic stress ratio, is a nonlinear function that decreases with increased normal stress. To incorporate the nonlinear effect of decreasing cyclic stress ratio with increasing confining pressure, Seed [47] recommended incorporation of a correction factor, $K_\sigma$, for overburden pressures greater than 100 kPa. This factor allows correction of results obtained from the simplified procedure to overburden pressures that are greater than those generally found in the observational data base from which the procedure was derived. Because of the lack of case history data, extrapolation of the simplified procedure to depths greater than 15 m using $K_\sigma$ factors yields results, such as factors of safety, that are less certain than at shallower depths.

The $K_\sigma$ values developed by Seed [47] were obtained by normalizing cyclic resistance ratios of isotropically consolidated cyclic triaxial compression tests to CRR values associated with an effective confining pressure of 100 kPa. For confining pressures greater than 100 kPa, the $K_\sigma$ correction factor is less than one and decreases with increasing pressure. The original analyses by Seed [47] yielded a band of suggested $K_\sigma$ factors that decreased approximately linearly with effective overburden pressure from a value of 1.0 at 100 kPa to values ranging from about 0.40 to 0.65 at 800 kPa (Figure 5.7). Seed and

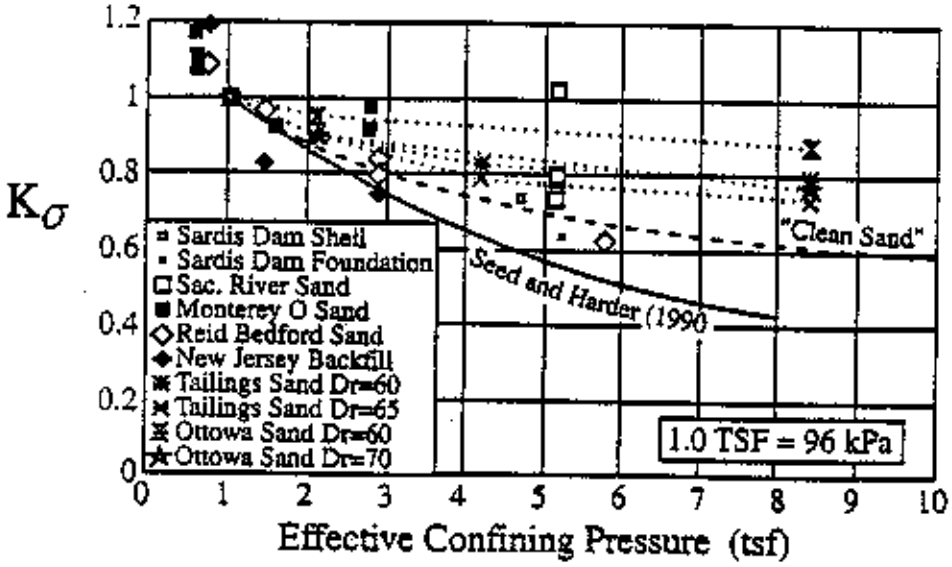


**Figure 5.7:** $K_o$ **values determined by various investigators (After Seed and Harder, [48])**

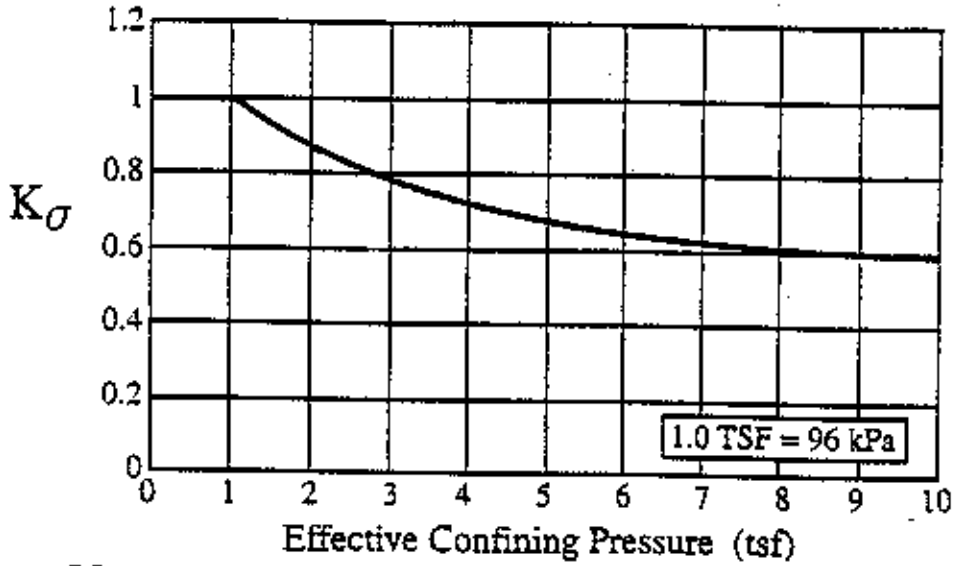


**Figure 5.8: Minimum Values for $K_o$ Recommended for Clean and Silty Sands and Gravels (After Harder and Boulanger, [52]).**

Harder [48] analyzed additional data and suggested generally lower values that are defined by a single concave curve with a $K_\sigma$ value of 0.44 at an effective confining pressure of 800 kPa. Vaid et al. [49] and Vaid and Thomas [50] performed constant-volume cyclic simple shear tests on clean sands and derived smaller decreases in $K_\sigma$. From tests on mine-tailing, Ottawa, and Frazer Delta sands (Figure 5.7), several investigators (Byrne and Harder, [51]; Arango, [46]) calculated values for $K_\sigma$ ranging from about 0.75 to 0.90 for effective overburden pressures of 1,000 kPa to minimal values of 0.67 for effective overburden pressures as great as 2,600 kPa. These analyses indicate that lower relative densities generally produced higher $K_\sigma$ values. The various analyses confirm the considerable variability in derived $K_\sigma$ values, and that the factors developed by Seed and Harder were overly conservative.

Based on the above discussion and a review of test results presented by Harder and Boulanger [52], the workshop participants gained consensus that the Seed and Harder $K_\sigma$ values were too conservative and that an increase is recommended for general engineering practice. Based on this review, the workshop recommended $K_\sigma$ values represented by the curve in Figure 5.8 as minimal values for engineering practice for both clean and silty sands and for gravels.

**$K_\sigma$ Correction Factor for Sloping Ground**

Sloping ground induces static shear within the body of a soil mass before the onset of earthquake shaking. The relative magnitude of the static shear, $\tau_{st}$, on the horizontal plane can be assessed by normalizing it with respect to the effective vertical stress, $\sigma'_{vo}$. The resulting parameter is called the alpha ratio, where $\alpha = \tau_{st}/\sigma'_{vo}$. For level ground conditions, the alpha ratio is zero. Early researchers suggested that the presence of a static shear stress always improved the cyclic resistance of a soil because higher cyclic shear stresses were required to cause stress reversal. This conclusion is true for dense soils under relatively low confining pressures. However, loose soils and some soils under high confining pressures have lower liquefaction resistance under the influence of initial static shear stresses than in the absence of these stresses. This behavior is due to the potential strain softening nature of very loose soils.

To incorporate the effect of static shear stresses on liquefaction resistance of soils, Seed [47] recommended use of a correction factor $K_\alpha$. This factor is used to correct results obtained from the simplified procedure for level ground to sloping ground sites with constant static shear stress.

For the workshop Harder and Boulanger [52] reviewed past publications, tests, and analyses relative to Kα. They concluded that the wide ranges in potential $K_\alpha$ values developed by past investigators indicate a lack of consensus and a need for continued research and field verification of the effects of static shear stress on liquefaction resistance. Different rates of pore pressure generation and different limiting values for excess pore pressure at different locations within a slope make liquefaction analyses for sloping ground conditions extremely complicated.

The workshop participants agreed that the evaluation of liquefaction resistance beneath sloping ground or embankments (slopes greater than about six percent) is not well understood and that such evaluations are beyond rountine application of the simplified procedure. Although curves relating $K_\alpha$ to $\alpha$ have been published (Harder and Boulanger), the participants concluded that general recommendations for use of $K_\alpha$ by the engineering profession is not advisable at this time.

**Influence of Age of Deposit**

Several investigators have shown that liquefaction resistance of soils increases with age. For example, Seed [52] observed significant increases in liquefaction resistance with age of reconstituted sand specimens tested in the laboratory. Cyclically loaded tests were conducted on freshly reconstituted sand specimens and on similar sand specimens at periods ranging up to one hundred days. Increases of as much as 25 percent in cyclic resistance ratio were noted between the freshly constituted and the 100-day-old specimens. Youd and Hoose [54] and Youd and Perkins [28] note that liquefaction resistance increases markedly with geologic age. Sediments deposited within the past few hundred years are generally much more susceptible to liquefaction than older Holocene sediments; Pleistocene sediments are even more resistant; and Pre-Pleistocene sediments are essentially insusceptible to liquefaction. Although qualitative increases in liquefaction resistance have

been well documented insufficient quantitative data have been assembled from which correction factors for age can be defined.

The age, and concomitantly the liquefaction resistance, of naturally sedimented deposits generally increases with depth. In natural soils, this increase may partially or wholly counteract the influence of the $K_\sigma$ factor which generates an apparent decreases in liquefaction resistance with depth. In the absence of quantitative correction factors for age, engineering judgment is required in assessing liquefaction resistance of sediments older than a few thousand years old, knowledgeable engineers have ignored the $K_\sigma$ factor as partial compensation for unquantifiable, but known increases in liquefaction resistance with age. For man-made structures, such as thick fills and embankment dams, aging effects are generally minimal and should be ignored in calculating liquefaction resistance.

Application of the simplified procedure for evaluating liquefaction resistance requires estimates of earthquake magnitude and peak horizontal ground acceleration. In the procedure, these factors characterize duration and intensity of ground shaking, respectively. The workshop addressed the following questions with respect to selection of magnitude and peak acceleration.

## 5.8 EARTHQUAKE MAGNITUDE

Records from past earthquakes indicate that the relationship between duration and magnitude is rather uncertain and that factors other than magnitude influence duration. For example, unilateral faulting, in which rupture begins at one end of the fault and propagates to the other, usually produces longer shaking duration for a given magnitude than bilateral faulting, in which slip begins near the midpoint on the fault and propagates in both directions. Duration also generally increases with distance from the seismic energy source and may vary with site conditions and with bedrock topography (basin effects). The workshop addressed the following questions with respect to the use of magnitude as an index for shaking duration, and developed the following consensus answers.

**Question:** Should correlations or correction factors be developed to adjust duration of shaking to account for the influence of earthquake source mechanism and other factors?

**Answer:** Faulting characteristics and variations in shaking duration are difficult to predict in advance of an earthquake event. The influence of distance is generally of secondary importance within the range of distances to which potentially damaging effects of liquefaction commonly develop. Basin effects are not yet sufficiently predictable to be adequately accounted for in engineering practice. Thus workshop participants recommend continued use of conservative relationship between magnitude and duration embodied in the simplified procedure for routine evaluation of liquefaction resistance.

**Question:** Which magnitude scale should be used by engineers in selecting a magnitude for use in liquefaction resistance analyses?

**Answer:** Seismologists commonly calculate earthquake magnitudes using five different scales: (1) local or Richter magnitude, $M_L$; (2) surface-wave magnitude, $M_s$; short-period body-wave magnitude $m_b$; (4) long-period body-wave magnitude $m_B$ and (5) moment magnitude, $M_w$. Moment magnitude is the scale most commonly used for engineering applications and is the scale preferred for calculation of liquefaction resistance. As shown on Figure 5.9, magnitudes from other scales may be substituted directly from Mw within the following limits: $M_L < 6$, $m_B < 7.5$, and $6 < M_s < 8$. $M_b$, a scale commonly applied in the eastern US, may be used for magnitudes between 5 and 6, provided such magnitudes are corrected to $M_w$ using the curves plotted in Figure 5.9 (Idriss, [55]).

## 5.9 PEAK ACCELERATION

In the simplified procedure, peak horizontal acceleration ($a_{max}$) is used to characterize the intensity of ground shaking. To provide guidance for estimation of $a_{max}$, the workshop addressed the following questions.

**Question:** What procedures are preferred for estimating $a_{max}$ at potentially liquefiable sites?

**Answer:** The following three methods, in order of preference, may be used for estimating $a_{max}$:

(1) The preferred method of estimating $a_{max}$ at a site is through application of empirical correlations for attenuation of $a_{max}$ as a function of earthquake magnitude, distance from the seismic energy source, and local site conditions. Several correlations have

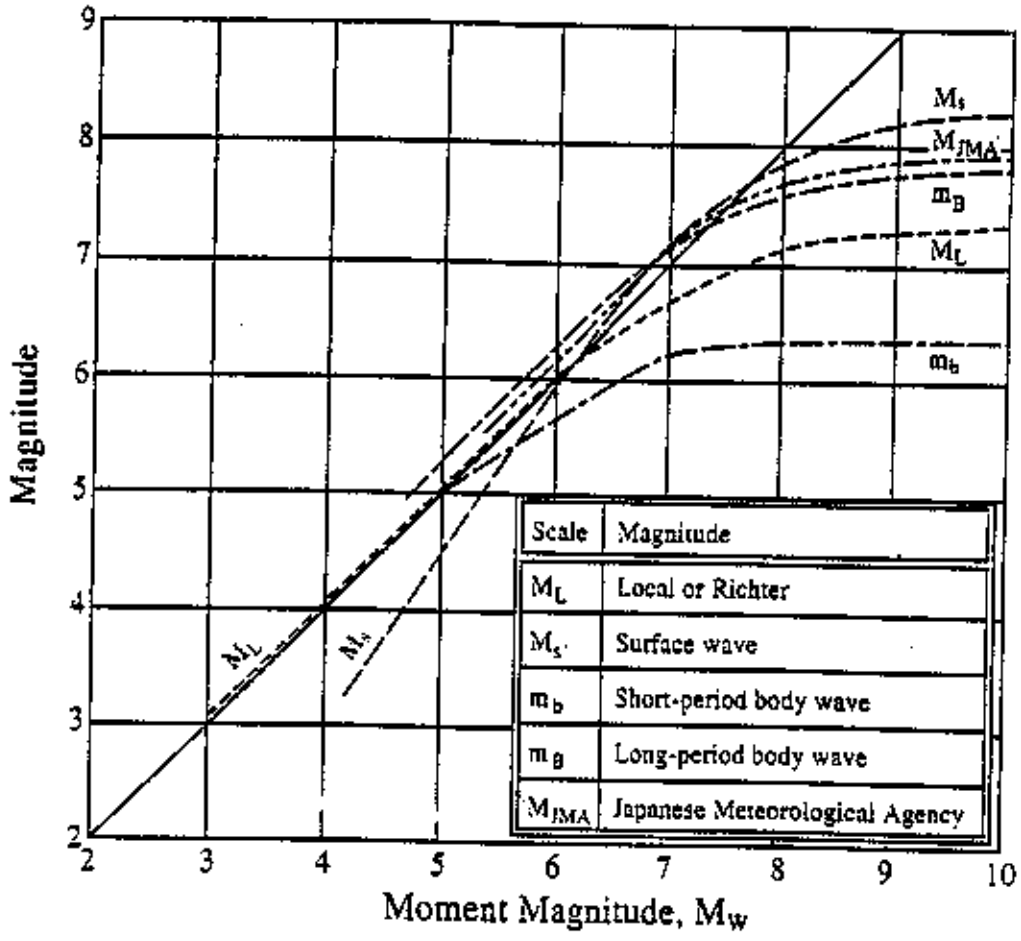


**Figure 5.9: Relationship between Moment, $M_w$, and Other Magnitude Scales [57].**

been developed for estimating $a_{max}$ for sites on bedrock or stiff to moderately stiff soils. Preliminary attenuation relationships have also been developed for soft soil sites (Idriss, [56]). Selection of an attenuation relationship should be based on factors such as region of the country, type of faulting, site condition, etc.

(2) For soft sites and other soil profiles that are not compatible with available attenuation relationships $a_{max}$ may be estimated from local site response analyses. Computer programs such as SHAKE, DESRA, etc., may be used for these calculations. Input ground motions in the form of recorded accelerograms are preferable to synthetic records. Accelerograms derived from white noise should be avoided. A suite of plausible earthquake records should be used in the analyses, including as many records as feasible from earthquakes with similar magnitudes, source distances, etc.

(3) The third and least desirable method for estimating peak ground acceleration is through amplification ratios, such as those developed by Idriss [56, 58], Seed et al. [59], and NEHRP [60]. These factors use a multiplier or ratio by which bedrock outcrop motions are amplified to estimate motions at ground surface. Because amplification ratios are influenced by strain level, earthquake magnitude, and perhaps frequency content, caution and considerable engineering judgment are required in the application of these relationships.

**Question:** Which peak acceleration should be used? (a) the largest horizontal acceleration recorded on a three-component accelerogram; (b) the geometric mean (square root of the product) of the two maximum horizontal components; or (c) a vectorial combination of horizontal accelerations.

**Answer:** According to I.M. Idriss (oral communication at workshop), where recorded motions were available, the larger of the two horizontal peak components of acceleration were used in the original development of the simplified procedure. Where recorded values were not available, which was the circumstance for most sites in the data base, peak acceleration values were estimated from attenuation relationships based on the geometric mean of the two orthogonal peak horizontal accelerations. In nearly all instances where recorded motions were used, the peaks from the two horizontal records were approximately equal. Thus where a single peak was used that peak and the geometric mean of the two

peaks were about the same value. Based on this information, the workshop participants concurred that use of the geometric mean is more consistent with the derivation of the procedure and is preferred for use in engineering practice. However, use of the larger of the two orthogonal peak accelerations would be conservative and is allowable. Vectorial accelerations are seldom calculated and should not be used. Peak vertical accelerations are ignored for calculation of liquefaction resistance.

**Question:** Liquefaction usually develops at soil sites where ground motion amplification may occur and where sediments may soften as excess pore pressures develop. How should investigators account for these factors in estimating peak acceleration?

**Answer:** The procedure recommended by the workshop is to calculate or estimate a peak acceleration that incorporates the influence of site amplification, but neglects the influence of excess pore-water pressure. Simply stated, the peak acceleration to be used in liquefaction resistance evaluations is the peak horizontal acceleration that would have occurred at ground surface at the site in the absence of increased pore-water pressure or the occurrence of liquefaction.

**Question:** Should high-frequency spikes (periods less than 0.1 sec) in acceleration records be considered or ignored?

**Answer:** In general, short-duration, high-frequency acceleration spikes should be ignored for liquefaction resistance evaluations. By using attenuation relationships for estimation of peak acceleration, as noted above, high frequency spikes are essentially ignored because few high-frequency peaks are incorporated in data bases from which attenuation relationships have been derived. Similarly, ground response analyses programs such as SHAKE and DESRA generally attenuate or filter out high-frequency spikes, reducing their influence. Where amplification ratios are used engineering judgment should be used to determine which bedrock accelerations should be amplified.

## 5.10 RESULTS OF LIQUEFACTION EVALUATION

We have written a Computer Program based on the updated simplified procedure to perform liquefaction analysis. Factor of safety, F.S., against liquefaction at a point in a soil deposit is defined by the ratio of cyclic resistance (CRR) to the cyclic stress (CSR) induced

by the design earthquake. Soil deposits with F.S. < 1 are marked as liquefiable. We selected the maximum likely earthquake for each city in the study area. Published ground motion attenuation relationships were used to estimate peak horizontal ground accelerations for the earthquakes selected. A summary of the earthquake parameters used in liquefaction evaluation for each city in study area is listed in Table 5.3.

Standard Penetration (SPT) and shear-wave velocity (VS) measurements conducted in study cities and reported in Appendices (B & F) were interpolated by the liquefaction analysis program.

Liquefaction analysis using the simplified procedure indicates that the majority of the liquefiable sediment layers are in the sabkha of Jizan city at different depths from ground surface as shown in Table 5.4. The liquefaction evaluation results are listed in Appendix C.

**Table (5.4):** Depth Ranges of Liquefiable Layers in Study Cities

| City | Site # | Depth Range (m) |
|---|---|---|
| Haql | 6 | 4 – 4.50 |
| | 6 | 11.2 – 14.3 |
| Al-Wajh | 3 | 0 – 1.5 |
| | 3 | 3.4 – 12.2 |
| | 3 | 18.2 – 15.8 |
| Jizan | 1 | 0.90 – 12.00 |
| | 2 | 1.20 – 9.30 |
| | 3 | 1.20 – 9.30 |
| | 4 | 3.20 – 4.70 |
| | 4 | 9.00 – 9.90 |
| | 5 | 2.40 – 20.00 |
| | 6 | 2.30 – 20.90 |
| | 7 | 0.0 – 8.00 |
| | 9 | 0.40 – 0.70 |
| | 9 | 1.50 – 23.10 |
| | 10 | 0.70 – 10.20 |
| | 11 | 0.0 – 22.00 |
| | 12 | 0.70 – 20.50 |
| | 14 | 0.00 – 14.10 |

# CHAPTER 6

# RESULTS AND DISCUSSION

## 6.1 SUMMARY OF SWV RESULTS

The field measurements of the shear wave velocity (SWV) profiles presented in set of figures in Appendix (F) are summarized here in tabulated forms for the analysis purpose. The results are presented in the following tables according to city order in the field tests: Table 6.1 for City of Haql, Table 6.2 for City of Alwajh, Table 6.3 for City of Yanbu, Table 6.4 for City of Jeddah, and Table 6.5 for City of Jizan. Each table includes a data set of SWV depth profile of each site tested in the respective city. For each data set, the data are organized in columns indicating depth (D) in m up to the bottom of the respective layer, SWV (Vs) in m/s, and layer thickness in m, respectively.

Depth's limit shown is 30 m in accordance with the proposed site classification method of the NEHRP [11] which explained earlier in Section 1.2 of Chapter 2. The bottom of each data set shows the respective average SWV to 30 m depth computed as the average of the layered SWV inverse values, as illustrated later by equations 6.1 and 6.2.

Table 6.1: SWV Measurements and Shear Modulus (G) in City of Haql.

| Site | Haql Site # 1 | | | Haql Site # 2 | | | Haql Site # 3 | | | Haql Site # 4 | | |
|---|---|---|---|---|---|---|---|---|---|---|---|---|
| Parameters | D (m) | SWV (m/s) | Thickness (m) | D (m) | SWV (m/s) | Thickness (m) | D (m) | SWV (m/s) | Thickness (m) | D (m) | SWV (m/s) | Thickness (m) |
| | 2.31 | 294.94 | 2.31 | 1.1 | 124.24 | 1.17 | 2.12 | 257.46 | 2.12 | 0.60 | 175.56 | 0.60 |
| | 3.34 | 405.25 | 2.03 | 2.14 | 258.51 | 0.97 | 4.31 | 351.93 | 2.19 | 1.16 | 243.25 | 0.56 |
| | 6.38 | 491.90 | 2.04 | 3.48 | 364.06 | 1.34 | 7.59 | 389.76 | 3.28 | 2.21 | 328.59 | 1.05 |
| | 8.68 | 485.90 | 2.30 | 5.99 | 533.51 | 2.50 | 10.00 | 383.76 | 2.41 | 3.28 | 322.59 | 1.0 |
| | 10.13 | 369.00 | 1.45 | 7.69 | 527.51 | 1.70 | 11.72 | 319.00 | 1.72 | 4.41 | 284.98 | 1.14 |
| SWV | 14.83 | 356.50 | 4.70 | 9.93 | 376.86 | 2.24 | 14.41 | 298.17 | 2.68 | 5.24 | 346.64 | 0.83 |
| Profile | 18.28 | 369.20 | 3.45 | 13.62 | 360.67 | 3.69 | 18.62 | 433.82 | 4.21 | 6.48 | 393.93 | 1.24 |
| | 21.21 | 460.83 | 2.93 | 15.69 | 313.56 | 2.07 | 24.31 | 427.82 | 5.69 | 7.96 | 38.93 | 1.48 |
| | 26.55 | 480.36 | 5.35 | 19.48 | 340.87 | 3.79 | 30.00 | 559.98 | 5.69 | 9.21 | 443.61 | 1.25 |
| | 30.00 | 543.25 | 3.45 | 22.76 | 409.43 | 3.28 | | | | 11.9 | 474.90 | 2.76 |
| | | | | 25.34 | 489.51 | 2.59 | | | | 13.82 | 468.90 | 1.84 |
| | | | | 30.00 | 563.16 | 4.66 | | | | 30.00 | 642.09 | 16.18 |
| Avg. SWV | | 416.65 | | | 373.88 | | | 390.99 | | | 473.72 | |
| Range of G (MPaP | | 140 - 480 | | | 25 - 530 | | | 100 – 500 | | | 48 - 700 | |

Table 6.1: SWV Measurements and Shear Modulus (G) in City of Haql. (Continued)

| Site | Haql Site # 5 | | | Haql Site # 6 | | | Haql Site # 7 | | | Haql Site # 8 | | |
|---|---|---|---|---|---|---|---|---|---|---|---|---|
| Parameters | D (m) | SWV (m/s) | Thickness (m) | D (m) | SWV (m/s) | Thickness (m) | D (m) | SWV (m/s) | Thickness (m) | D (m) | SWV (m/s) | Thickness (m) |
| | 1.38 | 156.40 | 1.38 | 0.83 | 195.05 | 0.83 | 1.11 | 281.55 | 1.11 | 1.55 | 220.18 | 1.55 |
| | 2.76 | 228.68 | 1.38 | 1.86 | 225.92 | 1.03 | 1.60 | 309.16 | 0.48 | 2.79 | 274.22 | 1.24 |
| | 3.90 | 357.09 | 1.15 | 2.63 | 285.40 | 0.77 | 2.62 | 303.16 | 1.03 | 3.55 | 413.98 | 0.76 |
| | 5.17 | 469.22 | 1.27 | 3.36 | 279.40 | 0.72 | 3.44 | 374.13 | 0.82 | 5.14 | 563.14 | 1.59 |
| | 6.08 | 580.87 | 0.90 | 4.07 | 210.67 | 0.71 | 6.02 | 587.83 | 2.58 | 6.78 | 751.55 | 1.64 |
| | 7.72 | 574.87 | 1.65 | 4.52 | 233.51 | 0.45 | 7.54 | 729.04 | 1.51 | 8.42 | 745.55 | 1.64 |
| | 11.72 | 470.21 | 4.00 | 5.66 | 308.43 | 1.14 | 9.54 | 784.80 | 2.00 | 12.96 | 515.60 | 5.54 |
| SWV | 15.53 | 464.21 | 3.81 | 8.95 | 348.08 | 3.29 | 10.72 | 778.80 | 1.18 | 14.67 | 408.29 | 1.71 |
| Profile | 19.08 | 426.85 | 3.55 | 10.00 | 342.08 | 1.05 | 12.70 | 520.79 | 1.97 | 19.65 | 697.86 | 4.98 |
| | 20.98 | 552.78 | 1.90 | 11.25 | 314.98 | 1.25 | 13.88 | 699.12 | 1.18 | 30.00 | 870.96 | 10.35 |
| | 23.07 | 555.37 | 2.08 | 12.57 | 271.33 | 1.32 | 16.38 | 886.84 | 2.50 | | | |
| | 30.00 | 751.08 | 6.93 | 14.34 | 268.95 | 1.78 | 21.25 | 880.84 | 4.87 | | | |
| | | | | 16.72 | 351.33 | 2.38 | 30.00 | 1029.84 | 8.75 | | | |
| | | | | 20.69 | 416.14 | 3.96 | | | | | | |
| | | | | 29.14 | 559.33 | 8.45 | | | | | | |
| | | | | 30.00 | 647.43 | 0.86 | | | | | | |
| Avg. SWV | | 450.22 | | | 357.96 | | | 682.41 | | | 570.09 | |
| Range of G (MPaP | | 40 - 900 | | | 60 - 670 | | | 120 – 1700 | | | 75 - 1200 | |

Table 6.2: SWV Measurements and Shear Modulus (G) in City of ALWahj.

| Site | Wahj Site # 1 | | | Wahj Site # 2 | | | Wahj Site # 3 | | | Wahj Site # 4 | | |
|---|---|---|---|---|---|---|---|---|---|---|---|---|
| Parameters | D (m) | SWV (m/s) | Thickness (m) | D (m) | SWV (m/s) | Thickness (m) | D (m) | SWV (m/s) | Thickness (m) | D (m) | SWV (m/s) | Thickness (m) |
| | 2.31 | 248.55 | 2.31 | 1.45 | 318.69 | 1.45 | 0.60 | 125.77 | 0.60 | 1.05 | 206.91 | 1.05 |
| | 5.14 | 529.57 | 2.83 | 2.83 | 512.00 | 1.38 | 1.48 | 156.50 | 0.88 | 1.84 | 361.55 | 0.79 |
| | 6.34 | 523.57 | 1.20 | 4.87 | 804.78 | 2.04 | 2.66 | 153.50 | 1.17 | 2.50 | 461.11 | 0.66 |
| | 7.45 | 376.76 | 1.11 | 8.49 | 798.78 | 3.62 | 3.41 | 136.90 | 0.76 | 5.92 | 502.10 | 3.42 |
| SWV | 14.92 | 542.65 | 7.47 | 12.70 | 630.57 | 4.21 | 4.83 | 135.10 | 1.41 | 7.10 | 496.10 | 1.18 |
| Profile | 18.23 | 536.65 | 3.31 | 15.46 | 486.86 | 2.76 | 6.59 | 136.48 | 1.76 | 10.13 | 332.10 | 3.03 |
| | 21.71 | 723.24 | 3.48 | 22.07 | 556.63 | 6.61 | 10.20 | 187.21 | 3.61 | 13.28 | 379.38 | 3.15 |
| | 30.00 | 742.11 | 8.29 | 30.00 | 909.04 | 7.93 | 14.67 | 214.50 | 4.48 | 19.34 | 509.18 | 6.06 |
| | | | | | | | 30.00 | 312.52 | 15.33 | 29.21 | 524.17 | 9.87 |
| | | | | | | | | | | 30.00 | 663.84 | 0.79 |
| Avg. SWV | | 537.69 | | | 634.88 | | | 220.37 | | | 446.17 | |
| Range of G (MPaP | | 100 - 880 | | | 150 - 1300 | | | 25 – 150 | | | 65 - 700 | |

Table 6.2: SWV Measurements and Shear Modulus (G) in City of ALWahj (continued)

| Site | Wahj Site # 5 | | | Wahj Site # 6 | | | Wahj Site # 7 | | | Wahj Site # 8 | | |
|---|---|---|---|---|---|---|---|---|---|---|---|---|
| Parameters | D (m) | SWV (m/s) | Thickness (m) | D (m) | SWV (m/s) | Thickness (m) | D (m) | SWV (m/s) | Thickness (m) | D (m) | SWV (m/s) | Thickness (m) |
| | 0.96 | 196.86 | 0.96 | 1.21 | 366.50 | 1.21 | 1.21 | 154.10 | 1.21 | 0.31 | 353.93 | 0.31 |
| | 1.53 | 270.63 | 0.57 | 3.34 | 704.89 | 2.14 | 3.00 | 207.86 | 1.79 | 0.69 | 570.70 | 0.38 |
| | 2.83 | 383.51 | 1.30 | 5.72 | 729.95 | 2.38 | 6.56 | 332.96 | 3.56 | 1.31 | 595.96 | 0.62 |
| | 4.14 | 399.84 | 1.31 | 6.86 | 723.95 | 1.14 | 9.35 | 410.36 | 2.79 | 1.90 | 589.96 | 0.59 |
| | 5.62 | 393.84 | 1.48 | 7.52 | 644.00 | 0.66 | 12.33 | 641.03 | 2.98 | 2.69 | 645.29 | 0.79 |
| | 8.49 | 486.15 | 2.87 | 8.79 | 592.86 | 1.28 | 13.28 | 724.81 | 0.95 | 3.48 | 639.29 | 0.79 |
| SWV | 12.57 | 480.15 | 4.08 | 11.63 | 893.61 | 2.83 | 20.66 | 718.81 | 7.38 | 5.17 | 672.08 | 1.69 |
| Profile | 15.26 | 398.36 | 2.70 | 12.09 | 887.61 | 0.47 | 30.00 | 840.11 | 9.34 | 7.10 | 666.08 | 1.93 |
| | 21.21 | 364.83 | 5.94 | 13.67 | 665.43 | 1.58 | 30.00 | 942.96 | 0.00 | 10.39 | 568.78 | 3.29 |
| | 30.00 | 507.35 | 8.79 | 15.72 | 628.57 | 2.05 | | | | 11.91 | 562.78 | 1.51 |
| | | | | 21.30 | 622.57 | 5.58 | | | | 15.69 | 821.71 | 3.78 |
| | | | | 23.44 | 811.58 | 2.14 | | | | 19.48 | 1123.81 | 3.79 |
| | | | | 30.00 | 1109.96 | 6.56 | | | | 22.59 | 1117.81 | 3.10 |
| | | | | | | | | | | 30.00 | 1054.46 | 7.41 |
| Avg. SWV | | 415.59 | | | 728.77 | | | 489.48 | | | 795.34 | |
| Range of G (MPaP | | 60 - 400 | | | 210 - 2000 | | | 35 – 1400 | | | 200 - 1800 | |

Table 6.2: SWV Measurements and Shear Modulus (G) in City of AlWahj (Continued).

| Site | Wahj Site # 9 | | | Wahj Site # 10 | | | | | | | | |
|---|---|---|---|---|---|---|---|---|---|---|---|---|
| Parameters | D (m) | SWV (m/s) | Thickness (m) | D (m) | SWV (m/s) | Thickness (m) | D (m) | SWV (m/s) | Thickness (m) | D (m) | SWV (m/s) | Thickness (m) |
| SWV Profile | 0.79 | 169.22 | 0.79 | 0.53 | 127.07 | 0.53 | | | | | | |
| | 1.71 | 220.96 | 0.92 | 1.64 | 239.79 | 1.11 | | | | | | |
| | 2.50 | 273.54 | 0.80 | 2.91 | 305.24 | 1.27 | | | | | | |
| | 3.23 | 267.54 | 0.73 | 4.97 | 299.24 | 2.05 | | | | | | |
| | 4.33 | 245.49 | 1.10 | 7.17 | 402.56 | 2.21 | | | | | | |
| | 5.79 | 326.09 | 1.46 | 9.34 | 415.98 | 2.17 | | | | | | |
| | 8.49 | 320.09 | 2.70 | 11.25 | 409.98 | 1.91 | | | | | | |
| | 11.55 | 340.82 | 3.07 | 14.14 | 458.56 | 2.89 | | | | | | |
| | 18.62 | 401.28 | 7.07 | 17.96 | 452.56 | 3.852 | | | | | | |
| | 25.00 | 635.20 | 6.38 | 25.92 | 567.71 | 7.96 | | | | | | |
| | 30.00 | 848.24 | 5.00 | 30.00 | 630.13 | 4.08 | | | | | | |
| Avg. SWV | | 403.38 | | | 426.03 | | | | | | | |
| Range of G (MPaP | | 140 - 1100 | | | 25 - 640 | | | | | | | |

Table 6.3: SWV Measurements and Shear Modulus (G) in City of Yanbu.

| Site | Yanbu Site # 1 | | | Yanbu Site # 2 | | | Yanbu Site # 3 | | | Yanbu Site # 4 | | |
|---|---|---|---|---|---|---|---|---|---|---|---|---|
| Parameters | D (m) | SWV (m/s) | Thickness (m) | D (m) | SWV (m/s) | Thickness (m) | D (m) | SWV (m/s) | Thickness (m) | D (m) | SWV (m/s) | Thickness (m) |
| | 0.90 | 205.53 | 0.90 | 1.17 | 403.48 | 1.17 | 1.58 | 392.97 | 1.58 | 1.21 | 225.69 | 1.21 |
| | 1.82 | 301.02 | 0.92 | 1.89 | 617.85 | 0.72 | 2.17 | 611.52 | 0.59 | 1.71 | 315.76 | 0.50 |
| | 2.59 | 427.26 | 0.77 | 3.38 | 851.40 | 1.49 | 3.36 | 755.97 | 1.18 | 3.35 | 491.59 | 1.64 |
| | 3.40 | 421.26 | 0.81 | 6.02 | 845.40 | 2.64 | 4.93 | 855.66 | 1.58 | 5.70 | 750.08 | 2.35 |
| | 4.75 | 385.39 | 1.35 | 8.09 | 592.00 | 2.07 | 5.53 | 849.66 | 0.59 | 7.66 | 835.94 | 1.96 |
| | 6.34 | 427.40 | 1.58 | 10.33 | 465.43 | 2.23 | 6.71 | 682.35 | 1.18 | 8.17 | 829.94 | 0.50 |
| SWV | 8.23 | 575.50 | 1.89 | 14.23 | 396.83 | 3.91 | 7.76 | 959.35 | 1.05 | 9.43 | 610.52 | 1.26 |
| Profile | 10.95 | 624.84 | 2.72 | 18.51 | 609.77 | 4.28 | 8.95 | 1095.99 | 1.18 | 10.31 | 446.40 | 0.88 |
| | 14.16 | 618.84 | 3.21 | 26.90 | 603.77 | 8.39 | 10.86 | 1089.99 | 1.91 | 16.63 | 446.85 | 6.33 |
| | 17.56 | 691.27 | 3.40 | 30.00 | 658.88 | 3.10 | 14.14 | 1108.22 | .3.29 | 20.88 | 640.83 | 4.25 |
| | 21.23 | 1003.54 | 3.67 | | | | 16.84 | 1102.22 | 2.70 | 30.00 | 772.11 | 9.12 |
| | 30.00 | 1120.34 | 8.77 | | | | 20.66 | 896.04 | 3.82 | | | |
| | | | | | | | 24.88 | 1463.78 | 4.23 | | | |
| | | | | | | | 30.00 | 1475.78 | 5.12 | | | |
| Avg. SWV | | 630.22 | | | 569.27 | | | 973.09 | | | 566.04 | |
| Range of G (MPaP | | 60 – 2000 | | | 250 – 700 | | | 250 – 3500 | | | 80 - 950 | |

Table 6.3: SWV Measurements and Shear Modulus (G) in City of Yanbu (continued)

| Site | Yanbu Site # 5 | | | Yanbu Site # 6 | | | Yanbu Site # 7 | | | Yanbu Site # 8 | | |
|---|---|---|---|---|---|---|---|---|---|---|---|---|
| Parameters | D (m) | SWV (m/s) | Thickness (m) | D (m) | SWV (m/s) | Thickness (m) | D (m) | SWV (m/s) | Thickness (m) | D (m) | SWV (m/s) | Thickness (m) |
| | 0.59 | 180.69 | 0.59 | 0.73 | 180.70 | 0.73 | 0.61 | 287.27 | 0.61 | 1.10 | 236.54 | 1.10 |
| | 1.92 | 356.74 | 1.34 | 1.47 | 332.69 | 0.74 | 1.05 | 443.16 | 0.44 | 2.66 | 634.30 | 1.55 |
| | 3.60 | 519.74 | 1.68 | 2.91 | 474.57 | 1.43 | 1.24 | 437.16 | 0.19 | 3.62 | 757.29 | 0.97 |
| | 5.54 | 513.74 | 1.94 | 5.39 | 804.79 | 2.49 | 1.59 | 305.43 | 0.35 | 4.24 | 751.29 | 0.62 |
| | 8.51 | 408.00 | 2.97 | 8.29 | 798.79 | 2.89 | 2.34 | 273.08 | 0.75 | 5.52 | 558.29 | 1.28 |
| SWV | 11.90 | 402.57 | 3.38 | 11.27 | 763.53 | 2.98 | 3.65 | 320.27 | 1.31 | 7.55 | 585.21 | 2.03 |
| Profile | 17.78 | 382.57 | 5.89 | 15.66 | 757.53 | 4.39 | 4.84 | 314.27 | 1.19 | 9.49 | 579.21 | 1.94 |
| | 24.14 | 630.26 | 6.36 | 19.28 | 884.37 | 3.62 | 6.49 | 405.87 | 1.65 | 12.56 | 440.43 | 3.07 |
| | 30.00 | 849.24 | 5.86 | 23.45 | 1069.09 | 4.17 | 12.31 | 399.87 | 5.82 | 16.37 | 422.67 | 3.81 |
| | | | | 30.00 | 1063.09 | 6.55 | 22.45 | 337.55 | 10.14 | 20.65 | 416.67 | 4.28 |
| | | | | | | | 29.08 | 529.43 | 6.63 | 26.70 | 394.10 | 6.05 |
| | | | | | | | 30.00 | 588.51 | 0.92 | 30.00 | 639.58 | 3.30 |
| Avg. SWV | | 483.40 | | | 752.74 | | | 384.25 | | | 460.92 | |
| Range of G (MPaP | | 50 – 1100 | | | 48 – 1700 | | | 120 – 500 | | | 84 - 600 | |

Table 6.3: SWV Measurements and Shear Modulus (G) in City of Yanbu (Continued).

| Site | Yanbu Site # 9 | | | Yanbu Site # 10 | | | | | | | | |
|---|---|---|---|---|---|---|---|---|---|---|---|---|
| Parameters | D (m) | SWV (m/s) | Thickness (m) | D (m) | SWV (m/s) | Thickness (m) | D (m) | SWV (m/s) | Thickness (m) | D (m) | SWV (m/s) | Thickness (m) |
| SWV Profile | 1.38 | 178.54 | 1.38 | 0.90 | 308.79 | 0.90 | | | | | | |
| | 3.16 | 290.07 | 1.78 | 2.14 | 357.63 | 1.24 | | | | | | |
| | 5.00 | 284.07 | 1.84 | 2.93 | 436.81 | 0.79 | | | | | | |
| | 7.96 | 339.33 | 2.96 | 4.28 | 430.81 | 1.34 | | | | | | |
| | 11.51 | 410.34 | 3.55 | 5.86 | 381.84 | 1.58 | | | | | | |
| | 16.45 | 404.34 | 4.93 | 7.76 | 352.70 | 1.91 | | | | | | |
| | 20.86 | 552.31 | 4.41 | 12.63 | 315.74 | 4.87 | | | | | | |
| | 29.83 | 723.79 | 8.97 | 16.72 | 325.83 | 4.09 | | | | | | |
| | 30.00 | 1218.11 | 0.17 | 18.62 | 433.36 | 1.90 | | | | | | |
| | | | | 23.97 | 501.75 | 5.35 | | | | | | |
| | | | | 30.00 | 495.75 | 6.03 | | | | | | |
| Avg. SWV | | 425.84 | | | 394.54 | | | | | | | |
| Range of G (MPaP | | 45 – 2000 | | | 140 – 380 | | | | | | | |

Table 6.4: SWV Measurements and Shear Modulus (G) in City of Jeddah.

| Site | Jeddah Site # 1 | | | Jeddah Site # 2 | | | Jeddah Site # 3 | | | Jeddah Site # 4 | | |
|---|---|---|---|---|---|---|---|---|---|---|---|---|
| Parameters | D (m) | SWV (m/s) | Thickness (m) | D (m) | SWV (m/s) | Thickness (m) | D (m) | SWV (m/s) | Thickness (m) | D (m) | SWV (m/s) | Thickness (m) |
| | 0.46 | 146.27 | 0.46 | 1.28 | 197.91 | 1.28 | 0.66 | 126.67 | 0.66 | 0.79 | 160.14 | 0.79 |
| | 1.45 | 334.68 | 0.99 | 3.36 | 517.43 | 2.08 | 0.90 | 210.80 | 0.24 | 1.66 | 216.45 | 0.86 |
| | 4.52 | 867.66 | 3.07 | 4.54 | 615.59 | 1.18 | 1.83 | 330.19 | 0.93 | 2.97 | 279.21 | 1.31 |
| | 8.29 | 1284.02 | 3.77 | 6.25 | 609.59 | 1.71 | 3.41 | 324.19 | 1.59 | 5.72 | 403.75 | 2.76 |
| | 9.67 | 1278.02 | 1.38 | 8.95 | 709.04 | 2.70 | 5.03 | 406.33 | 1.62 | 9.47 | 397.75 | 3.75 |
| SWV | 15.92 | 808.29 | 6.25 | 12.50 | 703.04 | 3.55 | 7.17 | 443.43 | 2.14 | 11.91 | 573.19 | 2.43 |
| Profile | 30.00 | 3128..95 | 14.08 | 15.79 | 533.29 | 3.29 | 9.67 | 483.25 | 2.50 | 14.41 | 567.19 | 2.50 |
| | | | | 23.28 | 893.05 | 7.49 | 11.38 | 477.25 | 1.71 | 17.83 | 658.03 | 3.42 |
| | | | | 30.00 | 1001.03 | 6.72 | 13.62 | 537.62 | 2.24 | 26.21 | 808.27 | 8.38 |
| | | | | | | | 18.97 | 595.19 | 5.35 | 30.00 | 1549.82 | 3.79 |
| | | | | | | | 26.72 | 613.16 | 7.76 | | | |
| | | | | | | | 30.00 | 1109.17 | 3.28 | | | |
| Avg. SWV | | 1158.92 | | | 661.94 | | | 496.83 | | | 530.47 | |
| Range of G (MPaP | | 32 – 1450 | | | 60 – 1600 | | | 22 – 1900 | | | 40 - 3800 | |

Table 6.4: SWV Measurements and Shear Modulus (G) in City of Jeddah (continued)

| Site | Jeddah Site # 5 | | | Jeddah Site # 6 | | | Jeddah Site # 7 | | | Jeddah Site # 8 | | |
|---|---|---|---|---|---|---|---|---|---|---|---|---|
| Parameters | D (m) | SWV (m/s) | Thickness (m) | D (m) | SWV (m/s) | Thickness (m) | D (m) | SWV (m/s) | Thickness (m) | D (m) | SWV (m/s) | Thickness (m) |
| SWV Profile | 1.45 | 340.46 | 1.45 | 0.62 | 156.41 | 0.62 | 0.44 | 104.04 | 0.44 | 0.54 | 105.37 | 0.54 |
| | 2.00 | 418.79 | 0.55 | 0.79 | 189.92 | 0.17 | 0.64 | 143.63 | 0.20 | 0.89 | 161.33 | 0.35 |
| | 2.48 | 536.87 | 0.48 | 1.10 | 226.46 | 0.31 | 0.99 | 166.67 | 0.34 | 1.42 | 230.19 | 0.53 |
| | 2.86 | 556.86 | 0.38 | 2.03 | 313.58 | 0.93 | 1.24 | 163.67 | 0.25 | 2.22 | 243.08 | 0.80 |
| | 3.38 | 550.86 | 0.52 | 3.00 | 354.52 | 0.97 | 1.38 | 154.30 | 0.14 | 2.69 | 237.08 | 0.47 |
| | 3.83 | 502.40 | 0.45 | 4.21 | 348.52 | 1.21 | 1.61 | 129.36 | 0.24 | 4.21 | 209.36 | 1.52 |
| | 4.15 | 416.57 | 0.32 | 5.66 | 299.46 | 1.45 | 2.90 | 145.48 | 1.29 | 6.55 | 230.17 | 2.34 |
| | 5.23 | 373.94 | 1.08 | 6.66 | 415.80 | 1.00 | 30.00 | 1222.01 | 27.10 | 10.72 | 341.98 | 4.17 |
| | 8.95 | 363.84 | 3.71 | 9.41 | 409.80 | 2.75 | | | | 15.72 | 454.27 | 5.00 |
| | 11.95 | 429.48 | 3.00 | 11.25 | 371.37 | 1.84 | | | | 24.31 | 542.27 | 8.59 |
| | 21.55 | 694.33 | 9.60 | 17.30 | 515.12 | 6.05 | | | | 30.00 | 846.03 | 5.69 |
| | 28.97 | 1058.50 | 7.40 | 28.27 | 701.56 | 10.97 | | | | | | |
| | 30.00 | 1772.91 | 1.03 | 30.00 | 1100.37 | 1.73 | | | | | | |
| Avg. SWV | | 585.19 | | | 474.13 | | | 697.56 | | | 384.33 | |
| Range of G (MPaP | | 180 – 5000 | | | 40 – 1900 | | | 15 – 2400 | | | 16 - 1100 | |

Table 6.4: SWV Measurements and Shear Modulus (G) in City of Jeddah (Continue).

| Site | Jeddah Site # 9 | | | Jeddah Site # 10 | | | | | | | | |
|---|---|---|---|---|---|---|---|---|---|---|---|---|
| Parameters | D (m) | SWV (m/s) | Thickness (m) | D (m) | SWV (m/s) | Thickness (m) | D (m) | SWV (m/s) | Thickness (m) | D (m) | SWV (m/s) | Thickness (m) |
| | 0.99 | 435.35 | 0.99 | 0.39 | 229.41 | 0.39 | | | | | | |
| | 1.91 | 760.13 | 0.92 | 1.16 | 292.97 | 0.77 | | | | | | |
| | 3.16 | 1013.05 | 1.25 | 1.69 | 286.97 | 0.53 | | | | | | |
| | 4.61 | 1007.05 | 1.45 | 2.43 | 379.77 | 0.74 | | | | | | |
| | 8.20 | 824.90 | 3.60 | 3.68 | 496.94 | 1.26 | | | | | | |
| SWV | 9.83 | 1113.70 | 1.63 | 5.59 | 805.31 | 1.91 | | | | | | |
| Profile | 12.96 | 1107.70 | 3.13 | 7.83 | 799.31 | 2.24 | | | | | | |
| | 18.59 | 699.00 | 5.63 | 9.01 | 956.15 | 1.18 | | | | | | |
| | 23.10 | 814.50 | 4.51 | 10.66 | 950.15 | 1.64 | | | | | | |
| | 30.00 | 1575.00 | 6.90 | 14.74 | 903.55 | 4.08 | | | | | | |
| | | | | 21.21 | 1092.06 | 6.47 | | | | | | |
| | | | | 30.00 | 1674.10 | 8.79 | | | | | | |
| Avg. SWV | | 915.39 | | | 870.38 | | | | | | | |
| Range of G (MPaP | | 300 – 4000 | | | 82 – 4500 | | | | | | | |

Table 6.5: SWV Measurements and Shear Modulus (G) in City of Jizan.

| Site | Jizan Site # 1 | | | Jizan Site # 2 | | | Jizan Site # 3 | | | Jizan Site # 4 | | |
|---|---|---|---|---|---|---|---|---|---|---|---|---|
| Parameters | D (m) | SWV (m/s) | Thickness (m) | D (m) | SWV (m/s) | Thickness (m) | D (m) | SWV (m/s) | Thickness (m) | D (m) | SWV (m/s) | Thickness (m) |
| | 0.24 | 124.44 | 0.24 | 0.59 | 102.33 | 0.59 | 0.59 | 102.33 | 0.59 | 0.53 | 119.54 | 0.53 |
| | 0.56 | 152..01 | 0.31 | 1.24 | 125.29 | 0.65 | 1.24 | 125.29 | 0.65 | 0.99 | 219.34 | 0.46 |
| | 0.90 | 149.01 | 0.34 | 1.80 | 123.49 | 0.56 | 1.80 | 123.49 | 0.56 | 1.84 | 213.34 | 0.86 |
| | 1.24 | 141.94 | 0.34 | 2.87 | 125.41 | 1.07 | 2.87 | 125.41 | 1.07 | 3.29 | 197.01 | 1.45 |
| | 1.80 | 111.24 | 0.56 | 4.61 | 123.61 | 1.73 | 4.61 | 123.61 | 1.73 | 4.67 | 173.09 | 1.38 |
| SWV | 2.87 | 125.41 | 1.07 | 9.31 | 174.70 | 4.70 | 9.31 | 174.70 | 4.70 | 7.30 | 211.41 | 2.63 |
| Profile | 3.93 | 158.29 | 1.06 | 23.79 | 441.39 | 14.48 | 23.79 | 441.39 | 14.48 | 9.87 | 205.41 | 2.57 |
| | 7.48 | 231.79 | 3.55 | 30.00 | 712.34 | 6.21 | 30.00 | 712.34 | 6.21 | 13.09 | 240.68 | 3.22 |
| | 12.04 | 308.25 | 4.56 | | | | | | | 16.55 | 254.31 | 3.46 |
| | 18.42 | 375.16 | 6.38 | | | | | | | 23.28 | 437.94 | 6.72 |
| | 23.79 | 516.48 | 5.37 | | | | | | | 30.00 | 535.64 | 6.72 |
| | 30.00 | 712.29 | 6.21 | | | | | | | | | |
| Avg. SWV | | 315.09 | | | 281.64 | | | 281.64 | | | 283.86 | |
| Range of G (MPaP | | 20 – 700 | | | 15 – 700 | | | 15 – 700 | | | 22 - 400 | |

Table 6.5: SWV Measurements and Shear Modulus (G) in City of Jizan (Continue).

| Site | Jizan Site # 5 | | | Jizan Site # 6 | | | Jizan Site # 7 | | | Jizan Site # 8 | | |
|---|---|---|---|---|---|---|---|---|---|---|---|---|
| Parameters | D (m) | SWV (m/s) | Thickness (m) | D (m) | SWV (m/s) | Thickness (m) | D (m) | SWV (m/s) | Thickness (m) | D (m) | SWV (m/s) | Thickness (m) |
| | 0.66 | 88.11 | 0.66 | 0.39 | 111.02 | 0.39 | 7.91 | 141.79 | 7.91 | 0.57 | 172.94 | 0.57 |
| | 1.48 | 119.94 | 0.83 | 0.90 | 166.63 | 0.51 | 30.00 | 843.65 | 22.09 | 1.76 | 229.22 | 1.19 |
| | 2.48 | 129.67 | 1.00 | 1.21 | 226.01 | 0.31 | | | | 3.31 | 244.15 | 1.56 |
| | 3.03 | 127.87 | 0.55 | 1.77 | 220.01 | 0.56 | | | | 4.80 | 322.96 | 1.49 |
| | 4.28 | 101.14 | 1.24 | 2.31 | 139.50 | 0.54 | | | | 6.32 | 316.96 | 1.51 |
| | 6.71 | 152.79 | 2.43 | 2.97 | 168.42 | 0.66 | | | | 30.00 | 1986.23 | 23.68 |
| SWV | 9.54 | 191.64 | 2.83 | 3.24 | 165.422 | 0.28 | | | | | | |
| Profile | 11.97 | 215.94 | 2.43 | 3.90 | 132.98 | 0.66 | | | | | | |
| | 20.00 | 326.98 | 8.03 | 5.07 | 122.16 | 1.17 | | | | | | |
| | 30.00 | 529.97 | 10.00 | 7.37 | 153.14 | 2.30 | | | | | | |
| | | | | 9.54 | 186.07 | 2.17 | | | | | | |
| | | | | 12.63 | 182.07 | 3.09 | | | | | | |
| | | | | 20.86 | 246.26 | 8.23 | | | | | | |
| | | | | 30.00 | 341.57 | 9.14 | | | | | | |
| Avg. SWV | | 241.86 | | | 216.97 | | | 365.96 | | | 829.61 | |
| Range of G (MPaP | | 11 – 400 | | | 17 – 160 | | | 32 – 1100 | | | 48 - 6000 | |

Table 6.5: SWV Measurements and Shear Modulus (G) in City of Jizan (Continued).

| Site | Jizan Site # 9 | | | Jizan Site # 10 | | | Jizan Site # 11 | | | Jizan Site # 12 | | |
|---|---|---|---|---|---|---|---|---|---|---|---|---|
| Parameters | D (m) | SWV (m/s) | Thickness (m) | D (m) | SWV (m/s) | Thickness (m) | D (m) | SWV (m/s) | Thickness (m) | D (m) | SWV (m/s) | Thickness (m) |
| | 0.45 | 100.64 | 0.45 | 0.76 | 90.91 | 0.76 | 0.51 | 90.79 | 0.51 | 0.50 | 109.34 | 0.50 |
| | 0.69 | 144.31 | 0.24 | 1.04 | 91.48 | 0.28 | 1.41 | 140.37 | 0.90 | 0.71 | 149.02 | 0.21 |
| | 1.11 | 181.40 | 0.43 | 2.02 | 89.68 | 0.98 | 1.76 | 176.27 | 0.34 | 0.83 | 147.22 | 0.11 |
| | 1.53 | 177.40 | 0.41 | 3.59 | 88.94 | 1.57 | 2.59 | 187.08 | 0.83 | 1.25 | 106.90 | 0.42 |
| | 2.45 | 194.62 | 0.92 | 10.15 | 168.51 | 6.56 | 3.07 | 183.08 | 0.49 | 1.52 | 93.03 | 0.27 |
| SWV | 3.24 | 190.62 | 0.79 | 30.00 | 1044.15 | 19.85 | 3.86 | 129.23 | 0.79 | 1.86 | 89.50 | 0.35 |
| Profile | 5.00 | 137.33 | 1.76 | | | | 5.53 | 170.92 | 1.66 | 2.41 | 103.31 | 0.55 |
| | 6.84 | 145.93 | 1.84 | | | | 9.87 | 172.86 | 4.35 | 4.21 | 103.79 | 1.79 |
| | 9.87 | 155.04 | 3.03 | | | | 22.04 | 295.07 | 12.17 | 10.26 | 178.26 | 6.06 |
| | 14.31 | 219.72 | 4.44 | | | | | | | 20.52 | 292.82 | 10.25 |
| | 23.10 | 321.62 | 8.80 | | | | | | | 30.00 | 958.06 | 9.48 |
| | 30.00 | 702.96 | 6.90 | | | | | | | | | |
| Avg. SWV | | 245.90 | | | 306.28 | | | 290.26 | | | 252.17 | |
| Range of G (MPaP | | 14 – 700 | | | 12 – 1600 | | | 12 – 130 | | | 17 - 1300 | |

Table 6.5: SWV Measurements and Shear Modulus (G) in City of Jizan (Continued).

| Site | Jizan Site # 13 | | | Jizan Site # 14 | | | | | | | | |
|---|---|---|---|---|---|---|---|---|---|---|---|---|
| Parameters | D (m) | SWV (m/s) | Thickness (m) | D (m) | SWV (m/s) | Thickness (m) | D (m) | SWV (m/s) | Thickness (m) | D (m) | SWV (m/s) | Thickness (m) |
| | 0.321 | 140.67 | 0.31 | 4.48 | 121.29 | 4.48 | | | | | | |
| | 2.41 | 225.78 | 2.10 | 6.16 | 122.64 | 1.68 | | | | | | |
| SWV | 3.67 | 260.84 | 1.26 | 8.55 | 156.34 | 2.39 | | | | | | |
| Profile | 8.68 | 296.26 | 5.01 | 11.05 | 188.65 | 2.50 | | | | | | |
| | 12.24 | 989.75 | 3.56 | 14.14 | 206.28 | 3.09 | | | | | | |
| | 30.00 | 1787.63 | 17.76 | 30.00 | 1244.31 | 15.86 | | | | | | |
| Avg. SWV | | 641.44 | | | 280.59 | | | | | | | |
| Range of G (MPaP | | 28 - 4000 | | | 20 - 2200 | | | | | | | |

## 6.2 NEHRP SOIL PROFILE CLASSIFICATION

As per NEHRP [11] recommendations explained in Chapter 2, the Seismic Soil Profile Classification (Site Class) is defined in terms of a weighted average of SWV ($\overline{V}_S$), which can be computed for the top 30 m as follows:

$$\overline{V}_S = \frac{\sum_{i=1}^{n} d_i}{\sum_{i=1}^{n} \frac{d_i}{v_{si}}} \qquad (6.1)$$

Where, the symbol **i** refers to any one of the layers between 1 and **n**, $V_{si}$ is the SWV and $\mathbf{d_i}$ is the depth of the respective layer, in consistent units.

If SWV data is unavailable, NEHRP also recommends similar classification based on weighted average of Standard Penetration Test (SPT) data for all soil types ($\overline{N}$), and untrained shear strength data for cohesive soil deposits ($\mathbf{S_u}$). Based on layered properties to 30 m depth, $\overline{N}$ is computed as follows:

$$\overline{N} = \frac{\sum_{i=1}^{n} d_i}{\sum_{i=1}^{n} \frac{d_i}{N_{si}}} \qquad (6.2)$$

Where, $N_{si}$ is SPT of the respective layer.

Sites are classified based on the criteria shown in Table 6.6, that are fully adopted in the UBC97 [12], and IBC2000 [13]:

**Table 6.6 NEHRP Soil Profile Type Classifications**

| Site Class | Soil Profile Name | AVERAGE SOIL PROPERTIES IN TOP 30 m. | | |
|---|---|---|---|---|
| | | Soil Shear Wave Velocity, $\overline{V}_S$ (m/s) | SPT, $\overline{N}$ | Unconfined Soil Shear Strength, $S_u$ (kPa) |
| A | Hard Rock | > 1,500 | not applicable | not applicable |
| B | Rock | 760 to 1,500 | not applicable | not applicable |
| C | Very Dense Soil and Soft Rock | 360 to 760 | > 50 | > 100 |
| D | Stiff Soil | 180 to 360 | 15 to 50 | 50 to 100 |
| E | Soft Soil | < 180 | < 15 | < 50 |
| F | 1-Liquefiable soils, quick and highly sensitive clays, collapsible weakly cemented soils<br>2-Layers of peats and/or highly organic clays with thickness (H) of more than 3 m.<br>3-Very high plasticity clays (PI > 75) with H > (8 m)<br>4-Very thick, soft/medium stiff clays with H > (36 m) | | | |

## 6.3 DISCUSSION ON THE RELIABILITY OF SWV MEASUREMENTS

In noninvasive testing, there is always the issue of valid comparisons with direct measurement methods. It is well accepted that cross-hole shear wave velocity (SWV) measurement is the only method to provide accurate comparisons for the CXW method. Down-hole SWV measurements can be useful for such comparison; however, they are less precise and more operator-subjective than the cross-hole measurements. However, the cost of such comparisons is prohibitive in most cases. It was excluded from the project plan because of the limited budget allocated for the project. Moreover, we believe that such comparisons may not be necessary because CXW has been thoroughly investigated.

Many investigators have used the CXW database available in more than 400 sites in Japan, California, New York, Alaska, and Hawaii for site-specific seismic response studies. In Japan, there is a database that includes more than 20 sites where comparative cross- and down-hole SWV measurements were obtained to depth of 30 m in several different geologic formations. The Japanese Ministry of Construction (JMC) in March 1997 used this database for approving the CXW method as a standard method. The JMC certification in Japan is similar to test methods such as American Society of Testing and Materials (ASTM). Based on recent CXW results from Japan and Alaska, the CXW has been

proposed as a standard method and it is now being considered for adoption by ASTM Committee D18 (ASTM STP 1350, January 1998). Several independent researchers show good correlation of CXW results with direct SWV measurements. Park and others [60] used CXW to map seismic site response in Southern California. Nath and others [61] showed very good correlation between CXW and direct SWV measurements.

In the present study, soil profiles classified based on the CXW results were checked using the results of the bore -hole tests conduced in cities of Haql and AlWajh, and are reported in the Chapter 4. The soil profiles in these sites were checked under the NEHRP' concept of using ($\overline{N}$) as an alternative criterion for definition of soil profile in case SWV data is not available. In this context, $\overline{V}_S$, and $\overline{N}$ were calculated in accordance with equations 6.1 and 6.2 respectively for 5 sites in each city of haql and Alwajh. They were then used to classify the soil profiles based on the criteria of Table6.6. Table 6.7 shows that site classes that are defined based on $\overline{N}$, are either consistent or more conservative than those based on $\overline{V}_S$. This is expected as per the commentary of NEHRP [62] as it states the following:

Table 6.7 Comparisons Between Definitions of Soil Profiles in Cities of Haql and Alwjh

| City | Sites No. | Definition Based on SWV | | Definition Based on SPT | |
|---|---|---|---|---|---|
| | | $\overline{V}_S$ m/s$^2$ | Site Class* | $\overline{N}$ | Site Class* |
| Haql | 1 | 417 | C | 66 | C |
| | 2 | 374 | C | 73 | C |
| | 3 | 391 | C | 100 | C |
| | 4 | 474 | C | 100 | C |
| | 5 | 450 | C | 48 | D |
| Alwajh | 1 | 538 | C | 56 | C |
| | 2 | 635 | C | 48 | D |
| | 3 | 220 | D | 8.4 | E |
| | 4 | 446 | C | 81 | C |
| | 5 | 416 | C | 31 | D |

* See Table 6.6

"**Use of Geotechnical Parameters Instead of** $\overline{V}_S$: Based on the studies and observations discussed above, the site categories in the 1994 provisions are defined in terms of the average shear wave velocity in the top 100 ft (30.5 m) of the profile, $\overline{V}_S$. If the shear wave velocities are available for the site, they should be used. However, in recognition of the fact that in many cases the shear wave velocities are not available, alternative definitions of the site categories also are included in the 1994 provisions. They use the standard penetration resistance for cohesion less soil layers and the undrained shear strength for cohesive soil layers. These alternative definitions are rather conservative since the correlation between site amplification and these geotechnical parameters is more uncertain than that with $\overline{V}_S$. ----------. Also, the reader must not interpret the site category definitions as implying any specific numerical correlation between shear wave velocity on the one hand and standard penetration or shear strength on the other".

Based on the above discussion, it seems that measurements of SWV obtained using CXW method are reliable enough to be utilized for seismic classifications of the soil profiles of the study sites.

## 6.4 SEISMIC SOIL CATEGORIES OF THE STUDY SITES

As per the NEHRP provisions discussed above, the soil profiles of the study sites were classified and listed in Table 6.8. The classes' definitions of Table 6.6 were used based on $\overline{V}_S$ values given in Tables 6.1 to 6.5.

**Table 6.8 Seismic Soil Categories of the Study Sites**

| Haql City | | Wajh City | | Yanbu City | | Jeddah City | | Jizan City | |
|---|---|---|---|---|---|---|---|---|---|
| Site* | Class | Site | Class | Site | Class | Site | Class | Site | Class |
| 1 | SC | 1 | SC | 1 | SC | 1 | SB | 1 | SD? |
| 2 | SC | 2 | SC | 2 | SC | 2 | SC | 2 | SD? |
| 3 | SC | 3 | SD? | 3 | SB | 3 | SC | 3 | SD? |
| 4 | SC | 4 | SC | 4 | SC | 4 | SC | 4 | SD? |
| 5 | SC | 5 | SC | 5 | SC | 5 | SC | 5 | SD? |
| 6 | SD? | 6 | SC | 6 | SC | 6 | SC | 6 | SD? |
| 7 | SC | 7 | SC | 7 | SC | 7 | SC | 7 | SC |
| 8 | SC | 8 | SB | 8 | SC | 8 | SC | 8 | SB |
| | | 9 | SC | 9 | SC | 9 | SB | 9 | SD? |
| | | 10 | SC | 10 | SC | 10 | SB | 10 | SD? |
| | | | | | | | | 11 | SD? |
| | | | | | | | | 12 | SD? |
| | | | | | | | | 13 | SC |
| | | | | | | | | 14 | SD? |

* See Appendix A for Sits' Locations

? Results of the liquefaction study presented in Chapter 6 indicate that these sites have high potential of liquefaction. This may justify classifying these sites to softer soil such as SE or even SF. These sites therefore require site-specific geotechnical evaluation, especially for buildings that are classified as special or essential in the seismic design code.

## 6.5 SITE COEFFICIENTS

Site coefficient, as an amplification index of the site-specific design ground motions, was calculated for each site as per the recent Two-Factor approach of NEHRP [11] that recognizes the non-linearity of the soil factors. This approach assigns two coefficients for a specific site: short-period site coefficient ($F_a$), and long-period site coefficient ($F_v$). It has been adopted in NEHRP since 1994 and is based on recommendations of NCEER/SEAOC/BSSC Site Response Workshop mentioned in Chapter 2. Both $F_a$ and $F_v$ are functions of site conditions and shaking intensity. NEHRP 1994 provisions defined the shaking intensity by, the effective peak acceleration ($A_a$), and the effective peak related acceleration ($A_v$) for $F_a$ and $F_v$ respectively. In UBC1997, the shaking intensity is defined

by the seismic zone factor (Z) that is assigned for the respective city, and $F_a$ and $F_v$ are not used directly. In this code, two seismic coefficients $C_a$ and $C_v$ are used as direct input of respectively, the short period and long period design ground motions. These coefficients are conceptually based on the following NEHRP formulas:

$C_a=A_aF_a$ and $C_v=A_vFv$ , where both $A_a$ and $A_v$ are considered to be equal to Z

In this study, UBC1997 provisions were employed to determine values of $C_a$ and $C_v$, and are summarized in Table 6.9, as functions of the site profile class and Z of the respective city. Values of Z were based on the outcome of the research project AR-9-31 [17].

**Table 6.9 Seismic Site Coefficients of the Study Sites**

| Haql City Z=0.2 | | | WajhCity Z=0.075 | | | Yanbu City Z=0.075 | | | Jeddah City Z=0.15 | | | Jizan City Z=0.2 | | |
|---|---|---|---|---|---|---|---|---|---|---|---|---|---|---|
| Site* | $C_a$ | $C_v$ | Site | $C_a$ | $C_v$ | Site | $C_a$ | $C_v$ | Site | $C_a$ | $C_v$ | Site | $C_a$ | $C_v$ |
| 1 | 0.24 | 0.32 | 1 | 0.09 | 0.13 | 1 | 0.09 | 0.13 | 1 | 0.15 | 0.15 | 1? | 0.34 | 0.64 |
| 2 | 0.24 | 0.32 | 2 | 0.09 | 0.13 | 2 | 0.09 | 0.13 | 2 | 0.18 | 0.25 | 2? | 0.34 | 0.64 |
| 3 | 0.24 | 0.32 | 3? | 0.19 | 0.26 | 3 | 0.08 | 0.08 | 3 | 0.18 | 0.25 | 3? | 0.34 | 0.64 |
| 4 | 0.24 | 0.32 | 4 | 0.09 | 0.13 | 4 | 0.09 | 0.13 | 4 | 0.18 | 0.25 | 4? | 0.34 | 0.64 |
| 5 | 0.24 | 0.32 | 5 | 0.09 | 0.13 | 5 | 0.09 | 0.13 | 5 | 0.18 | 0.25 | 5? | 0.34 | 0.64 |
| 6? | 0.34 | 0.64 | 6 | 0.09 | 0.13 | 6 | 0.09 | 0.13 | 6 | 0.18 | 0.25 | 6? | 0.34 | 0.64 |
| 7 | 0.24 | 0.32 | 7 | 0.09 | 0.13 | 7 | 0.09 | 0.13 | 7 | 0.18 | 0.25 | 7 | 0.24 | 0.32 |
| 8 | 0.24 | 0.32 | 8 | 0.08 | 0.08 | 8 | 0.09 | 0.13 | 8 | 0.18 | 0.25 | 8 | 0.20 | 0.20 |
| | | | 9 | 0.09 | 0.13 | 9 | 0.09 | 0.13 | 9 | 0.15 | 0.15 | 9? | 0.34 | 0.64 |
| | | | 10 | 0.09 | 0.13 | 10 | 0.09 | 0.13 | 10 | 0.15 | 0.15 | 10? | 0.34 | 0.64 |
| | | | | | | | | | | | | 11? | 0.34 | 0.64 |
| | | | | | | | | | | | | 12? | 0.34 | 0.64 |
| | | | | | | | | | | | | 13 | 0.24 | 0.32 |
| | | | | | | | | | | | | 14? | 0.34 | 0.64 |

* See Appendix A for Sits' Locations

? These values were calculated considering soil profile class SE instead of SD that was assigned for such sites in Table 6.8. This conservative assumption was made to account for the susceptibility of these sites to liquefaction. Moreover, as mentioned in the footer of Table 6.8, these sites require site-specific evaluation for soil class SF, especially for buildings that are classified as special or essential in the seismic design code.

# CHAPTER 7

# SUMMARY, CONCLUSIONS, AND RECOMMENDATIONS

## 7.1 SUMMARY

This Final Report (Part 1-main Report and Part 2- Appendices) of the research project AR-14-77 culminates the study reported earlier in six progress reports. The idea of this study is to initiate and explore the concept of the seismic microzonation of selected cities in the Kingdom of Saudi Arabia (KSA). Microzonation (the site-specific seismic zonation) has long been recognized as the most appropriate and economical solution of site categorization. Experts in many countries consider the seismic microzonation mapping based on site-specific soil conditions as the most essential element for their urban land use management plans and seismic risk reduction programs.

The scope of the study was limited to five cities located on the western coast of the Kingdom. These cities are Haql, Yanbu, Jeddah, Jizan, and Al-Wajh. Efforts of the study involved systematic geotechnical and geophysical field-tests at 8 to 14 carefuly-selected sites in each city, to accomplish the following objectives:

a) Characterizing the soil profile and assessment of the dynamic soil properties that included a vast site characterization database of shear wave velocity (SWV) profiles to depths reaching 50 m.

b) Evaluation of the potential of amplification of the seismic response of the ground and the associated soil site coefficients. Site coefficients were defined based on the mean shear wave velocity in the upper 30 m of the soil profile according to the current trend of provisions on the effect of local site conditions on ground motions.

c) Evaluation of the liquefaction potential.

## 7.2 SIGNIFICANT RESULTS

The most significant and conspicuous results that have been achieved in this study can be summarized as follows:

(1) The large geotechnical data of soil tests collected for the cities of Yanbu, Jeddah, and Jizan, are compiled in Chapter 4 of this report. The analysis of the data indicated that more than 90% of the collected drilling logs were shallower than 10 m., which is inconsistent with the criteria of seismic classification of soil profiles that is based on SPT of the top 30m of the profile. However, the collected data was utilized for general soil classification (as reported in Chapter 4) while the seismic classification of the soil profiles of the study sites, were mainly based on the SWV tests. The soil profiles of both Haql and Alwajh sites were also characterized based on the results of the SPT results of 10 bore holes conducted on these cities. The profiles' classes were found to be fairly consistent with those based on SWV.

(2) Vertical Electrical Sounding (VES) measurements were conducted at 5 sites in each city to define the groundwater and depth to the bedrock. The results revealed that the depth of the bedrock in all the study sites is greater than 60 m. The level of groundwater is very shallow in Jizan (about 0.5m). It varies in the areas that are closer to the shore. It varies from 2m to 4m in Jeddah, Yanbu, and Alwajh, while it is from 3 to 10m in Haql.

(3) The liquefaction potential of the study sites was investigated by employing a refined simplified approach. A computer program incorporating the SPT and SWV measurements in the analysis was developed for this purpose. The results revealed that the liquefaction susceptibility could be generalized for Jizan. In Haql only one site (No. 6), similarly site No. 3 in Alwajh, were found to be susceptible to liquefaction.

(4) Advanced technique known as Controlled Source Spectral Analysis of surface waves (CXW) was employed for measurements of shear wave velocity (SWV) profiles to depths reaching up to 50 on, 8 sites in Haql, 10 sites in each of Wajh, Yanbu, and Jeddah, and 14 sites in Jizan. The results are presented in Appendix F in form of profiling logs and are listed in tabulated forms in Chapter 6. These were comprehensively utilized to classify the soil profiles of the study sites as per the recent state of knowledge of the soil-site categories for building design codes. Specifically, the current provisions of NEHRP on soil profile definitions [11], which are adopted in both UBC 1997 [12] and IBC 2000 [13], were used in this study. These provisions consider the mean shear wave velocity $\overline{V}_S$ in the upper 30

m of the soil profile as the main definition of the site category. Value of $\overline{V}_S$ was calculated for each site and listed in the bottom of Tables 6.1 to 6.5 for, Haql, Wajh, Yanbu, Jeddah, and Jizan respectively. The soil profile classes corresponding to the $\overline{V}_S$ values of the respective sites were listed in Table 6.6.

(5) UBC1997 provisions were employed to determine the seismic coefficients: $C_a$ and $C_v$ of the short-period and long period design ground motions as functions of the site profile class and the seismic zone factor Z of the respective city. Values of $C_a$ and $C_v$ are presented in Table 6.9.

## 7.3 CONCLUSIONS AND RECOMMENDATIONS

Based on discussion of pertinent results, the conclusions that may be drawn, and the recommendations that may be forwarded are given as follows:

(1) The majority of the tested soil profiles in Haql (except site No. 6) can be classified as very dense soil and soft rock with seismic site-soil category SC. The seismic coefficients recommended for this type of profiles (for Z=0.2) are: $C_a$=0.24 and $C_v$=0.32. The soil profile could not be finalized for site No. 6. This site as shown on the city map (Appendix A) is in sandy deposit terrain located in the coastal lowland section of Haql. Although, this site can be defined as SD class based solely on $\overline{V}_S$ value, the liquefaction potential of this site suggests its soil profile to be fitted in softer class. Therefore, seismic coefficients recommended for this type of profiles were based on site-soil category SE: $C_a$=0.34 and $C_v$=0.64. These coefficients are only recommended for design of the conventional buildings. The buildings that are classified as special or essential in the seismic design code require geotechnical site-specific evaluation to check for soil class SF.

(2) Similar to Haql, the majority of the tested soil profiles in Alwajh (except site No. 3) can be classified as very dense soil or soft rock with seismic site-soil category SC. The seismic coefficients recommended for this type of profiles and those associated with Alwajh Z are: $C_a$=0.09 and $C_v$=0.13. The soil profile could not be finalized for site No. 3. This site as shown on the city map (Appendix A) is in loose to medium dense terrain located at Wadi Zaem north of Alwajh. Although, this site can be defined as SD class based solely on $\overline{V}_S$ value, the liquefaction potential of this site

suggests its soil profiles to be fitted in a softer class. Therefore, seismic coefficients recommended for this type of profiles were based on site-soil category SE: $C_a$=0.34 and $C_v$=0.64. These coefficients are only recommended for design of the conventional buildings. However, the buildings that are classified as special or essential in the seismic design code require geotechnical site-specific evaluation to check for soil class SF.

(3) Soil class SC that is associated with very dense soil and soft rock can be generalized for Yanbu. The seismic coefficients recommended for this type of profiles and associated with Yanbu Z are: $C_a$=0.09 and $C_v$=0.13. Harder soil (Rock) profile of class SB can be selected for site No 1, which as shown on the city map (Appendix A) is in a newly developed section located in the far north (about15 km) of the city.

(4) Most of the soil profiles tested in Jeddah were classified as class SC (dense soil and soft rock). Under this soil class and for Jeddah Z value, $C_a$ is 0.18 and $C_v$ is 0.25. Profiles of three sites located in the north sections of the city (Alzahra, Alrawhda, and Almuhamadia) toward Abhur, are qualified for rock of class SB. Both $C_a$ and $C_v$ for such sites can be taken as 0.15.

(5) In Jizan city, the soil profiles cannot be classified solely based on $\overline{V}_S$ values. This is because of the inferred problematic soil formation and pertinent liquefaction potential in this city. As shown in Fig.11, there are two main soil formations in Jizan. These are, the elevated terrain, and sabkah soil. The elevated terrain is underlain by the salt dome that is the predominant structural feature in the coastal area. Therefore, the hard soil profiles of soft rock (SC) and rock (SB) that were revealed by $\overline{V}_S$ values in this terrain (Sites No 7,8, and 13) can be attributed to existing of dense layer of salt rock. Construction in such areas is prohibitive due to the high susceptibility of large settlement of foundations as consequence of salt dissolution. In the Alsabka terrains all soil profiles were basically, related to $\overline{V}_S$, defined as stiff soil of class SD, and were then modified to softer class because of their high potential of liquefaction. The predominant liquefaction potential in the Alsabka terrains justify classifying these sites to fit softer soil classes such as SE or even SF. These sites therefore requiring site-specific geotechnical evaluation,

especially for buildings that are classified as special or essential in the seismic design code. For the conventional buildings, which are defined as standard buildings in the design code, seismic coefficients associated with the soil profile SE are suggested for Alsabka terrains. Specifically, $C_a$=0.34 and $C_v$=0.64.

The above discussion of the pertinent conclusions reveal that the main finding of this study is a preliminarily site-specific seismic zonation (microzonation), at least of the tested sites of the five cities considered in the study. The local municipalities can use the site-soil categorizations along with the associated seismic coefficients assigned for such sites, in their urban land use management plans and seismic risk reduction programs. The results are also essential for updating the seismic design criteria proposed for KSA and evaluation of the seismic performance of existing buildings. Engineering and consulting offices as well as researchers can benefit from the results.

The gained experience and mobilization of advanced equipment during the course of this study provide enough impetus for further similar effort aiming at detailed seismic microzonation of seismically active regions of the KSA

# REFERENCES


[1] Uniform Building Code (UBC 94), The International Conference of Building Officials, Whittier, California, 1994.

[2] NEHRP, Recommended Provisions for the Development of Seismic Regulations for New Buildings, Building Seismic Safety Council, Washington, D.C., 1991.

[3] American Society for Testing and Material, "Standard Method for Penetration Test and Split – Barrel Sampling of Soils", ASTM: D 1586-84, Vol. 4.08, Section 4, pp. 242-246, Philadelphia, 1992.

[4] Rodriguez-Ordonez, J.A., "New Method for Interpretation of Surface Wave Measurements in Soil", Ph.D. Dissertation, North Carolina State University, Civil Engineering Department, August 1994.

[5] ATC-3-06, 1978, Tentative Provisions for the Development of Seismic Regulations for buildings; Applied Technology Council, ATC 3-06, 505 p., Palo Alto, California, 1978.

[6] UBC 1991, Uniform Building Code, The International Conference of Building Officials, Whittier, California, 1991.

[7] Boore, D.M. and W.B.Joyner , Prediction of Ground Motion in North America, Applied Technology Council, ATC-35-1, Palo Alto, California, 1994.

[8] Borcherdt, R.D. (1994), New Developments in Estimating Site effects on Ground Motion, in Proc. Seminar on New Developments in Earthquake Ground Motion Estimation and Implications for Engineering Design Practice, ATC-35-1.

[9] Boore, D.M, W.B.Joyner and T.E. Fumal, Estimation of Response Spectra and Peak Accelerations From Western North American Earthquakes: An Interim Report, USGS Open File Report 93-509, Menlo Park, CA, (1993).

[10] Rinne, E.E., (1994), "Development of New Site Coefficients for Building Codes", Proceeding of 5th U.S. Nat. Conf. on Earthquake Engineering, July10-14, 1994, Chicago, Illinois.

[11] NEHRP, Recommended Provisions for the Development of Seismic Regulations for New Buildings, Building Seismic Safety Council, Washington, D.C., 1994.

[12] Uniform Building Code (UBC 97), The International Conference of Building Officials, Whittier, California, 1997.

[13] International Building Code 2000 (IBC2000), Final Draft, International Code Council (ICC), Falls Church, Virginia, 1998.

[14] Campbell, K.W. and Y.Bozorognia, Near-Source Attenuation of Peak Horizontal Acceleration from Worldwide Accelerogram Recorded from 1957 to 1993, 5th US National Conf. on Earthq. Eng., Chicago, (1994)

[15] Al-Haddad, M., Al-Dail, M., Al-Amri, A. "Preliminary Reconnaissance Report on the November 1995 Gulf of Aqaba Earthquake (Saudi Arabian Side)", Proceedings of the Eleventh World Conference on Earthquake Engineering (11WCEE), Acapulco, Mexico, 1996.

[16] Gulf of Aqaba Earthquake (22 November 1995), Ministry of Petroleum and Mineral Resources, Deputy Minister of Mineral Resource, Technical Report DMMR-TR-96-1, Jeddah, 1996.

[17] Al-Haddad, M.S., Siddiqi, G. H., Al-Zaid, R., Arafah, A., Necioglu, A., Turekeli, N., "A Study Leading To Preliminary Seismic Design Criteria In The Kingdom Of Saudi Arabia", AR-9-31, Final Report, KACST, Riyadh, 1992.

[18] Rowaihy, M.. Geologic Map of the Haql Quadrangle, Sheet 29A, GM-80C, Director General of Mineral Resources, Jeddah, Saudi Arabia, 1985.

[19] Davies, F.B. Geologic Map of the Al Qajh Quadrangle. Sheet 26B,GM-83C, Deputy Ministry for Mineral Resources, Jeddah, Saudi Arabia, 1985.

[20] Pellaton, C., Geologic Map of the Yanbu Al Bahr Quadrangle, Sheet 24C, GM-48A, Director General for Mineral Resources, Jeddah, Saudi Arabia, 1979.

[21] Moore, T. and Al-Rehaili, M., Geologic Map of the Makkah Quadrangle, Sheet 21D, GM-107C, Director General for Mineral Resources, Jeddah, Saudi Arabia, 1989.

[22] Skipwith, S.P., The Red Sea and Coastal Plain of the Kingdom of Saudi Arabia, Director General for Mineral Resources, Jeddah, Saudi Arabia, 1973.

[23] Blank, R., Johnson, P., Gettings, M., and Simmons, G., Explanatory Notes to the Geologic Map of Jizan Quadrangle, Sheet 16F, Deputy Ministry for Mineral Resources, Jeddah, Saudi Arabia, p. 25, 1986.

[24] Dobry, R. and Vucetic, M., "State-of-the-art Report: Dynamic Properties and Response of Soft Clay Deposits", Proc. Intl. Symp. On Geotec. Eng. Of Soft Soils, Mexico City, Vol. 2, pp. 51-87, 1987.

[25] Seed, H.B., Romo, M.P., Sun, J.I., Jaime, A. and Lysmer, J., "The Mexico Earthquake of September 19, 1985 – Relationships Between Soil Conditions and Earthquake Ground Motioins", Earthquake Spectra No. 4, pp. 687-729, 1988.

[26] Borcherdt, R., Glassmoyer, G., Andrews, M. and Cranswick, E., "Armenia Earthquake Reconnaissance Report: Effect of Site Conditions on Ground Motion and Damage", Earthquake Spectra Spec. Issue, pp. 23-42, Aug. 1989.

[27] Vucetic, M., "Correlation Between the Response of Soils to Earthquake Loads and Standard Soil Characteristics", NCEER Bull, Buffalo, N.Y., Vol. 3, No. 2, pp. 6-7, April, 1989.

[28] Youd, T.L., and Perkins, D.M., "Mapping of Liquefaction-Induced Ground Failure Potential", Journal of the Geotechnical Engineering Division, ASCE, Vol. 104, No. GT4, pp. 433-446, 1978.

[29] Erol, A. Orhan, "Engineering Geological Considerations in a Salt Dome Region Surrounded by sabkha Sediments, Saudi Arabia", Engineering Geology, 26, pp. 215-232, 1989.

[30] Al-Muhendis, "Jazan Town Planning and Structural Engineering Studies", Unpublished Report, Ministry of Municipal and Rural Affairs, Riyahd, Saudi Arabia, 1985.

[31] Seed, H.B., and Idriss, I.M., 1971, "Simplified Procedure for Evaluating Soil Liquefacfion Potential," Journal of the Soil Mechanics and Foundations Division, ASCE, Vol. 97, No. SM9, p. 1249-1273..

[32] Summary Report -1997-NCEER Workshop on Evaluation of Liquefaction Resistance of Soils. Technical Report NCEER-97-0022.

[33] Liao, S.S.C., Veneziano, D., and Whitman, R.V., 1988, "Regression Models for Evaluating Liquefaction Probability," Journ.. Of Geotechnical Engineering, Vol. 114, No. 4, p. 3 89-411.

[34] Youd, T.L., and Noble, S.K., 1996, "Liquefaction Criteria Based on Probabilistic Analyses," Proceeding of the NCEER Workshop on Evaluation of Liquefaction Resistance of Soils. Technical Report NCEER-97-0022, p. 201-216.

[35] Seed, H.B., and Idriss, I.M., 1982, "Ground Motions and Soil Liquefaction During Earthquakes," Earthquake Engineering Research Institute Monograph.

[36] Seed, H.B., Tokimatsu, K., Harder, L.F., and Chung, R.M., 1985, "The Influence of SPT Procedures in Soil Liquefaction Resistance Evaluations," Journal of Geotechnical Engineering, ASCE, Vol. III, No. 12, p. 1425-1445.

[37] Liao, S.S.C. and Whitman, R.V., 1986, "Overburden Correction Factors for SPT in Sand," Journal of Geotechnical Engineering, Vol. 112, No. 3, p. 373-377.

[38] Stokoe, K.H., II, Roesset, J.M., Blei-schwale, J.G., and Aoouad, M., 1988, "Liquefaction Potential of Sands From Shear Wave Velocity," Proceedings, 9th World Conf. On Earthquake Engineering, Tokyo, Japan, Vol. 111, p. 213-218.

[39] Tokimatsu, K., Kuwayama, S., and Tamura, S., 199 I, "Liquefaction Potential Evaluation Based on Rayleigh Wave Investigation and Its Comparison with Field Behavior, "Proceedings, 2nd Int. Conf. On Recent Advances in Geotechnical

Earthquake Engineering and Soil Dynamics, held in St. Louis, Missouri, S. Prakash, Ed., University of Missouii-Rolla, Vol. 1, p. 357-364.

[40] Robertson, P.K., Woeler, D.J., and Finn, W.D.L., 1992, "Seismic Penetration Test for Evaluating Liquefaction Potential Under Cyclic Loading," Canadian Geotechnical Journal, Vol. 29, p. 686-695.

[41] Kayen, R.E., Mitchell, J.K., Saeed, R.B., Lodge, A., Nisho, S., and Coutinho, R., 1992, "Evaluation of SPT-CPT-, and Shear Wave-Based Methods for Liquefaction Potential Assessment Using Loma Prieta Data, "Proceedings, 4th Japan-US Workshop on Earthquake Resistant Design of Lifeline Facilities and Countermeasures for Soil Liquefaction, Honolulu, Hawaii, NCEER, Buffalo, NY, Technical Report NCEER-920019, Vol. 1, p. 177-204.

[42] Andrus, R.D., 1994, "In Situ Characterization of Gravelly Soils That Liquefied in the 1983 Borah Peak Earthquake," Ph.D. Dissertation, University of Texas at Austin, p. 533.

[43] Lodge, A.L., 1994, "Shear Wave Velocity Measurements for Subsurface Characterization," Ph.D. Dissertation, University of California at Berkeley.

[44] Andrus, R.D. and Stokoe, K.H., 1996, "Liquefaction Resistance Based on Shear Wave Velocity". Proceedings of the NCEER Workshop on evaluation of liquefaction resistance of soils, FHWA, Salt Lake City, Utah, p. 89-128.

[45] Ambraseys, N.N., 1988, "Engineering Seismology," Earthquake Engineering and Structural Dynamics, Vol. 17, p. 1-105.

[46] Arango, I., 1996, "Magnitude Scaling Factors for Soil Liquefaction Evaluations," Journal of Geotechnical Engineering, ASCE, Vol. 122, No. I 1, p. 929-936.

[47] Seed, H.B., 1983, "Earthquake Resistant Design of Earth Dam," Symposium of Seismic Design of Earth Dams and Caverns, ASCE, New York, p. 41-64.

[48] Seed, R.B., and Harder, L.F., Jr., "SPT-Based Analysis of Cyclic Pore Pressure Generation and Undrained Residual Strength", Proceedings, H. Bolton Seed Memorial symposium, May 1990, BiTech Publishers, Ltd., pp. 315-376, 1990.

[49] Vaid, Y.P., Chem, Jing C., and Tumi, Hadi, 1985, "Confining Pressure, Grain Angularity, and Liquefaction," Journal of Geotechnical Engineering, ASCE, Vol. 111, No. 10, October.

[50] Vaid, Y.P., and Thomas, J., 1994, "Post Liquefaction Behavior of Sand," Proceedings of the 13th Int. Conf. On Soil Mechanics and Foundation Engineering, New Delhi, India.

[51] Byrne, P.M. and Harder, L.F., Jr., 1991, "Terzaghi Dam, Review of Deficiency Investigation, Report No. 3," prepared for B C Hydro, Vancouver, British Columbia.

[52] Harder, L.F. Jr. And Boulanger, R., 1996 "Application of $K_\sigma$, and $K_\alpha$ Correction Factor", Proceedings of the NCEER Workshop on Evaluation of Liquefaction Resistance Soils. Technical Report NCEER-97-0022, p. 167-190.

[53] Seed, H.B., 1979, "Soil Liquefaction and Cyclic Mobility Evaluation for Level Ground During Earthquakes," Journal of Geotech-nical Engineering, ASCE, Vol. 105, No. GT2, p. 201-255.

[54] Youd, T.L., and Hoose, S.N., 1977, "Liquefaction Susceptibility and Geologic Setting," Proceeding, 6th World Conference on Earthquake Engineering, Prentice-hall, Inc., Vol. 3, pp. 2189-2194.

[55] Idriss, I.M., 1985, "Evaluating Seismic Risk in Engineering Practice," Proceedings, 11th Int. Conf. On Solid Mechanics and Foundation Engineering, San Francisco, Vol. 1, p. 255-320.

[56] Idriss, I.M., 1991, "Earthquake Ground Motions at Soft Soil Sites," Proceedings, 2nd Int. Conf On Recent Advances in Geotechnical Earthquake Engineering and Soil Dynamics, Vol. 3, p. 2265-2271.

[57] Heaton, T.H., Tajima, F., and Mori, A.W., 1982, "Estimating Ground Motions Using Recorded Accelerograms," unpublished report by Dames and Moore to Exxon Production Res. Co., Houston, Texas.

[58] Idriss, I.M., 1990, "Response of Soft Soil Sites During Earthquakes," Proceedings, H. Bolton Seed Memorial Symposium, Vol. 2, BiTech Publishers Ltd, Vancouver, B.C. Canada, p. 273-290.

[59] Seed, R.B., Dickenson, S.E., Rau, G.A., White, R.K., and Mok, C.M., 1994, "Site Effects on Strong Shaking and Seismic Risk: Recent Developments and Their Impact on Seismic Design Codes and Practice," Proceedings, Structural Congress II, ASCE, Vol. 1, p. 573-578.

[60] Park, S. and Elrick S., "Predictions of Shear Wave Velocities in Southern California Using Surface Geology", Bulletin of the Seismological Society of American, Vol. 88, No. 3, pp. 677-685, June 1998.

[61] Nath, S.K., Chatterjee, D., Biswass, N.N., Dravinski, M., Cole, D.A., Papageorgiou, A., Rodriguez, J.A., and Poran, C.J., "Correlation Study of Shear Wave Velocity in Near Surface Geological Formations in Anchorage, Alaska, "Earthquake Spectra, Vol. 13, No. 1, pp. 55-75, February 1997.

[62] NEHRP Recommended Provisions for Seismic Regulations for New Buildings, Pail 2-Conunentaiy, Federal Emergency Management Agency, 1994 Edition, Building Seismic Safety Council, Washington, D.C., p. 335.